Symmetry protected measurement-based quantum computation in finite spin chains

by

Arnab Adhikary

B.Tech, Jadavpur University, 2018

A THESIS SUBMITTED IN PARTIAL FULFILLMENT
OF THE REQUIREMENTS FOR THE DEGREE OF

Master of Science

in

THE FACULTY OF GRADUATE AND POSTDOCTORAL STUDIES
(Physics)

The University of British Columbia
(Vancouver)

August 2021

The following individuals certify that they have read, and recommend to the Faculty of Graduate and Postdoctoral Studies for acceptance, the thesis entitled:

Symmetry protected measurement-based quantum computation in finite spin chains

submitted by **Arnab Adhikary** in partial fulfillment of the requirements for the degree of **Master of Science** in **Physics**.

Examining Committee:

Robert Raussendorf, Physics
Supervisor

Mona Berciu, Physics
Supervisory Committee Member

Abstract

We consider ground states of quantum spin chains with symmetry-protected topological (SPT) order and their usefulness as resources for measurement-based quantum computation (MBQC). It is known that SPT phases (applicable to infinite spin chains) protected by a finite abelian symmetry group exhibit uniform computational power. In this work, we extend these ideas to finite spin chains which are more realistic resources for physical computation. Herein, we relate the usefulness of MBQC resource states to a non-vanishing string-order parameter. Furthermore, using the techniques developed, we show that hard-to-think-about regimes of computation are actually more efficient than the textbook prescription. Our results strengthen the connection between condensed matter and quantum computation and also provide the necessary tools to explore such connections in the state-of-the-art noisy small quantum devices. As an outlook, we discuss how this newly developed formalism can potentially be used to identify non-traditional resource states for MBQC and be extended to higher dimensions, leading to universal quantum computation.

Lay Summary

In middle school, we were all told that there are three phases of matter – solid, liquid and gas. If you were a little curious like me, you may have found out a "secret": there is a fourth phase of matter called "plasma". At any rate, it should not come as a surprise that in reality, nature exhibits far more interesting phenomenon than we were let in on as kids. It turns out that there are not three phases of matter, nor four, but many. A key insight of modern physics, due to Lev Landau, is that these phases are characterized by their symmetries. It was indeed remarkable that a theory based on such general principles could describe all phases of matter known to us at the time. However, starting from the 1980s, exotic phases of matter were discovered which are beyond the Landau paradigm. A particularly striking example of such unconventional phases is the so-called symmetry-protected topological order. Recently, such phases of matter have been recognized as a resource for building the much-coveted quantum computer. In this work, we explore how these states can still be useful as computational resources in situations where the concept of phase itself is murky i.e. in *finite* quantum spin chains.

Preface

The work presented in this thesis is primarily the result of an ongoing collaboration with my supervisor Dr. Robert Raussendorf. All the initial motivation and drive for this project was provided by him. As far as the results go, the discussion in Sec. 5.2 is entirely his work although it was motivated by my numerical results in Fig. 5.1. Talking about numerics, all the computer simulations included in this manuscript have been performed by me. Apart from this, my main contribution to this project has been the discussion of decoherence management schemes in finite systems and the discovery of counter-intuitive yet efficient regimes of computation as outlined in Sec. 5.5.

The entirety of this thesis has been written in my own words and this work has not yet been published anywhere else.

Table of Contents

List of Figures

List of Symbols

Note: All the matrix representations are in the computational (Pauli-Z) basis.

Quantum circuit components

Quantum wire — $\begin{bmatrix} 1 & 0 \\ 0 & 1 \end{bmatrix}$

Computational basis measurement — 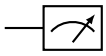 $\Pi_0 = \begin{bmatrix} 1 & 0 \\ 0 & 0 \end{bmatrix}$, $\Pi_1 = \begin{bmatrix} 0 & 0 \\ 0 & 1 \end{bmatrix}$

Single qubit gates

Pauli-X — 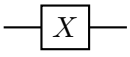 $\begin{bmatrix} 0 & 1 \\ 1 & 0 \end{bmatrix}$

Pauli-Y — 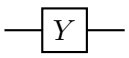 $\begin{bmatrix} 0 & -i \\ i & 0 \end{bmatrix}$

Pauli-Z — 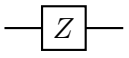 $\begin{bmatrix} 1 & 0 \\ 0 & -1 \end{bmatrix}$

Hadamard — 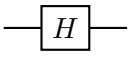 $\frac{1}{\sqrt{2}} \begin{bmatrix} 1 & 1 \\ 1 & -1 \end{bmatrix}$

$R_x(\theta) \equiv e^{-i\theta X/2}$ — 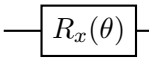 $\begin{bmatrix} \cos\frac{\theta}{2} & -i\sin\frac{\theta}{2} \\ -i\sin\frac{\theta}{2} & \cos\frac{\theta}{2} \end{bmatrix}$

$R_z(\theta) \equiv e^{-i\theta Z/2}$ — 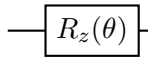 $\begin{bmatrix} e^{-i\theta/2} & 0 \\ 0 & e^{i\theta/2} \end{bmatrix}$

Two qubit gates

Controlled-Z (CZ) —  $\begin{bmatrix} 1 & 0 & 0 & 0 \\ 0 & 1 & 0 & 0 \\ 0 & 0 & 1 & 0 \\ 0 & 0 & 0 & -1 \end{bmatrix}$

List of Abbreviations

- AKLT state: Affleck, Lieb, Kennedy and Tasaki state
- BCS: Bardeen, Cooper and Schrieffer
- CZ gate: Controlled-Z gate/Controlled-phase gate
- DMRG: Density-matrix renormalisation group
- LP (metric): Loss in purity (metric)
- MBQC: Measurement-based quantum computation
- MPO: Matrix product operator
- MPS: Matrix product state
- NISQ: Noisy intermediate-scale quantum
- PEPS: Projected entangled-pair states
- SOP: String order parameter
- SPT(O): Symmetry-protected topological/trivial (order)
- SRE: Short-range entangled

Acknowledgments

I will be eternally grateful to my supervisor, Robert Raussendorf, for accepting me as a graduate student despite my engineering background and giving me the opportunity to work on such an intriguing problem. I attribute the success of my degree to his constant support, tutelage, and generosity with his time. No part of this project would have been possible without him.

Additionally, I would like to thank the other members of the UBC quantum information group including Paul Herringer and Michael Zurel for interesting discussions about quantum information and life in general. Special thanks to Ryohei Weil for answering all my typesetting problems and proofreading the thesis. Furthermore, I am thankful to David T. Stephen for being so generous with his time in numerous fruitful discussions over Zoom. Shout-out to the lovely people at the Flatiron Institute for developing the open-source ITensor Julia package that enabled me to perform the numerical simulations for this project. They were so patient in answering my stupid questions and providing instant customisation for their users.

In my life outside university, I am grateful to my long-time friends Sourav and Soumik for their companionship throughout the years. I have also thoroughly enjoyed the company of my friends at UBC Physics Circle.

Finally, I am most grateful to my parents, whose unwavering support has helped me in all aspects of life. Despite the challenges that come from being raised in a rural lower-middle-class family, they made it their life's mission to provide me with a better education. I will be eternally indebted to them for standing by me through thick and thin. This thesis is dedicated to them.

Chapter 1

Introduction

For almost three decades now, a universal quantum computer has been widely believed to be able to efficiently solve (specific) problems that are intractable for its classical counterparts. Originally conceived by Feynman [Fey82] as a way to simulate exponentially complex quantum systems that cannot possibly be efficiently simulated classically, the idea of quantum computers has gained unprecedented traction in recent years. Such kindled interest in the field has primarily been fuelled by the development of quantum algorithms that serve broader goals than that of the condensed matter enthusiast. The canonical examples that come to mind is that of Shor's algorithm [Sho97] for factoring integers[1] and Grover's algorithm [Gro96] for unstructured search. Both of these algorithms are *asymptotically* more efficient than that of any known classical algorithm. However, such claims are based on scaling arguments and we would need to build large-scale fault-tolerant quantum computers to see a practical improvement over relevant existing classical algorithms. On the other hand, recent experiments from Google [AAB$^+$19] and others [ZWD$^+$21] have (allegedly [ZSW20, PR21]) demonstrated such *quantum supremacy* in real-life noisy quantum devices for the (useless?) problem of sampling from random distributions.

These facts notwithstanding, an age-long question regarding the foundation of the field remains unanswered: what exactly makes quantum computing work? Different answers regarding counter-intuitive quantum phenomena like superposition [Deu85], interference, the largeness of Hilbert space, entanglement [JL03] and contextuality [HWVE14] have been suggested but it is safe to say that the "magical essence" that makes the paradigm of quantum computing (QC) superior remains elusive to date. It is worth pointing out that an answer to this fundamental question promises to provide insights into identifying "useful" problems that may have quantum speedups. In this spirit, it is instructive to look at the measurement-based quantum computing model (MBQC) [RB01] in which one starts out with a specific entangled state and performs only single qubit (adaptive) measurements on it to carry out the desired computation. As surprising as it may sound, such a model of computation can be proven to be universal given that the initial state is a *universal resource state*. This model provides an alternative vantage

[1] and thereby breaking the RSA public cryptosystem: a primary reason why the intelligence community (CIA/NSA) is willing to invest billions in the field.

point for investigating the power of QC as it relies solely on the initial resource to provide the magic/resource for the supremacy of QC. Given the concentrated power of computation on the initial state in the MBQC setting, the natural question becomes: what connects the universal resource states providing the quantum speed up? This has turned out to be a remarkably difficult question to answer in general but it is known that these states are extraordinarily rare in Hilbert space [GFE09].

As with almost everything in physics, the situation simplifies when one adds symmetry to the mix and considers the ground state of some local Hamiltonian, invariant under a symmetry transformation, as the resource state. In an attempt to classify different MBQC schemes by symmetry (in a similar way as, say, elementary particles), one conjectures: the power of MBQC is uniform throughout a symmetry-protected topological (SPT) phase. This is known to be true at least for 1D (infinite) spin chains [RWP$^+$17, SWP$^+$17] where there are only two phases: the cluster phase (computational resource) and the product (trivial) phase. These two "phases" are distinguished by the fact that the parent Hamiltonians[2] of the states in the two phases cannot be adiabatically deformed from one onto the other through a symmetry respecting path that doesn't close the energy gap above the ground state [Wen95]. There exists an equivalent fancy mathematical classification of these phases in terms of group cohomologies and cocycles [CGLW13].

All of this is very elegant mathematics but here comes the catch: real computation takes place in finite systems and for them, the energy gap *never* closes when one adiabatically connects the cluster state to the product state through a symmetry respecting path. But then what is it that defines the phases and what characterizes the phase transition between them? Note that in a finite system, one cannot refer to the thermodynamic limit – thereby making the idea of physical phases also murky. On the other hand, realistically speaking, the idea of quantum computational power is defined specifically in finite systems[3] and there is where we seem to arrive at an impasse.

In this work, we provide an alternative formalism that classifies the aforementioned states in terms of their computational power as a MBQC resource state, but crucially, such a prescription is equally at ease in discussing finite systems. This new formalism, seemingly innocuous at first sight, replaces all the previous techniques that were developed in terms of the ansatz of matrix product states (MPS) and solely focuses on the quantum state under consideration. Such an operational point of view not only allows us to analyze finite systems but also extends the previous formalism developed in [RWP$^+$17]. As evidence for the superiority of the new methods, we further show that, for computation in any finite chain, the most efficient regime of operation is precisely the *opposite* of the "safe" regime prescribed in the earlier literature. Overall, this thesis puts the connection between SPT states and MBQC on firmer ground by extending such notions to finite systems and along the way shows that the usefulness of MBQC

[2] of which the concerened states are ground states of

[3] the thermodynamic limit is only invoked as a stand-in for discussing large but finite systems.

resource states is inextricably related to string order – a concept well-known to the topological condensed matter physicist [HPGCS12]. Additionally, our methods apply to arbitrarily small systems, making investigations in NISQ (noisy intermediate-scale quantum) era devices feasible.

In the following chapter, we provide the reader with the necessary background in quantum computation via local measurements and (symmetry-protected) quantum phases. We first introduce some computational primitives that show us how MBQC works and why it is a universal model of quantum computation. Next, we move on to the notion of SPT order. We end the chapter by introducing the ansatz of matrix product states (MPS) that play a seminal role in the analytical and numerical analysis of 1D spin chains. In Chapter 3, we review earlier works that established a deep connection between the entanglement structure in SPT phases and their usefulness in MBQC. The culmination of this line of inquiry leads to the idea of "computational phases of quantum matter". In Chapter 4, we discuss all the trouble that comes with trying to apply the traditional methods to finite systems and conjecture that the earlier techniques may be inadequate in dealing with real-life finite resources. Fortunately, in Chapter 5, we succeed in coming up with a rather different formulation that works for any system size. Using these techniques, we draw a direct connection between long-range string-order in SPT ordered states and their computational usefulness in MBQC. Such methods also allow us the investigate exotic regimes of computation that we prove to be efficient. Finally, in Chapter 6, we discuss the possible ramifications of our work and how they can be used to further the grander goal of classifying MBQC schemes just by analyzing their algebraic structure (symmetry).

Chapter 2

Background

The purpose of this chapter is to set up the groundwork for understanding the results of the thesis. No prior knowledge outside standard quantum mechanics has been assumed. Keeping in mind that this thesis lies at the intersection of quantum computation and condensed matter physics, in the following sections, we intend to present the reader with a bird's eye view of (measurement-based) quantum computation and its relation to symmetry-protected topological (SPT) phases. The chapter concludes with an introduction to tensor networks with an emphasis on matrix product states (MPS) which are excellent ansatz to study quantum spin chains and have been used extensively for the numerical results presented in the thesis.

Primer on quantum computation

Quantum computation is a novel paradigm of harnessing nature to perform computations using the (admittedly weird) rules of quantum mechanics. The fundamental difference between a quantum computer and your favorite electronic device is the basic unit of information used. In classical computation, the simplest system of interest can be in either of two distinct states - thereby encoding a *bit*. In the quantum mechanical setting, a two-level system encodes a *qubit*. Formally, the state of a qubit is associated with the Hilbert Space $\mathbb{C}^2$ and can be expanded in the computational basis $\{|b\rangle|\ b \in \mathbb{Z}_2\}$ as $|\Psi\rangle = \alpha_0|0\rangle + \alpha_1|1\rangle$. For the well-known quantum circuit model, one considers a state of n-qubits initialized to $|0\rangle^{\otimes n}$ and performs a quantum circuit by applying a unitary transformation $u \in U(2^n)$ to it, prior to the final measurement in the computational basis. The exponential freedom in the choice of this unitary operator allows us to explore the whole Hilbert space but also raises a natural question: Is it possible to restrict ourselves to a strict subset of unitaries (which are "easy" to implement physically) and still harness the full power of quantum computation to arbitrary precision? Fortunately for us, the answer turns out to be yes and gate sets with this property are known as universal for quantum computation. It is not hard to prove that the set of single-qubit rotations along with the 2-qubit entangling Controlled-Z (CZ) gate (defined in Eq. 2.2) is an example of such a universal gate set. Mathematically speaking, this is not a particularly deep result, but physically

it is significant. It tells us that if we are able to faithfully perform generic single-qubit rotations along with the 2-qubit CZ gate, we will be able to build up any general quantum circuit, no matter how complex, to arbitrary precision. For completeness, let us note that this gate set can be further significantly reduced to a finite set which is paramount for discussions of fault tolerance [KLZ98] and quantum computation using magic states [BK05]. However, these analyses will not be particularly relevant for proving the universality of an equivalent model of quantum computation which is introduced in the following section.

2.1 Measurement-based quantum computation

As evident from the previous section, in the quantum circuit model, the unitary evolution of the quantum mechanics takes center-stage and the (projective) measurements at the end are merely used as readout procedures, thereby playing a secondary role. In the measurement-based quantum computational (MBQC) model introduced by Raussendorf and Brigel [RB01], the roles of unitary evolution and projective measurements are more or less reversed. First of all, no entangling unitary gate is available to us on the fly. Instead, all the entanglement that is to be used up in the computation is prepared in the form of a particular many-body (highly) entangled quantum state (known as a *universal resource*) before any computation starts. Once this state is given to us as a *resource*, the computation is executed by performing (adaptive) single-qubit projective measurements[1] on this state. It is imperative to stress here that the initial resource state is universal in the sense that *any* arbitrary quantum computation can be performed by adjusting the (single-qubit) measurement pattern on *this specific state*.

The cluster state(s)

As we might suspect, universal resource states for MBQC are indeed very special and are in fact extraordinarily rare in the Hilbert space. The reason is also intriguing. Most states are *too entangled*[2] to be useful [GFE09] for MBQC schemes. Nevertheless, there are a few explicitly known such universal resource states, the most natural of which is the so-called 2-dimensional cluster state. Here we first introduce an explicit method of how to create such a state and then describe a mathematical formalism to define and deal with it efficiently.

Consider a two-dimensional square lattice $\mathcal{L}_2$ where each vertex $a \in V(\mathcal{L}_2)$ denotes a qubit and the edges $e \in E(\mathcal{L}_2)$ denote interactions between the lattice qubits. Given this setting, the two dimensional cluster state $|C\rangle_{\mathcal{L}_2}$ is created in two simple steps.

1. Prepare all the qubits on vertices $a \in V(\mathcal{L}_2)$ in the $+1$ eigenstate of the Pauli-X operator i.e. $|+\rangle_a := \frac{1}{\sqrt{2}}(|0\rangle_a + |1\rangle_a)$

[1] The careful reader may be (justifiably) worried about how this computational scheme might be affected by the fundamental randomness and irreversibility involved in quantum measurements. This is indeed a non-trivial problem and requires classical side-processing during and at the end of the computation. We will discuss this in considerable detail after Eq. 2.8.

[2] with respect to the geometric entanglement measure.

2. Turn on a translation-invariant Ising interaction for a fixed time T

$$U = \exp\left\{ \left\{ -i\frac{gT}{\hbar} \sum_{\langle i,j \rangle} (1 - Z_i)(1 - Z_j) \right\} \right\} \quad \text{with} \quad \frac{gT}{\hbar} = \frac{\pi}{4}.$$

To a quantum information theorist, the more familiar equivalent operation is a Controlled Phase (CZ) gate applied between all neighbouring qubits resulting in

$$|C\rangle_{\mathcal{L}_2} = \left[\prod_{(a,b) \in E(\mathcal{L}_2)} CZ_{a,b} \right] \bigotimes_{a \in V(\mathcal{L}_2)} |+\rangle_a \tag{2.1}$$

wherein the CZ gate is a symmetric operation (which squares to the identity) between the control (c) and target (t) qubits that can be represented as

$$CZ_{c,t} = |0\rangle_c\langle 0| \otimes \mathbb{I}_t + |1\rangle_c\langle 1| \otimes Z_t = \mathbb{I}_{c,t} - 2|11\rangle_{c,t}\langle 11| \tag{2.2}$$

This implies, in the computational basis expansion of a two-qubit state, that the CZ operation only flips the sign of the $|11\rangle$ coefficient.

The CZ gate can be shown to obey the following useful propagation identities

$$\begin{aligned} CZ_{a,b}\, X_a\, CZ_{a,b} &= X_a\, Z_b, \\ CZ_{a,b}\, X_b\, CZ_{a,b} &= Z_a\, X_b, \\ CZ_{a,b}\, Z_a\, CZ_{a,b} &= Z_a, \\ CZ_{a,b}\, Z_b\, CZ_{a,b} &= Z_b. \end{aligned}$$

Applying these relations recursively results in the identity

$$\begin{aligned} &\left[\prod_{(a,b) \in E(\mathcal{L}_2)} CZ_{a,b} \right] X_u \left[\prod_{(a,b) \in E(\mathcal{L}_2)} CZ_{a,b} \right] = X_u \prod_{v \in n(u)} Z_v, \\ \Rightarrow \quad &\left[\prod_{(a,b) \in E(\mathcal{L}_2)} CZ_{a,b} \right] X_u = X_u \left[\prod_{v \in n(u)} Z_v \prod_{(a,b) \in E(\mathcal{L}_2)} CZ_{a,b} \right]. \end{aligned}$$

where the neighbourhood set $n(u)$ contains all the vertices v that are connected to the vertex u via edges $(u, v) \in E(\mathcal{L}_2)$. Applying this identity to the initial product state $|+\rangle|+\rangle \cdots |+\rangle$, we arrive at the set of stabiliser relations

$$|C\rangle_{\mathcal{L}_2} = \left[X_u \prod_{v \in n(u)} Z_v \right] |C\rangle_{\mathcal{L}_2} \; ; \quad \forall u \in V(\mathcal{L}_2) \tag{2.3}$$

$$= K_u \; |C\rangle_{\mathcal{L}_2} \; ; \quad \forall u \in V(\mathcal{L}_2). \tag{2.4}$$

This set of equations turns out to be enough to uniquely specify the cluster state given the lattice $\mathcal{L}_2$. Thus, together with Eq. 2.1, the cluster state can be alternatively defined as the *unique* $+1$ eigenstate of the independent commuting Pauli observables (which form the so called "stabilizer group" of the state)

$$K_u := X_u \prod_{v \in n(u)} Z_v \; ; \quad \forall u \in V(\mathcal{L}_2) \; . \tag{2.5}$$

This definition is independent of any particular experimental preparation procedure and generalizes the idea of a cluster state to a larger family of states called graph states.

Definition 1 (Graph and Cluster States). *Given any graph G with vertex set V_G and edge set E_G, we can define the graph state $|G\rangle$ as the unique simultaneous $+1$ eigenstate of the Pauli observables*

$$K_u := X_u \prod_{v \in n(u)} Z_v \; ; \quad \forall u \in V_G \; ,$$

wherein $n(u) := \{v \mid (u,v) \in E_G\}$ i.e. $K_u |G\rangle = (+1)|G\rangle$ for all vertices u. The d-dimensional cluster state is a special graph state corresponding to the graph $G = \mathcal{L}_d$.

Additionally, this stabilizer definition of the cluster-like states naturally translates into the Hamiltonian picture in condensed matter physics and thereby to symmetry-protected topological phases. We will explore this connection in all its glory in the following chapters. But for now, having defined them, let us see some simple examples of 1D cluster states.

- **Two qubit cluster state**: The simplest non-trivial cluster state is of 2 qubits and can be expanded in the computational basis as

$$\begin{aligned} |C_2\rangle := CZ_{1,2}|+\rangle_1|+\rangle_2 &= CZ_{1,2}\left(\frac{|0\rangle_1 + |1\rangle_1}{\sqrt{2}}\right)\left(\frac{|0\rangle_2 + |1\rangle_2}{\sqrt{2}}\right) \\ &= \frac{1}{2}(|00\rangle_{1,2} + |01\rangle_{1,2} + |10\rangle_{1,2} - |11\rangle_{1,2}) \\ &= \frac{|0+\rangle_{1,2} + |1-\rangle_{1,2}}{\sqrt{2}}. \end{aligned}$$

  The final expression looks very close to the maximally entangled two qubit states known as Bell pairs. In fact, the two qubit cluster state is just a locally (Hadamard) rotated version of the first Bell pair

$$(I_1 \otimes H_2)\,|C_2\rangle = \frac{|00\rangle_{1,2} + |11\rangle_{1,2}}{\sqrt{2}} =: |B_{00}\rangle \; .$$

- **Three qubit cluster state**: Using the same Def. 2.1 the three qubit cluster state on a

chain can be expanded as

$$\begin{aligned}|C_3\rangle &:= CZ_{2,3}\, CZ_{1,2}\, |+\rangle_1|+\rangle_2|+\rangle_3 \\ &= \frac{1}{\sqrt{2}} CZ_{2,3}\, CZ_{1,2}\, |+\rangle_1(|0\rangle_2 + |1\rangle_2)|+\rangle_3 \\ &= \frac{|+0+\rangle_{1,2,3} + |-1-\rangle_{1,2,3}}{\sqrt{2}}\ .\end{aligned}$$

In the final line qubit 2 was chosen as the control qubit for both the Controlled-Z gates to obtain a compact expression efficiently. This state is again local unitarily equivalent to the so-called Greenberger-Horne-Zeilinger (GHZ) state as

$$(H_1 \otimes I \otimes H_3)\, |C_3\rangle = \frac{|000\rangle_{1,2,3} + |111\rangle_{1,2,3}}{\sqrt{2}} =: |\mathsf{GHZ}\rangle\ .$$

2.1.1 Simple one qubit gates using teleportation on cluster states

The first step towards demonstrating the universality of MBQC is to show that quantum information can be faithfully transmitted between different qubits in this computational scheme. To see this, let us consider a two-qubit cluster state *with input* i.e. a two-qubit cluster state where one of the (edge) qubits has been used to encode a logical state. Thus the initial state of the circuit can be written as $|\mathsf{in}\rangle_1 \otimes |+\rangle_2$ where the input logical state can be expanded in the local computational basis $|\mathsf{in}\rangle = \alpha_0|0\rangle + \alpha_1|1\rangle$. Next, the logical qubit is encoded by entangling it with the second qubit using the CZ gate. Let us now consider measurement on the first qubit in different bases and see what effect it has on the logical information that was initially encoded in $|\mathsf{in}\rangle_1$.

- **Quantum wire**: Immediately after the CZ encoding, the two-qubit state can be compactly expressed as $|\Psi\rangle = \alpha_0|0+\rangle + \alpha_1|1-\rangle$. Now let us see what happens when we measure the first qubit in the (Pauli-)X basis. Expanding the state $|\Psi\rangle$ in the $\{|+\rangle_1, |-\rangle_1\}$ basis (eigenbasis of the measurement observable) and rearranging, we arrive at

$$\begin{aligned}|\Psi\rangle &= \alpha_0|0+\rangle_{1,2} + \alpha_1|1-\rangle_{1,2} \\ &= \tfrac{\alpha_0}{\sqrt{2}}|++\rangle + \tfrac{\alpha_0}{\sqrt{2}}|-+\rangle + \tfrac{\alpha_1}{\sqrt{2}}|+-\rangle + \tfrac{\alpha_1}{\sqrt{2}}|--\rangle \\ &= |+\rangle(\tfrac{\alpha_0}{\sqrt{2}}|+\rangle + \tfrac{\alpha_1}{\sqrt{2}}|-\rangle) + |-\rangle(\tfrac{\alpha_0}{\sqrt{2}}|+\rangle - \tfrac{\alpha_1}{\sqrt{2}}|-\rangle) \\ &= \tfrac{1}{\sqrt{2}}(|+\rangle_1 H|\mathsf{in}\rangle_2 + |-\rangle_1 HZ|\mathsf{in}\rangle_2)\ . \quad (\text{as } H|+\rangle = |0\rangle,\ H|-\rangle = |1\rangle)\end{aligned}$$

Thus, if we measure the first qubit in the X basis and obtain an outcome $\mathbf{s} \in \{0,1\}$,[3] the

[3] 0 corresponds to the post measurement state of $|+\rangle_1$ and 1 to the post measurement state of $|-\rangle_1$

second qubit is left in the final state

$$|\text{out}\rangle = HZ^s|\text{in}\rangle\,. \tag{2.6}$$

Although mathematically almost trivial, physically this is a rather intriguing result. At time $t = 0$ we had encoded our logical information (contained in the coefficients α_0, α_1) solely in qubit 1. Naively one would think that this information is destroyed as an irreversible measurement is performed on this qubit. However, it is the entanglement between the two qubits that allows this information to be perfectly transmitted to qubit 2. If we are supplied with the one-bit information about the measurement outcome i.e. s, this information can be perfectly recovered. Those familiar with the famous quantum teleportation protocol [BBC$^+$93] will recognize the present circuit as just a variant of the teleportation set-up with a minor difference: here, only one bit of classical information needs to be exchanged. In MBQC language, this operation is known as *"quantum wire"* or the half-teleportation circuit [CLN05]. One might be worried about the Hamadard operation sitting in front but as we will see next this can be dealt with pretty easily by using larger cluster states. Still, at this point, the pessimist might argue that all we have done is perform (close to) an identity gate via local measurements and we are far away from carrying out arbitrary unitary operations. This is however not the case as we will see next.

- **Arbitrary z-rotations**: Let us now consider a slight variant of the quantum wire scenario, where we would like to perform a rotation about the z-axis on our logical qubit. In other words, given a state $|\text{in}\rangle$, we want to transform our final state to $|\text{out}\rangle = R_z(\beta)|\text{in}\rangle =: \exp\Big(-i\frac{\beta}{2}Z\Big)|\text{in}\rangle$ for some rotation angle $\beta \in \mathbb{R}$.

  It is immediately clear that given a two-qubit cluster state with input, if we allow our encoding scheme to include a $R_z(\beta)$ and implement quantum wire as outlined earlier, we get $|\text{out}\rangle = HZ^s|\text{in'}\rangle = HZ^sR_z(\beta)|\text{in}\rangle$ (See Fig. 2.1a). However, the reader should immediately take issue with this suggestion as the whole point of MBQC is that we are not allowed any unitary operations on the fly.[4] Nevertheless, we will use this construction as a conceptual tool to understand how the same unitary operation can be carried out just via a rotation of our measurement axis for the first qubit. First of all, let us note that the CZ gate and $R_z(\beta)$ are diagonal in the Z basis and thereby they commute. Once the $R_z(\beta)$ gate is propagated (See Fig. 2.1c) just next to the measurement device for qubit 1, we can group them together and hope to construct a new measurement device which has the same effect as the grouped object. This is a simple linear algebra problem that we consider in generality below.

  Consider a quantum circuit that involves a unitary operation U followed by a Pauli measurement[5] of the observable A. The projector for such measurement observables can be

[4] Apart from the CZ gates that were used in creating the cluster state in the first place.

[5] In fact, this is true for measurement of any observable with eigenvalues ± 1

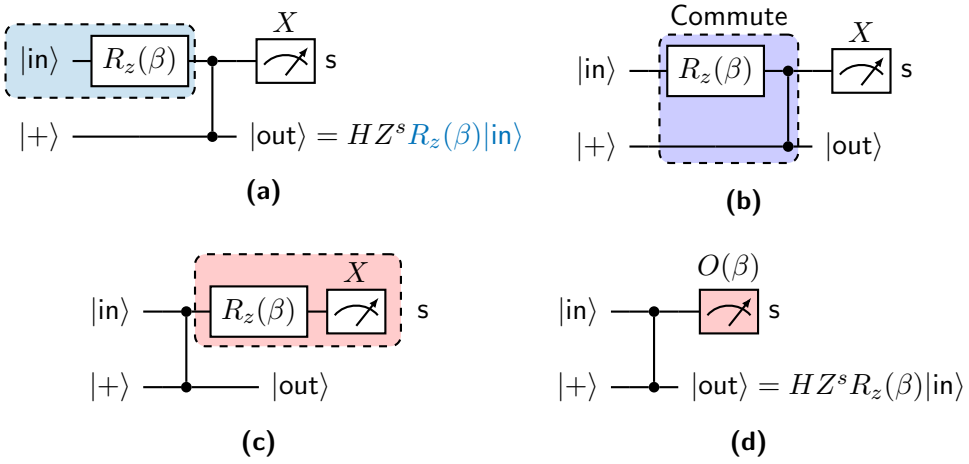

Figure 2.1: Explanation of arbitrary z-rotations

written as $\Pi_A = \frac{\mathbb{I}\pm A}{2}$. Thereby the action of the entire quantum circuit can be expressed and rearranged as

$$\begin{aligned}
\Pi_A\, U &= \frac{\mathbb{I}\pm A}{2}\, U \\
&= (UU^\dagger)\frac{\mathbb{I}\pm A}{2}\, U \quad (\because UU^\dagger = \mathbb{I}) \\
&= U\ (U^\dagger \frac{\mathbb{I}\pm A}{2}\, U) \quad (\because \text{associativity of multiplication}) \\
&= U\ \frac{\mathbb{I}\pm U^\dagger A U}{2} \qquad (\because U^\dagger U = \mathbb{I}) \\
&= U\ \Pi_{A_u}\,,
\end{aligned}$$

wherein the updated measurement observable is given by $\boldsymbol{A_u := U^\dagger A U}$. The reader would have noticed that the unitary U is now sitting *in front* of the projector. However, we are not particularly interested in the post-measurement state of the measured qubit and thus we don't care.

Circling back to our z-rotation unitary, the new measurement observable for the first qubit becomes

$$\begin{aligned}
O(\beta) &= R_z^\dagger(\beta)\ X\ R_z(\beta) \quad (X \text{ for the wire basis}) \\
&= \cos(\beta)X - \sin(\beta)Y\ .
\end{aligned} \tag{2.7}$$

To recap, to perform a rotation of angle β about the z-axis on our logical qubit, we can just implement the quantum wire circuit that was discussed in detail with a small but crucial difference. The last qubit is now measured in the eigenbasis of $O(\beta)$ as defined in Eq. 2.7. Thus just by changing single qubit the measurement axis, we can control what kind of logical operation we want to implement on our logical qubit. This is a

remarkable fact and is only possible because quantum measurement is a dynamical (and active) process.

One may still be worried about the Hadamard transform that always seems to sit at the front but it actually turns out to be quite convenient. By concatenating more and more qubits in construction, not only can we get rid of it but also use it to perform arbitrary rotations about the x-*axis*.

2.1.2 Implementing arbitrary one qubit gates and countering randomness

One of the pinnacles of Leonard Euler's work was the discovery that the ability to perform rotations about any two orthogonal axes is sufficient to execute arbitrary rotations in three dimensions. Till now, we have only shown the ability to implement z-rotations using MBQC. Next, we show how to use a three-qubit cluster state to perform x-rotations. Finally, we put everything together using the Euler decomposition to show that MBQC techniques suffice to carry out any one-qubit unitary gate.

- **Arbitrary x-rotations:** Let us consider a three qubit cluster state with input on which the first qubit is measured in the X basis, whereas the second is measured in the eigenbasis of the observable $O(\beta)$ as defined in Eq. 2.7. Using the techniques developed in the last section it is evident that the final qubit is left in the state

$$\begin{aligned}
|\text{out}\rangle &= [HZ^{s_2}R_z(\beta)] \,.\, [HZ^{s_1}] \,|\text{in}\rangle \\
&= H\ (Z^{s_2}R_z(\beta)H)\ Z^{s_1}\ |\text{in}\rangle && \text{(Associativity of unitaries)} \\
&= X^{s_2}R_x(\beta)Z^{s_1}|\text{in}\rangle && \text{(using the identity } HZH = X\text{)} \\
&= X^{s_2}Z^{s_1}\ R_x((-1)^{s_1}\beta)|\text{in}\rangle. && \text{(using the identity } XZ = -ZX\text{)} \qquad (2.8)
\end{aligned}$$

The final expression looks interesting. In front, we have the measurement dependent Pauli operator $X^{s_2}Z^{s_1}$ which is an example of a "*byproduct operator*" in the MBQC setting. Such operators are dealt with classical side processing at the end of the computation as long as we keep a record of all our measurement outcomes. On the other hand, at first glace, it seems like the x-rotation angle (intended to be β) can either be β or $-\beta$ depending on the measurement outcome of the first measurement which is fundamentally random. But actually, this is the wrong way of looking at things. If the measurement of the first qubit is made *before* the second, we can just choose the second measurement observable to be $O((-1)^{s_1}\beta)$ which results in the final state

$$\begin{aligned}
|\text{out'}\rangle &= X^{s_2}Z^{s_1}\ R_x((-1)^{s_1}\{(-1)^{s_1}\beta\})|\text{in}\rangle \\
&= X^{s_2}Z^{s_1}\ R_x(\beta)|\text{in}\rangle.
\end{aligned}$$

It is in this sense that the measurements in MBQC are adaptive and cannot just be

performed in parallel at the same instance of time.[6]

- **Arbitrary one qubit unitaries:** Now that we are equipped with all the necessary tools, let us show how to use a five qubit [7] cluster state to implement any unitary $U \in U(2)$ on our logical qubit. Taking hints from our earlier construction, we perform the measurements corresponding to the following observables on this five qubit cluster state with input: $O(\varphi_1 = 0) = X,\ O(\varphi_2),\ O(\varphi_3),\ O(\varphi_4)$. The values of $\varphi_2, \varphi_3, \varphi_4$ are left as variables for now and will depend on the specific unitary we want to implement. Thus, the fifth qubit is left in the state

$$\begin{aligned} |\text{out}\rangle &= [HZ^{s_4}R_z(\varphi_4)] \,.\, [HZ^{s_3}R_z(\varphi_3)] \,.\, [HZ^{s_2}R_z(\varphi_2)] \,.\, [HZ^{s_1}] \,|\text{in}\rangle \\ &= X^{s_4}R_x(\varphi_4)Z^{s_3}R_z(\varphi_3)X^{s_2}R_x(\varphi_2)Z^{s_1}|\text{in}\rangle \\ &= X^{s_4+s_2}Z^{s_3+s_1}\ R_x((-1)^{s_3+s_1}\varphi_4)\ R_z((-1)^{s_2}\varphi_3)\ R_x((-1)^{s_1}\varphi_2)\ |\text{in}\rangle \qquad (2.9) \\ &=: B(\mathbf{s})\ R_x((-1)^{s_3+s_1}\varphi_4)\ R_z((-1)^{s_2}\varphi_3)\ R_x((-1)^{s_1}\varphi_2)\ |\text{in}\rangle, \end{aligned}$$

wherein the byproduct operator is denoted as $B(\mathbf{s}) := X^{s_4+s_2}Z^{s_3+s_1}$.

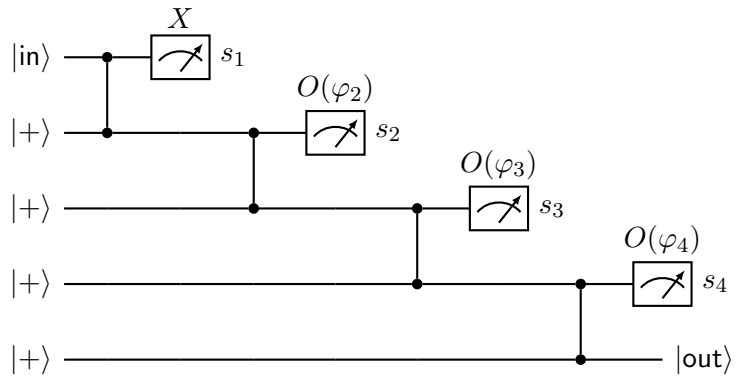

Figure 2.2: Arbitrary one qubit rotations with a 5-qubit cluster state

The resulting unitary transformation (up to $B(\mathbf{s})$) looks tantalisingly close to the Euler decomposition which tells us for any unitary[8] $U \in U(2)$

$$\exists\, \alpha, \beta, \gamma \in \mathbb{R}\ :\ U = R_x(\alpha)R_z(\beta)R_x(\gamma). \qquad (2.10)$$

In fact, they can be made the same if we choose our measurement angles to adaptively

[6] This can be made rigorous. Any MBQC scheme that doesn't require temporal ordering can be just simulated classically as they are equivalent to Clifford unitary operations.

[7] one can get away with four but the construction is "uglier" with Hadamards still sitting around.

[8] up to an irrelevant global phase $e^{i\delta}$.

be,

$$\varphi_2 = (-1)^{s_1}\gamma,$$
$$\varphi_3 = (-1)^{s_2}\beta,$$
$$\varphi_4 = (-1)^{s_3+s_1}\alpha.$$

This completes our proof that one qubit measurements on cluster states are sufficient to simulate *any one qubit* quantum circuit. Before moving on to two-qubit gates for which a 2-dimensional cluster state is necessary, let us note that measurements outside the Pauli basis are indispensable for getting us away from the arena of classically simulatable circuits. Without them, we are dealing with stabilizer circuits and thereby under the purview of the celebrated Gottesman-Knill Theorem [Got98].

2.1.3 Universality of MBQC

While the 1D cluster state is going to be used as the canonical example for a computational resource in the entire thesis, it is not a universal one. In fact, it is impossible for any 1D MBQC resource state to be able to simulate all quantum computations. The reason is rather intuitive. We can only encode one qubit in one of the edge modes of a 1D state. Thus it cannot be scaled up to perform general multi-qubit operations. This is a general feature of MBQC schemes. For any d-dimensional resource state, we can only hope to simulate quantum circuits in $(d-1)$ spatial dimensions as the remaining dimension is used up to simulate the temporal dimension in the circuit model. It turns out the two-dimensional cluster state can indeed be used to perform arbitrary quantum circuits. Although it will not be relevant for the scope of this thesis, for completeness' sake, we sketch a proof of this universality below.

Let us consider a cluster state supported on a 2D square grid of 4 rows and 4 columns. Our primary goal is to use the nearest-neighbour Ising interaction inherent in the physical qubit interactions to perform a Controlled-Z operation on the logical level. If we succeed in this endeavour, we will have proved that MBQC on 2D cluster states can simulate universal quantum computation since the CZ gate along with arbitrary single-qubit gates forms a universal gate set.

To simulate a CZ gate on this grid, we first perform a bunch of Z measurements on some of the qubits. Such measurements act as scissors removing the qubit being measured along with all the edges (representing interactions) associated with it. This is easy to understand if one is familiar with the stabilizer formalism but that's beyond the scope of this thesis. Let us just say that this is reasonable because all the interactions and the measurement observable under consideration are diagonal in the Z basis. As one can anticipate, such measurements are used to carve out the desired pattern that can be used for specific computations. The final step is to perform quantum wire (via measurements in the X basis) on the two horizontal and one vertical branches of our pattern. The resulting operation on our logical (control and target) qubits is

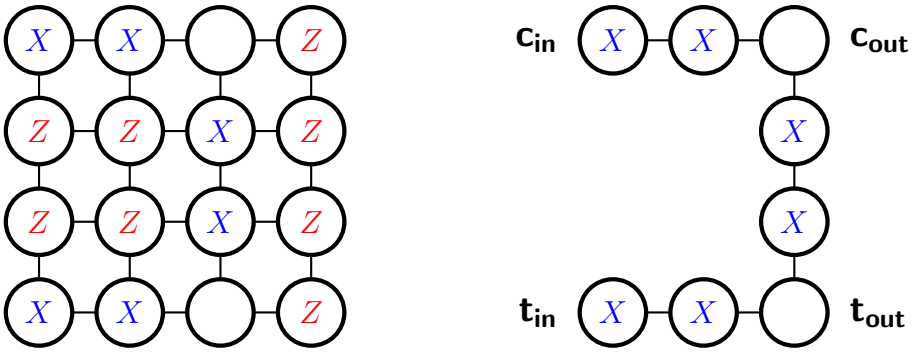

(a) Full measurement pattern. **(b)** Effective pattern after Z measurements.

Figure 2.3: Simulation of the entangling CZ gate using a cluster state supported on a 4×4 square grid. The upper and lower most qubits on the left denote control and target logical qubits that are given as input. The corresponding output qubits are shown on the right. Note that two consecutive X measurements on a line perform quantum wire up to byproduct operators.

a CZ gate (See Fig. 2.3). In this whole discussion, we have ignored the issue of byproduct operators which are always part of MBQC but let us assure the reader that they can be handled simply by classical post-processing.

2.2 Quantum phases and symmetry

Having reviewed the basic model of computation under consideration, we shift our attention to the required condensed matter background for this thesis. In this section, we review the basic idea of (symmetry-protected) quantum phases which serve as a classification tool[9] for MBQC resource states in 1D systems.

The study of distinct phases of matter and transitions amongst those phases is one of the central themes in both statistical mechanics and condensed matter physics. The classical definition of a phase, or to be more precise, a phase transition is associated with some non-analytical behaviour of the free energy of a system

$$F(\beta, \boldsymbol{\lambda}) = -\frac{\log\left(\mathrm{Tr}\ e^{-\beta H(\boldsymbol{\lambda})}\right)}{\beta}\ ,$$

where β is the inverse temperature, $\boldsymbol{\lambda}$ is a vector of parameters containing the details of our model and H is the Hamiltonian of our system. If we are interested in a "quantum" phase transition, the system needs to be cooled down to zero temperature. That is to say, to remove the dominant thermal fluctuations that might wash out the intrinsic quantum fluctuations, a quantum phase is defined in the zero temperature ($\beta \to \infty$) limit. In this regime, the free energy reduces to merely the ground state energy. Thus, *quantum phases are characterized by the ground state and the gap above it.*

The standard framework of phase transitions [Lan36], taught in a graduate statistical me-

[9] We will explore this connection in all its gory detail in Chapter 3.

chanics course, is due to Lev Landau. In this paradigm, the simplest of phase transitions can be explained by *spontaneous symmetry breaking*. For such phase transitions, the ground state has less symmetry than the original Hamiltonian. Hence, such phase transitions can be fully characterized by understanding the original symmetry group of the Hamiltonian and the broken symmetry subgroup of the ground state. A concrete example is that of the formation of Cooper pairs in BCS superconductivity which breaks the original $U(1)$ symmetry group to a discrete $\mathbb{Z}_2$ subgroup. All this analysis gives way to the primary object of phenomenological interest: the so-called *order parameter* η. Such a parameter can be used to distinguish between, for example, the disordered symmetric phase ($\eta = 0$) and the ordered symmetry-broken phase ($\eta \neq 0$). This simple theory was so successful that for a long time physicists believed that all possible phases in materials and thus all possible phase transitions can be described by Landau's symmetry-breaking argument.

However, starting from the late 1980s, physical phenomena were predicted and discovered in which different phases inherited the same symmetry and thus were beyond the Landau-Ginzburg paradigm. The fractional quantum hall effect [TSG82], the Haldane phase [Hal83] and the AKLT model [AKLT87] are some prominent examples of such phenomenon and each of these discoveries have led to numerous Nobel prizes. To deal with them under a unifying framework, Wen [Wen95] introduced the notion of topological order.

Definition 2(a) (Topological order). *Two gapped* [10] *quantum states* $|\Psi_0\rangle$ *and* $|\Psi_1\rangle$ *are said to be in the same phase if their parent Hamiltonians (of which they are ground states of)* H_0 *and* H_1 *can be smoothly connected through a continuous family of gapped Hamiltonians. A quantum state not residing in the trivial phase is said to possess topological order.*

An equivalent definition of phases comes from thinking about quantum circuits.

Definition 2(b) (Topological order). *Two gapped quantum states are said to be in the same phase if there exists some local quantum circuit (local implying that the depth of the circuit doesn't scale with system size) connecting them.*

The reader would have noticed that the above definition doesn't make any reference to the possible symmetries associated with the problem and such type of ordering of phases is known as *intrinsic* topological order. A state with trivial intrinsic topological order can be connected to the product state via a local quantum circuit. Such states are known as short-range entangled (SRE) states or finitely correlated states (FCS). Let us point out that all the states that we will be considering in this thesis are in fact SRE states. Thus, all of them have the same intrinsic (trivial) topological order. However, the phase diagram splits when one takes into account the symmetries of the problem and requires the quantum circuit to respect such symmetries. To this end, we define the concept of symmetry-protected topological (SPT) order.

[10] To be rigorous, this means that even in the thermodynamic limit there exists an energy gap between the ground state(s) and the first excitations.

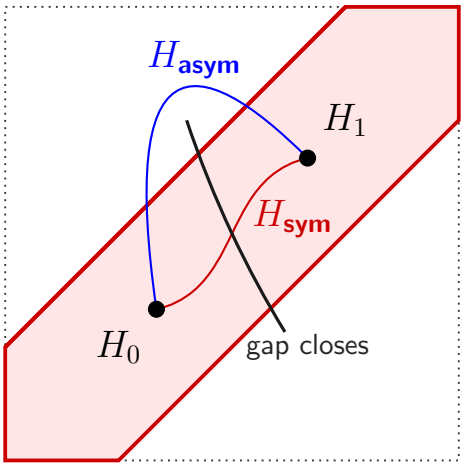

Figure 2.4: Illustration of SPT order: Two states $|\Psi_0\rangle$ and $|\Psi_1\rangle$ are said to be in distinct SPT phases if their parent Hamiltonians H_0 and H_1 cannot be smoothly deformed into one another via any symmetry respecting path without closing the gap in the thermodynamic limit. Note that if the path contains symmetry-breaking terms, the gap doesn't need to close, elucidating why such states are not genuinely topologically ordered. It is the imposing of the symmetry that protects the order in the phase diagram.

Definition 3 (SPT order). *A quantum state belongs to a non-trivial SPT phase if and only if it cannot be transformed to the product state by a local quantum circuit that commutes with the symmetry of the system.*

Such states are *symmetry-protected* as it is the symmetry respecting condition that ensures that they cannot be connected to the product state. At this point, it should be clear that SPT phases are not truly intrinsic topological phases as asymmetric local unitaries can connect states belonging to different SPT phases. Hence, many condensed matter physicists regard symmetry-protected topological order as a misnomer and use the same acronym SPT to mean symmetry-protected *trivial* order instead [hgw].

As pointed out earlier, states belonging to different phases of SPT ordering have different computational power as resource states of MBQC. The computational power has been proven to be uniform in the phases for 1D [RWP$^+$17, SWP$^+$17] and this fact has been conjectured to be true in higher dimensions. We will see an outline of these results in the next chapter but before going there let us establish some graphical notation that has been of central importance in the whole discussion of computation in SPT phases. It must be emphasized that remarkably for the results of this thesis, they *will not* play such pivotal roles as the fundamental objects of our theory. Nonetheless, this graphical language will allow us to introduce a simulation algorithm (DMRG) that has been extensively used to obtain the numerical results of the thesis.

2.3 Elements of technique: Tensor network methods

From the discussion in the previous section, we have seen that ground state wavefunctions play a central role in the classification of gapped phases of matter. However, due to the well-known problem of the exponential complexity involved in describing quantum states, one might question the feasibility of such a classification. To spell it out explicitly, for a N-body quantum system, one needs to keep track of exponentially many coefficients[11] to even describe the ground state, without any efficient faithful description. One such efficient description is the stabilizer formalism which we saw glimpses of while defining the family of graph states. However, these families of states turn out to be too restrictive and we need a different representation that is naturally suited to describe ground states of local gapped Hamiltonians. This is the graphical language of tensor networks which is a well-established tool for analytical and numerical investigations in many-body quantum systems.

Any N-body quantum state with local dimension d ($= 2$ for a spin-$1/2$ system) can be expanded in a specific local basis as

$$|\Psi\rangle = \sum_{i_1,i_2,\ldots,i_N=1}^{d} c_{i_1,i_2,\ldots,i_N} |i_1, i_2, \ldots, i_N\rangle. \tag{2.11}$$

One can always represent the (complex) amplitudes in the superposition above graphically by storing them in a tensor. In this language, a tensor is just a generalization of vectors and matrices. Thus, a rank-r tensor of dimension $d_1 \times d_2 \times \ldots \times d_r$ is just a tuple in $\mathbb{C}^{d_1 \times d_2 \times \ldots \times d_r}$. The central notion of tensor networks is to decompose this huge tensor in terms of a network of smaller tensors – thereby reducing the number of effective parameters required to describe the quantum state.

2.3.1 Matrix product states (MPS)

The canonical example of such a tensor network decomposition is the ansatz of matrix product state (MPS) where the coefficient tensor can be written as

$$c_{i_1,i_2,\ldots,i_N} = \sum_{\alpha_1,\alpha_2,\ldots,\alpha_N=1}^{D} A^{i_1}_{\alpha_1,\alpha_2} A^{i_2}_{\alpha_2,\alpha_3} \ldots A^{i_N}_{\alpha_N,\alpha_1}. \tag{2.12}$$

Herein, the key object of interest is the three index [12] tensor A with components $A^i_{\alpha,\beta}$. The index i, which runs over the dimension of the local Hilbert space ($= \mathbb{C}^2$ for a qubit), is known as the *physical index*. The indices α, β which are summed over are known as the *virtual indices*. The maximum value of these virtual indices (D) captures the entanglement structure in the quantum state and is known as the *bond dimension* of the tensor network. An alternative way

[11] $d^N - 2$ to be exact due to the normalization and irrelevancy of a global phase. However, for large N, this is a distinction without a difference

[12] For those familiar with the standard notion of tensors from general relativity, note that tensor indices here are *not* endowed with any fancy co- or contra-variant properties.

of expressing the MPS is to substitute the matrices $A^i = \sum_{\alpha,\beta=1}^{D} A^i_{\alpha,\beta} |\alpha\rangle\langle\beta|$, that act on the virtual space of the MPS, in the above Eq. 2.12 to arrive at

$$c_{i_1,i_2,\ldots,i_N} = \mathrm{Tr}[A^{i_1} A^{i_2} \ldots A^{i_N}]. \tag{2.13}$$

This form does justice to the name "matrix product state" as we see that for fixed value(s) of $i_1, i_2, \ldots, i_N$, the probability amplitude(s) can be constructed from the *product of local matrices*. Of course, for product states, this can be done with just complex numbers but for general entangled states, we require matrices instead. Please note that we have suppressed the site label for these matrices in the expression above and have also assumed periodic boundary conditions as is evident from the trace operation.
For open boundary conditions, our general quantum state can be written as

$$|\Psi\rangle = \sum_{i_1,\ldots,i_N} \langle L|A^{i_1} A^{i_2} \ldots A^{i_N}|R\rangle \, |i_1 \ldots i_N\rangle, \tag{2.14}$$

instead. Here the boundary conditions are specified by the left and right boundary vectors $|L\rangle$ and $|R\rangle$ living in the virtual space.

Given an arbitrary tensor (that represents a quantum state), one can arrive at the MPS description by performing a succession of Schmidt decompositions across neighboring sites, where the Schmidt rank becomes the bond dimension of the link between the relevant sites. This construction is exact and applies to arbitrary quantum states. For generic quantum states, the bond dimension D grows exponentially ($\approx d^{N/2}$) with the system size. At this point, it is not clear that we have done anything useful. We still have all the d^N coefficients in what looks like a more complicated form. However, it is for the ground states of gapped Hamiltonians following some area law (see Appendix A) that the MPS description becomes efficient as the bond dimension D grows polynomially with N. The reason behind this effective but efficient description is fascinating: for these physically relevant systems, the entanglement between any two subregions is mostly concentrated in the boundary between them. This in turns implies that the Schmidt coefficients decay quickly enough allowing us to throw away all but polynomially many of them. This truncation of the Schmidt decomposition allows us to represent our quantum state with only dD^2N coefficients as opposed to the d^N ones we started with.

All of this becomes self-evident in the graphical language. Here, we depict our MPS tensors A as a three-legged object

$$A^i_{\alpha,\beta} = \alpha \text{—} \overset{i}{\bullet} \text{—} \beta \,. \tag{2.15}$$

The horizontal lines represent the virtual indices while the vertical one represents the physical index. Next, we place these tensors in a line with the rule that connected indices are summed

over. This results in a graphical representation of the quantum state as

$$c_{i_1,i_2,\ldots,i_N} =$$ 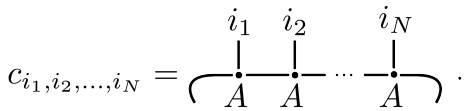 . (2.16)

Note that the longest link between the two ends represents the specific choice of boundary conditions and in general we have *not* assumed that the tensor components are the same at different sites[13]. This graphical notation is compact and allows us to calculate expectation values of local operators (like two-body correlators) efficiently.

The 1D cluster state as an MPS

To see an example of the MPS representation, let us consider the 1D cluster state. The circuit representation of the cluster state along with Eq 2.2 lets us expand the cluster state in the computational basis as:

$$|C\rangle_{\mathcal{L}_1} = \frac{1}{2^{N/2}} \sum_{i_1,i_2,\ldots,i_N} (-1)^{\#\text{ of neighbouring 1's}} |i_1, i_2, \ldots, i_N\rangle. \tag{2.17}$$

An obvious MPS representation[14] of this state is obtained by defining the components of a tensor C as the matrices,

$$C^0 = |0\rangle\langle +|, \qquad C^1 = |1\rangle\langle -|. \tag{2.18}$$

This definition is set up in a way that the trace evaluates to a sequence of inner products which are all 1 (ignoring normalization) except when the two neighbors are in the $|1\rangle$ state in which case we get an inner product of -1 (as $\langle -|1\rangle \cong -1$). Thus, the cluster state has a particularly nice representation as an MPS with a bond dimension of exactly $D = 2$ (size of the matrices above).

Although these expressions are simple enough, while using the cluster state for MBQC, it is quite useful to represent them in the wire (i.e. the Pauli-X) basis. To this end, we introduce the notation $A[b] := \sum_i \langle b|i\rangle\, A^i$, representing the contraction of the physical leg of the tensor with the basis state $|b\rangle$. Thus, the cluster state tensors can be written in the X basis as

$$\begin{aligned} C[+] &:= \frac{1}{\sqrt{2}}(C^0 + C^1) = H, \\ C[-] &:= \frac{1}{\sqrt{2}}(C^0 - C^1) = HZ\,. \end{aligned} \tag{2.19}$$

We will have more to say as to how the MPS picture is useful to argue in the presence of symmetries but let us postpone this discussion to the next chapter.

[13] Although for translationally invariant systems they will turn out to be the same.

[14] Note that this representation is not unique. This a general feature of MPS: there is always a gauge degree of freedom in choosing the tensors.

Injective MPS

In the discussion of SPT phases, all the MPS tensors considered are assumed to possess a property called *injectivity*. This condition is equivalent to numerous salient physical properties of our state and it serves as an essential tool in proving non-trivial theorems due to its connection to quantum channels.

To physically motivate this assumption, let us note that, to *every MPS*, we can associate a gapped, local *parent* Hamiltonian for which the MPS is a (possibly degenerate) ground state. The assumption of injectivity is equivalent to saying that the MPS is indeed the *unique* ground state of its parent Hamiltonian [PGVWC07]. From an experimental point of view, this uniqueness is essential if we hope to prepare this state by cooling down a physical system subject to the parent Hamiltonian.

To formally define injectivity, it is useful to first define the quantum channel[15]

$$\mathcal{E}_A(\cdot) = \sum_i A^i(\cdot)A^{i\dagger}. \tag{2.20}$$

Such a channel is naturally associated with every MPS A and encodes many physically relevant properties of the ground state that is being approximated. The largest eigenvalue of this mapping can always be normalized to 1. Since the channel is completely positive, it is guaranteed to have a positive fixed point ρ_{fix} [PGVWC07]. Arguably, the simplest definition of injectivity comes in terms of other eigenvalues of $\mathcal{E}_A$.

Definition 4 (Injectivity of an MPS). *An MPS A is said to be injective if the channel $\mathcal{E}_A$ has only one eigenvalue of modulus 1.*

Note that this definition immediately implies that, for such injective MPS, the fixed point ρ_{fix} is unique. Furthermore, although we have chosen this simple condition as our definition of injectivity, in [SPGWC10] the authors showed that there are a number of equivalent conditions on both $\mathcal{E}_A$ and the matrices A^i so that the MPS is injective.

Theorem 1 (Equivalent conditions of injectivity). *Given an MPS described by the matrices A^i, the following conditions are interchangeable.*

(1) The MPS is injective.

(2) The map defined by

$$\Gamma_L(\rho) = \sum_{i_1,..,i_L} \mathrm{Tr}\left(\rho\, A^{i_1}\dots A^{i_L}\right)|i_1\dots i_L\rangle$$

is injective for some finite L.

(3) The set of product matrices $\{A^{i_1}\cdot A^{i_2}\cdots A^{i_L}\}$ spans the whole space of $D\times D$ matrices for the same L as in condition (2).

[15] also known as the transfer matrix of the MPS.

(4) There exists some $l < L$ such that, for every density operator ρ, $\mathcal{E}_A^l(\rho)$ has full rank.

Although it may seem a bit excessive, all of these mathematically equivalent conditions help us greatly in understanding different phenomenological aspects of the state under consideration. Perhaps the most immediate consequence is that an injective MPS has a finite correlation length ζ. A straightforward calculation (See e.g. [ZCZW15]) shows that the correlation length of an MPS (defined in terms the channel $\mathcal{E}$ in Eq. 2.20) is given by $\zeta = -1/\ln|\lambda_1|$ where λ_1 is the second largest eigenvalue of $\mathcal{E}_A$. This is finite if and only if the MPS is injective.

On the other hand, as a consequence of condition (2), injectivity is crucial for computational readout of logical information that can potentially be encoded in the state [Ste17]. The map Γ_L can be interpreted as a map from the open boundary conditions of a chain of length L to the resulting quantum state (merely set $\rho = |R\rangle\langle L|$ to reconstruct Eq. 2.14). If this map is injective, a different choice of boundary conditions gives rise to different readout states. This is a necessary condition for encoding our logical information in the boundary vector $|L\rangle$. Otherwise, if different states $|L\rangle$ led to the same final physical state, we could not reliably deduce the information that has been encoded.

2.3.2 Matrix product operators (MPO)

A matrix product operator (MPO) is a generalisation of a matrix product state to the operator space. Formally speaking, an MPO can be expressed in a local basis as

$$O = \sum_{\substack{i_1,\ldots,i_N \\ j_1,\ldots,j_N}} \mathrm{Tr}(M^{i_1,j_1} M^{i_2,j_2} \ldots M^{i_N,j_N}) |i_1\rangle\langle j_1| \otimes |i_2\rangle\langle j_2| \ldots |i_N\rangle\langle j_N|. \tag{2.21}$$

Perhaps more illuminatingly, in graphical notation, O can be expressed in terms of a tensor with 4 legs. Two of these legs are external and un-contracted (i.e. an operator acting on physical dimension) while the other two are internal, contracted with neighboring tensors

$O =$ 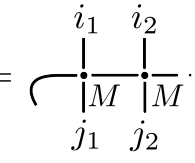

. (2.22)

Thus, an MPO can be understood as an MPS with two physical indices per site corresponding to the bra and the ket. MPOs with proper bond dimensions and boundary conditions can be used to represent density matrices, finite depth quantum circuits, and local Hamiltonians. For example, the N-body transverse field Ising Hamiltonian on a chain

$$H = -J \sum X_j X_{j+1} - h \sum_j Z_j, \tag{2.23}$$

can be represented as $H \equiv v_L M^N v_R^\dagger$, with the operator-valued matrix M and boundary vectors

v_L and v_R as defined below

$$M = \begin{pmatrix} \mathbb{I} & 0 & 0 \\ X & 0 & 0 \\ -hZ & -JX & \mathbb{I} \end{pmatrix}, \; v_L = \begin{pmatrix} 0 & 0 & 1 \end{pmatrix} \text{ and } v_R = \begin{pmatrix} 1 & 0 & 0 \end{pmatrix}. \tag{2.24}$$

2.3.3 Tensor network algorithms

Although the MPS language is very useful for some analytic arguments, their undisputed power comes from the efficient classical simulation algorithms they give birth to. These simulation algorithms allow us to approximate ground states of gapped local Hamiltonians by minimizing the so-called Reyleigh quotient of the Hamiltonian. As we know the exact solution is well approximated by an MPS, it suffices to restrict ourselves to the domain $\mathcal{D}$ of bounded bond dimension. Such an iterative algorithm yields an approximate solution ($|\Psi_{\text{opt}}\rangle$) given by

$$|\Psi_{\text{opt}}\rangle = \arg\min_{\Psi \in \mathcal{D}} \frac{\langle \Psi | H | \Psi \rangle}{\langle \Psi | \Psi \rangle} \tag{2.25}$$

The basic idea behind the well-known DMRG algorithm [Whi92, Sch11] is to start from some initial[16] MPS state - then variationally explore this domain, minimizing energy as we go. More specifically, the DMRG algorithm works by optimizing two neighboring MPS tensors simultaneously, combining them into a single tensor to be optimized. This is done using some interactive exact eigensolver algorithm such as Lanczos or Davidson. Before proceeding, the single tensor is factorized using the Schmidt decomposition in order to restore the MPS structure. During this decomposition, the bond dimension of the MPS can be adapted to meet the required accuracy of the solution. This adaptation is optimal in the sense that it preserves the distance between the network after the optimization step and the network with the restored MPS form.

A different class of tensor network algorithms, known as time-evolving block decimation (TEBD), evolve the initial MPS by acting with a quantum circuit (which can be represented as an MPO) at each time step. The resulting state is still represented by an MPS but with a blown-up bond dimension. To restrict the bond dimension from exploding over time, the crucial step is to truncate the MPS back to its original bond dimension by throwing away the smaller singular values. These types of algorithms are primarily used to capture time evolution but of course one can use imaginary time evolution to compute ground states.

The integration of these two classes of algorithms gives us a powerful armor of tools that can be used to analyze salient properties of many-body systems. Surprisingly, these tools even work well in the thermodynamic limit enabling detection of non-analytical behaviour in phase transitions. Interpreting the domain of search $\mathcal{D}$ as a non-linear manifold, one can also formulate

[16] Most of the time, it suffices to start with a random MPS with high bond-dimension although an educated guess helps in very quick convergence.

tangent-space methods to access other low-energy eigenstates apart from the ground state. Such an algorithm allows us to compute defining properties of our system of interest like ground state degeneracy and the energy gap above it. These methods have been used to obtain some numerical results of this thesis, e.g. Fig. 4.1.

Chapter 3

Computational Phases of Quantum Matter

In this chapter, we review the incredible joint progress that has been made in the last decade on the classification of SPT phases using tensor network methods and their usage as resource states for MBQC. To this end, the analysis will be fairly technical with particular emphasis on (projective) representations and group cohomology. While it is true that these methods will not play conspicuous roles in the results of the thesis, it is instructive to go through these arguments to understand where the difficulties lie with analyzing finite systems.

3.1 Classification of SPT phases

As was alluded to in the last chapter, SPT phases are said to be trivial in the bulk as, in the absence of a boundary, there is a unique gapped ground state with no bulk excitations. Thus, the non-trivial properties of SPT order are manifestly apparent on the boundary. In general, if a boundary is introduced in a system with on-site symmetry, it becomes necessary to decorate the symmetry with some non-trivial action localized near the boundary so that the ground state is still left invariant under the symmetry action. This results in the essence of SPT order: while the bulk symmetry action can be decomposed into a tensor product of on-site linear representations, the boundary action cannot be. This "boundary anomaly" makes sure that SPT ordered Hamiltonians *with boundaries cannot have a unique gapped ground state.*

In the following paragraphs, we discuss how to rigorously characterize these boundary anomalies first in terms of group cohomology and then tensor network techniques.

3.1.1 Group cohomology

SPT phases can be partially classified using the language of group cohomology [CGLW13]. In this formulation, one considers the cohomology classes $[\omega]$ which are elements of the k-th cohomology groups $H^k(G, U(1))$. Given a symmetry group G, the different bosonic SPT phase

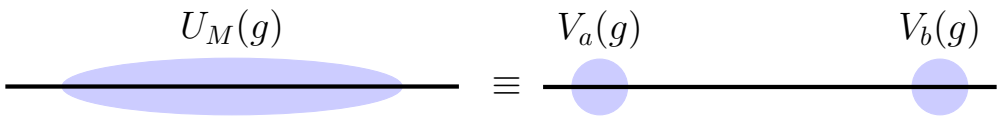

Figure 3.1: *Domain wall operators* in 1D systems: Effective edge representation of the symmetry that only acts at the boundary. In SPT phases, such operators $V(g)$ only need to be projective representations and are described by the language of group cohomology.

in d dimensions are labelled[1] by the elements of $H^{d+1}(G, U(1))$.

Below, we follow the discussion in [EN14], where the authors showed how to understand the cohomology class in terms of the anomalous action of the symmetry at the boundary and described an explicit procedure to extract it.

To start with, we introduce a boundary ∂M for our system by choosing some subregion M and removing all Hamiltonian terms that are not completely contained in M. This generically leads to new eigenstates (a.k.a. edge excitations) appearing below the bulk energy gap. The bulk symmetry $U_M(g) = \bigotimes_{i\in M} u_i(g)$ can be projected onto the low lying subspace to obtain an effective presentation of the symmetry $V_{\partial M}(g)$ which acts exclusively along the boundary. Hence, while $U_M(g)$ is a product of on-site linear representations, $V_{\partial M}(g)$ is not. We call such $V_{\partial M}(g)$ a *domain wall operator*. Next, we explain this procedure in detail for 1D systems. Extensions to higher dimensions look alike.

In 1D systems, M corresponds to a line segment while ∂M denotes the two endpoints (a and b) of the line. Assuming that the system size is significantly larger than the correlation length we can decompose $V_{\partial M}(g) = V_a(g) \otimes V_b(g)$ where the non-trivial action of $V_a(g)$ and $V_b(g)$ are localised near the points a and b respectively. As $V_{\partial M}(g)$ acts the same way as $U_M(g)$, it should be a linear representation. However, $V_a(g)$ only needs to be representation up to a phase (i.e. *projective representations*) as long as $V_b(g)$ carries the opposite phase factor. In other words, if we have the relation

$$V_a(g)\, V_a(h) = \omega(g,h)\, V_a(gh) \quad \text{for some phase factor } \omega(g,h)\ , \tag{3.1}$$

then $V_{\partial M}(g)$ is still a representation provided that $V_b(g)\, V_b(h) = \omega^{-1}(g,h)\, V_b(gh)$.

From the simple requirement of associativity of the projective representation, it is a straightforward to show that the phase factors would follow the so called *cocycle condition*

$$\omega(g,h)\,\omega(gh,m) = \omega(h,m)\,\omega(g,hm). \tag{3.2}$$

In mathematics, functions that take two elements of a group and return a phase factor $\in U(1)$ satisfying the above equation are known as *2-cocycles*. We are always allowed to rephase $V_a(g) \mapsto \Omega(g)V_a(g)$ as long as $V_b(g)$ is assigned to opposite phase factor. Hence, our

[1] In 4D or higher dimensions, there exist SPT phases that are beyond the group cohomology classification and require even more sophisticated mathematical structures like cobordisms [KTTW15].

cocycle is only defined up to the equivalence relation

$$\omega(g,h) \sim \Omega(g)\,\Omega(h)\,\Omega^{-1}(g,h)\,\omega(g,h). \tag{3.3}$$

The equivalence classes of 2-cocycles as defined in Eq. 3.2 modulo the *coboundary transformation* of Eq. 3.3 are known as *2-cohomology classes*. Under point-wise multiplication, the 2-cohomology classes $[\omega]$ form an abelian group called the *second cohomology group*, denoted by $H^2(G, U(1))$.

The cohomology group classifies inequivalent projective representations, corresponding to the different ways the symmetry can possibly act on the boundary of the system. As the different classes $[\omega]$ form a *discrete* group, one can handwavingly argue that it is impossible to smoothly interpolate between any two classes. This can be made rigorous by proving that a smooth change in a state can only modify the cocycle it is in, by a coboundary transformation. Such a transformation doesn't change the cohomology class implying that two systems with different cohomology classes must be in separate SPT phases.

The existence of robust zero-energy edge states in 1D SPT phases can be understood using the above result. If the low-energy subspace corresponding to boundary excitations has to transform as a non-trivial projective representation, it must have a degeneracy larger than one, since a 1D system cannot transform projectively. Generically speaking, the size of the edge mode in an SPT phase, labeled by a group G and a cohomology class $[\omega]$, is equal to the minimum dimension of an irreducible representation of G belonging to the class $[\omega]$. In the following section, we will see an example where this dimension is explicitly calculated.

3.1.2 SPT order in 1D cluster state

The above discussion about the cohomological classification of SPT phases was fairly abstract. To better understand the core of the issue, let us consider our old friend: the 1D cluster state, and see how it has non-trivial SPT order using cohomological tools.

Taking a cue from our definition of the 2D cluster state as defined in Eq. 2.1, the 1D cluster state on a periodic chain of N qubits can be defined via a local quantum circuit

$$|C\rangle = \left[\prod_{i=1}^{N} CZ_{i,i+1}\right] \; |++\cdots+\rangle, \tag{3.4}$$

where the $(N+1)$th qubit refers to the first qubit due to periodic boundary conditions. Equivalently, using the stabilizer formalism introduced earlier, one can define $|C\rangle$ as the unique ground state of the local Hamiltonian

$$H_C = -\sum_{i=1}^{N} Z_{i-1}X_iZ_{i+1}. \tag{3.5}$$

It is relatively straightforward to see that for even rings, the above Hamiltonian commutes with

a $\mathbb{Z}_2 \otimes \mathbb{Z}_2$ symmetry group generated by the operators

$$X_{\text{odd}} = \prod_{i=1}^{N/2} X_{2i-1} \quad \text{and} \quad X_{\text{even}} = \prod_{i=1}^{N/2} X_{2i}. \tag{3.6}$$

As the *unique* ground state, the cluster state $|C\rangle$ is invariant under this symmetry. Usually, the elements of symmetry ground are labelled by bit pairs (g_1, g_2) for $g_i \in \{0, 1\}$ and the symmetry is represented by $U(g_1, g_2) = X_{\text{even}}^{g_1} X_{\text{odd}}^{g_2}$. It is worth pointing out that although the entire local quantum circuit[2] commutes with the symmetries, the individual CZ gates *do not*. The reason behind this is the existence of non-trivial SPT order which we demonstrate below using cohomological arguments.

Let us consider an even number of sites $L < N$ as the subsystem M we are interested in. The truncated Hamiltonian, completely contained in M, is given by

$$H_{C,M} = -\sum_{i=2}^{L-1} Z_{i-1} X_i Z_{i+1}. \tag{3.7}$$

As the boundary stabilisers centered at site 1 and L have been removed, the ground space of $H_{C,M}$ becomes four-fold degenerate. To ascertain the action of the boundary on this degenerate subspace, we follow the methods outlined in [LG12, Yos16]. First, the ground state is characterised by the an effective algebra of Pauli operators $\bar{X}_1, \bar{X}_L, \bar{Z}_1, \bar{Z}_L$ which commute with the bulk Hamiltonian $H_{C,M}$ and thus preserve the ground space. If the truncated quantum circuit is defined as $U_{CZ,M} = \prod_{i=1}^{L-1} CZ_{i,i+1}$, its action on the boundary Pauli operators is determined by the relations

$$\begin{aligned} \bar{X}_1 &= U_{CZ,M} X_1 U_{CZ,M}^\dagger = X_1 Z_2, & \bar{Z}_1 &= U_{CZ,M} Z_1 U_{CZ,M}^\dagger = Z_1, \\ \bar{X}_L &= U_{CZ,M} X_L U_{CZ,M}^\dagger = X_L Z_{L-1}, & \bar{Z}_N &= U_{CZ,M} Z_N U_{CZ,M}^\dagger = Z_N. \end{aligned} \tag{3.8}$$

Using these effective Pauli operators, we can determine the action of the symmetry on the degenerate boundary space. Defining $U_M(g_1, g_2) = \prod_{i=1}^{L/2} X_{2i}^{g_1} X_{2i-1}^{g_2}$, we realise that the left boundary transforms as

$$U_M(g_1, g_2) \bar{X}_1 U_M^\dagger(g_1, g_2) = (-1)^{g_1} \bar{X}_1, \quad U_M(g_1, g_2) \bar{Z}_1 U_M^\dagger(g_1, g_2) = (-1)^{g_2} \bar{Z}_1. \tag{3.9}$$

The above relations imply that $U_M(g_1, g_2) \sim \bar{Z}^{g_1} \bar{X}^{g_2}$ at the left boundary. So we can write the anomalous action of the symmetry at the left edge: $V_a(g_1, g_2) = \bar{Z}^{g_1} \bar{X}^{g_2}$. Similar analysis for the right edge reveals $V_b(g_1, g_2) = \bar{X}^{g_1} \bar{Z}^{g_2}$. As far as the projective representation is concerned,

[2] that connects the cluster state to the product state.

we can just focus on the left edge to obtain the 2-cocyle,

$$\begin{aligned}\omega(g_1, g_2; h_1, h_2) &:= V_a(g_1, g_2)V_a(h_1, h_2)V_a^{-1}(g_1 \oplus h_1, g_2 \oplus h_2) \\ &= (-1)^{g_2 h_1}.\end{aligned} \tag{3.10}$$

where $\oplus$ denotes mod-2 addition. This belongs to the non-trivial cohomology class as it cannot be expressed in the form $\omega(g_1, g_2; h_1, h_2) = \Omega(g_1, g_2)\,\Omega(h_1, h_2)\,\Omega(g_1 \oplus h_1, g_2 \oplus h_2)$. To explicitly check this, consider the commutation relation:

$$\begin{aligned}\frac{\omega(g_1, g_2; h_1, h_2)}{\omega(h_1, h_2; g_1, g_2)} &= V_a(g_1, g_2)V_a(h_1, h_2)V_a^{-1}(g_1, g_2)V_a^{-1}(h_1, h_2) \\ &= (-1)^{g_2 h_1 \oplus g_1 h_2} \neq 1(\text{for trivial order}).\end{aligned} \tag{3.11}$$

Thus, we have rigorously proved that the 1D cluster state has non-trivial SPT order, as evidenced by the anti-commutation of the effective edge symmetry generators (U_M). Additionally, we note that there is no degeneracy respecting symmetric boundary Hamiltonian term that can be added in terms of the operators $\bar{X}_1, \bar{Z}_1$ as such a term have to commute with both $\bar{X}$, $\bar{Z}$ and must therefore be proportional to the identity matrix. Thus, *the boundary degeneracy cannot be lifted without breaking the bulk symmetry*.

3.2 Symmetries in tensor networks

In the last chapter, we saw how tensor network methods can be used to capture essential properties of gapped phases via numerical simulation algorithms. It turns out, the formalism of tensor networks also provides a uniquely clear vantage point for analyzing their symmetries and topological properties. It is indeed striking that even inherently non-local properties of a state (for example topological degeneracy or string order) can be understood locally just via the symmetries of the local tensors. Using such methods, we can make the procedure to extract cocycles, needed for classifying SPT order, more intuitive and rigorous compared to the process outlined in the previous section. Below we present a summary of this analysis in 1D systems.

3.2.1 Symmetries and SPT order in MPS

Let us consider how global on-site symmetries are realized in MPS. Suppose our local MPS tensors satisfy the following symmetry condition

(3.12)

where V is a unitary matrix. In index notation, the above condition can be rewritten as

$$u_{ij}A^j = VA^iV^\dagger. \tag{3.13}$$

In such a scenario, the state[3] $|\Psi\rangle$ has a global symmetry $u^{\otimes N}$ as the V and $V^\dagger$ coming from the neighbouring tensors cancel in the virtual bond between them. Graphically

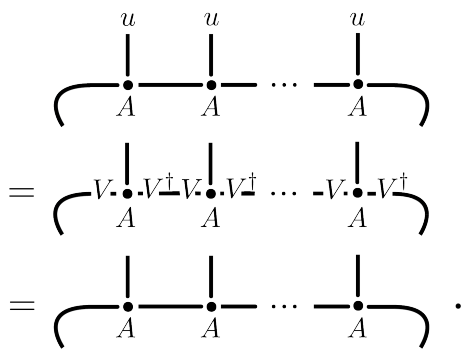

(3.14)

Although we will not prove it here, it turns out that, subject to some technicalities, this is the *only* way to encode a global symmetry into an injective MPS. In other words, if u is some global symmetry, we can always find a V such that Eq. 3.12 holds.

This is the central observation that leads to the classification of 1D SPT phases in the MPS picture. If we have a symmetry group G, acting with an on-site representation $u(g)$, this corresponds to a virtual representation $V(g)$ acting on the virtual space of the MPS as encoded by Eq. 3.12. Note that as $V(g)$ always appears with its own hermitian conjugate, it is only defined up to an arbitrary phase factor. Thus we are back to our familiar situation in the last section, where the boundary operators $V_{a/b}(g)$ had similar properties. In fact, $V(g)$ satisfies the exact same relations as $V_a(g)$, thereby forming a projective representation: $V(g)V(h) = \omega(g,h)V(gh)$. The 2-cocycle ω corresponds to some cohomology class $[\omega] \in H^2(G, U(1))$.

The advantage of the MPS formalism is that one can prove $[\omega]$ can not be changed under symmetric, gap preserving perturbations of the MPS tensor A [SPGC11]. Thus, we have a proof that states with different $[\omega]$ belong to separate SPT phases. Note that this is not completely rigorous as the MPS only approximates the gapped ground state. To have an air-tight argument, one would need to additionally construct a symmetric gapped path between an arbitrary gapped ground state and its MPS approximation.

3.2.2 Structure of MPS tensors in SPT phases

As we saw above, given an MPS tensor A with on-site symmetry $u(g)$ one can always extract its cohomology class $[\omega]$. Now we can ask ourselves if the reverse is true. In other words, given $[\omega]$ and $u(g)$, can we constrain the possible forms of the MPS tensors A that are consistent with the relation outlined in Eq. 3.12? The answer to this question turns out to be yes and it is of central importance for using SPT phases for MBQC. Below we rephrase the discussion in [ESBD12] to see how such constraints can be obtained.

[3] that is being approximated by the MPS tensors A

Consider a tensor A which satisfies the symmetry relation for a symmetry group G

$$\sum_j u(g)_{ij} A^j = V(g) A^i V^\dagger(g). \tag{3.15}$$

To make progress, we restrict ourselves to *finite abelian* groups, which implies that we can always choose a basis $\{|k\rangle\}$ of our physical on-site Hilbert space to diagonalize $u(g)$ such that $u(g)|k\rangle = \chi_k(g)|k\rangle$ for some 1D representations $\chi_k(g)$. For reasons that will become clearer later, we call this the *wire basis*. A further restriction is imposed on the cohomology class $[\omega]$ which is assumed to be *maximally non-commutative*, meaning that the subset $\{g \in G \mid \omega(g,h) = \omega(h,g)\ \forall h \in G\} = \{e\}$. In terms of the virtual representation $V(g)$, this condition implies that $V(g)V(h) = V(h)V(g)$ for all $h \in G$ if and only if $g = e$. It is known that any $V(g)$ having a maximally non-commutative cocycle can be written as

$$V(g) = \tilde{V}(g) \otimes \mathbb{I}, \tag{3.16}$$

where $\tilde{V}(g)$ is an irreducible representation of dimension $\sqrt{|G|}$. Such a relation tells us: in order for the SPT boundary to transform under such $V(g)$, it must support an edge mode of dimension at least $\sqrt{|G|}$.

In [ESBD12], the authors used Schur's lemma to prove that subject to the above two constraints, any injective MPS tensor A that transform as in Eq. 3.15 can be decomposed as

$$\boxed{A[k] = C[k] \otimes B[k],} \tag{3.17}$$

where $B[k]$ are arbitrary (junk) matrices and $C[k] = \tilde{V}(g_k)$ for a group element $g_k \in G$ that is determined by the equation, $\chi_k(g)\tilde{V}(g_k) = \tilde{V}(g)\tilde{V}(g_k)\tilde{V}^\dagger(g)$.

From Eq. 3.17, we see that the virtual space decomposes into two parts known as logical and junk subsystems. Importantly, as we move along the SPT phase, the matrices $B[k]$ which act on the junk subsystem vary while $C[k]$ do not. The entanglement structure in the logical subsystem is thus symmetry protected and doesn't depend on the precise point we are located in the phase. This uniform entanglement structure in the protected subspace can be used to perform MBQC throughout the phase given that we can find a single resource state in the phase.

However, please note that Eq. 3.17 only holds in the wire basis. Pictorially, letting C be a tensor defined by the components $C[k] = \tilde{V}(g_k)$ we can write

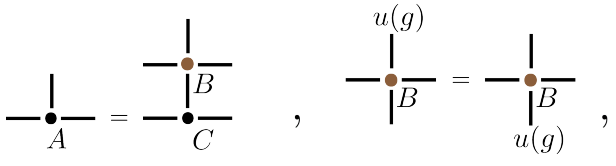

(3.18)

where B is some tensor describing an MPO. Keep in mind that fact that B commutes with the

symmetry action is essential for this statement to be non-trivial. Otherwise, by definition, any two states can be related to each other via a local quantum circuit which can be represented by an MPO. The symmetry condition on B ensures that upon contraction with the physical leg with state $|k\rangle$ in $u(g)$ basis, the final result is just Eq. 3.17 as the symmetry can just be pushed through.

As we will see shortly, this decomposition will be used to perform *quantum wire* throughout the SPT phase in the context of MBQC. Additionally, such a decomposition has been used, for example, to detect hidden symmetry breaking structures present in SPT phases, to quantify entanglement in SPT phases. In [PW15], the authors dropped both the assumptions of finite abelian group G and maximally non-commutative $[\omega]$ to arrive at a more general result using the formalism of Clebsch-Gordan coefficients. However, in such a general setting, nice decompositions like Eq. 3.17 have not been shown to exist and the connection to MBQC is not immediate. In [Ste17], it was shown that this structure can be preserved if just the maximally non-commutative constraint is removed.

Example: SPT order in 1D cluster state

As an example of the manifestation of SPT order in MPS, let us re-examine SPT order present in the 1D cluster state in terms of its MPS tensor components. Recall the 1D cluster state has a $\mathbb{Z}_2 \otimes \mathbb{Z}_2$ symmetry[4] generated by flipping spin at all even or odd sites (See Eq. 3.6). To fit it with the above formalism where the on-site symmetry is translationally invariant, we need to consider a two-qubit unit cell. If we project the cluster MPS tensors onto the X basis, we arrive at the 2-site blocked tensor components

$$\begin{aligned} C_b[++] &= C[+]C[+] = \mathbb{I}, \\ C_b[+-] &= C[+]C[-] = Z, \\ C_b[-+] &= C[-]C[+] = X, \\ C_b[--] &= C[-]C[-] = XZ, \end{aligned} \tag{3.19}$$

where we have used the relations obtained in Eq. 2.19. Pictorially such a blocking can be depicted as

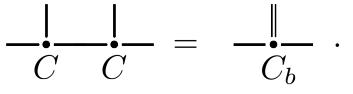

(3.20)

With a little bit of work, we can use Eq. 3.19 to find the unitary operator $V(g)$ in Eq. 3.15 as $V(g_1, g_2) = Z^{g_1} X^{g_2}$, in agreement with the result in Sec. 3.1.2. Such a representation satisfies our maximal non-commutativity condition. Furthermore, we can check that Eq. 3.17 holds as the wire basis is just the local X-basis and the matrices in Eq. 3.19 are of course elements of $V(g)$. Other states in the cluster phase can therefore be written in terms of the MPS tensors of the form Eq. 3.17 where $C = C_b$ and the junk matrices vary throughout the phase.

[4] inherited from its parent Hamiltonian.

3.3 MBQC with SPT phases

Till now, we have talked about SPT phases and their classification techniques. SPT phases are of independent interest to the condensed matter physicist as they are examples of exotic phases of matter that can not be captured by the celebrated Landau-Ginzburg theory of spontaneous symmetry breaking. However, our motivation for looking at SPT phases is their usefulness as resource states for driving MBQC. As alluded to earlier, it turns out that at least in some cases the computational capability of these resource states is uniform throughout the phase. Such phases of matter are known as *computation phases of matter*. In this setting, physical phases of matter coincide with that of uniform computation power. This was first noticed for the class of states containing the 1D AKLT state, which allows for universal MBQC on a single encoded qubit [BM08]. The 1D AKLT state can be thought of as an exactly solvable point in the 1D SPT phase, protected by the $SO(3)$ symmetry[5], often referred to as the 1D Haldane phase. The authors were able to construct an MBQC protocol in terms of the properties of the Haldane phase (which persists even when we move away from the 1D AKLT state), thereby establishing the first connection between MBQC and SPT order.

To gain an intuitive understanding of why SPT phases can be useful for MBQC, consider the following toy model. From Sec. 3.1, we know that SPT phases have robust edge modes. Thus, if we consider an SPT-ordered state on a half-infinite spin chain, there will be an edge mode degeneracy associated with the boundary of the chain. Specifically, for a $\mathbb{Z}_2 \otimes \mathbb{Z}_2$ chain like the 1D cluster state, this means that the ground state will be two-fold degenerate, with the two ground states differing by some operator localized near the edge.

Now let us encode our qubit state $|L\rangle$ in this edge mode. If the left most spin is measured, it will be projected to a product state $|s\rangle$ that depends on the random measurement outcome. As this spin is disentangled with the rest of the spin chain, we can just focus on the remaining smaller chain which will again have an edge mode $|L'\rangle$. The key result in the theory of SPT-MBQC formalism is that if the measurement basis is chosen correctly, the new edge state $|L'\rangle$ can be related to the original one $|L\rangle$ via a measurement dependent unitary: $|L'\rangle = U_s|L\rangle$. In other words, a measurement in the physical Hilbert space amounts to unitary evolution in the virtual Hilbert space where the logical qubit lives. As the edge modes are robust throughout an SPT phase, we might reasonably expect that our logical qubit is also protected under symmetry respecting perturbations. This is indeed the case for a quite broad class of 1D SPT phases as we will see next.

3.3.1 MBQC in correlation space

To flesh out the above structure some more, we consider the formalism of MPS where MBQC is said to carried out in *correlation space.* Note that this is just another way of expressing how our logical qubit evolves, under the measurement of the physical degrees of freedom, by analysing

[5]It was later observed that a finite abelian subgroup $\mathbb{Z}_2 \otimes \mathbb{Z}_2 \subset SO(3)$ is enough to protect the SPT order as $H^2(SO(3), U(1)) = H^2(\mathbb{Z}_2 \otimes \mathbb{Z}_2, U(1)) = \mathbb{Z}_2$.

the virtual degrees of freedom i.e. correlation space. To this end, consider an MPS with open boundary conditions, which can be written as

$$|\Psi\rangle = \sum_{i_1,\ldots,i_N} \langle L \left| A^{i_1} A^{i_2} \ldots A^{i_{N-1}} A^{i_N} \right| R\rangle \, |i_1, i_2, \ldots, i_N\rangle \,, \tag{3.21}$$

for some boundary vectors $\langle L|$ and $|R\rangle$. Suppose we have encoded our logical qubit in the left edge state $|L\rangle$. If we measure the left most spin (corresponding to the index label i_1) and obtain a measurement outcome corresponding to the eigenstate $|s\rangle$ of the measured observable, the post-measurement state of the unmeasured spin chain can be written as

$$\left|\Psi'\right\rangle = \sum_{i_2,\ldots,i_N} \left\langle L' \left| A^{i_2} \ldots A^{i_{N-1}} A^{i_N} \right| R\right\rangle |i_2, \ldots, i_N\rangle \,, \tag{3.22}$$

where the updated boundary vector is

$$\left|L'\right\rangle = A^{\dagger}[s]|L\rangle. \tag{3.23}$$

If $A[s]$ is unitary (which is not clear apriori), we have induced unitary evolution on the virtual space by measurement of the physical space. Note that $A[s]$ depends on the random measurement outcome s, which we cannot control. As the reader can guess from the discussion after Eq. 2.8, this can still be dealt with via byproduct propagation in the context of SPT phases.

3.3.2 Symmetry based MBQC on the 1D cluster state

To see how the above idea works in practice, let us consider a specific example of the 1D cluster state again. Recall that the cluster state tensor with two-site blocking can be represented by the matrices $A[a, b] = X^a Z^b$ where $a, b = 0, 1$ represented the projection on the state $|+\rangle$ and $|-\rangle$ respectively (See Eq. 3.19). Thus, measuring the two adjacent sites in the X-basis resents in an *byproduct operator* and it can be pushed to the end of the chain using the symmetry relations of the MPS tensor. As usual, these byproduct operators affect the logical processing of our encoded qubit via X and Z flips. Note that these Pauli byproduct operators are nothing but elements of the projective representation $V(g)$ for some element g in our symmetry group $\mathbb{Z}_2 \otimes \mathbb{Z}_2$. Pictorially we deal with the byproduct operator as follows

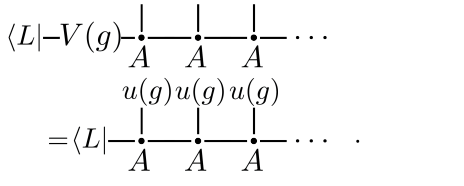

(3.24)

Here, we have made use of the symmetry propagation relations as depicted in Eq. 3.12. At the end of the day, all this means is that all the future measurement bases must be altered according to the symmetry operator $u(g)$ that now appears in the physical legs. This is just a symmetry-

based reformulation of the conventional framework of MBQC, where the measurement bases chosen are adaptive.

Using byproduct propagation, we can use the 1D cluster state as a "quantum wire", where measurements in the X basis deterministically shuttle the state $|L\rangle$ along the chain as we already saw in Sec. 2.1.1. We can perform non-trivial gates by rotating the measurement basis away from the wire basis. Suppose we define a general rotated basis spanned by the eigenstates

$$\begin{aligned} |\beta_+\rangle &= \cos(\beta)|+\rangle + i\sin(\beta)|-\rangle, \\ |\beta_-\rangle &= i\sin(\beta)|+\rangle + \cos(\beta)|-\rangle. \end{aligned} \tag{3.25}$$

If we measure the first qubit in the unit cell in this rotated basis and the second one in the X basis, we arrive at

$$\begin{aligned} A\left[\beta_+, b\right] &= \cos(\beta)A[+,b] - i\sin(\beta)A[-,b] = e^{-i\beta X}Z^b, \\ A\left[\beta_-, b\right] &= i\sin(\beta)A[+,b] + \cos(\beta)A[-,b] = e^{-i\beta X}XZ^b. \end{aligned} \tag{3.26}$$

In general, we have $A[\beta_a, b] = e^{-i\beta X}X^aZ^b$ implying that such a measurement results in a rotation by 2β about the x-axis on our logical qubit, up to the measurement dependent Pauli byproducts. Interchanging the measurement basis of the two qubits in the unit cell results in a rotation about the z-axis. As was noted in the first chapter, these two rotations concatenated together can generate any single-qubit unitary implying that the 1D cluster state is a *universal resource for single qubit* unitary operation.

3.4 Computational phases of matter in 1D

The universality of the 1D cluster state turns out to be a property of the SPT phase it resides in, protected by the $\mathbb{Z}_2 \otimes \mathbb{Z}_2$ symmetry (see Eq. 3.6). In fact, this is true of any abelian SPT phase with maximally non-commutative cocycles (defined in Sec. 3.2.2). For a rigorous proof of this general fact, we refer the reader to [SWP+17]. Below we depict the essential notions that ensures that the computational power across entire SPT phases is uniform.

3.4.1 Quantum wire in SPT phases

The fundamental computational primitive in the MBQC setting is that of quantum wire where we are merely transferring our encoded logical information from one spatial location to another. It turns out that for states connected to the cluster state, via a symmetric local quantum circuit, this can be done with *perfect fidelity*. To see why this is true, we go back to our master Eq. 3.17, a decomposition that holds in the entire cluster phase. We encode our logical state $|\psi\rangle$ only in the logical subsystem of the decomposition in Eq. 3.17. Thus, we can write $|L\rangle = |\psi\rangle \otimes |J\rangle$ for some arbitrary vector $|J\rangle$ in the junk subspace. Following Eq. 3.23, the updated boundary

vector under measurement in the wire basis can be written as

$$\big|L'\big\rangle = A^\dagger[k]|L\rangle = C^\dagger[k]|\psi\rangle \otimes B^\dagger[k]|J\rangle. \tag{3.27}$$

The crucial point to note is that the logical and the junk subsystems remain uncorrelated. Since $C[k] = \tilde{V}(g_k)$ (just Pauli matrices for the cluster case) and the virtual symmetry representation V acts non-trivially on the logical subspace only (see Eq. 3.16), the byproduct operators can still be propagated controllably to the end the computation just like the cluster state. Thus, the quantum wire can be implemented in the entire SPT phase as long as Eq. 3.17 holds for the corresponding MPS tensor. The junk subsystem evolves uncontrollably during this evolution via measurement. However, this is not a problem (not yet!) as the logical information never leaks out to this subsystem while implementing quantum wire.

3.4.2 1 qubit rotation in SPT phases

While it was straightforward to implement quantum wire in the entire cluster phase, the issue of implementing non-trivial unitary operations (e.g. z-rotations) on our encoded qubit turns out to be a much more complicated affair. The crux of the difficulty lies in the fact that simulating non-trivial unitary gates in MBQC involves measurements away from the wire basis and this is precisely when the neat decomposition into logical and junk subspaces (again, see Eq. 3.17) breaks down. This in turn implies that there is some inherent decoherence involved in carrying out non-trivial unitary operations in the phase (except for special fixed points like the cluster state itself) and one needs to come up with clever decoherence management schemes to make sure that such processes don't completely jeopardize our computational scheme.

To expand on the issue, consider performing a measurement in a rotated basis and obtaining some measurement outcome which is a superposition of states in the wire basis, $|b\rangle = \alpha|k\rangle + \beta|k'\rangle$. The evolution induced on correlation space via this measurement is given by

$$\big|L'\big\rangle = \alpha\,(C^\dagger[k]|\psi\rangle \otimes B^\dagger[k]|J\rangle) + \beta\,(C^\dagger[k']|\psi\rangle \otimes B^\dagger[k']|J\rangle), \tag{3.28}$$

which is an entangled state between the logical and junk subsystems unless $B[k] = B[k']$. Since we may have no knowledge about the junk tensor components $B[k]$ or $B[k']$, it becomes difficult to track the evolution of our logical state $|\psi\rangle$. A partial fix to this problem was provided in [MM15], where the authors used a *computational renormalization* scheme (inspired by Bartlett's earlier work [BBMR10]). However, the construction was fine-tuned to a certain subset of the Haldane phase and it was not clear how it can be extended to arbitrary SPT phases.

A general solution was provided in [RWP$^+$17, SWP$^+$17]. It was shown that the logical and junk systems, previously entangled, can be disentangled by splitting up the proposed rotation angle into very small parts and separating the rotation sites by a large number of spins in the middle, all of which are measured in the wire basis. Such a strategy works for any 1D SPT

phase protected by finite abelian groups, but the resulting set of logical gates is only guaranteed to be universal in the maximally non-commutative case [Ste17]. This is a seminal discovery in the context of using SPT phases in MBQC as it gives rise to the idea of *universal computational phases of matter* in 1D. Below, we highlight parts of the construction presented in [RWP$^+$17] that make the whole scheme work. This will not only give us a better sense of the clever techniques used but also help in putting the new results in context in so far that the results of Sec. 5.5 present a different point of view.

Raussendorf et al.'s oblivious wire trick:

Disclaimer: To be consistent with the previously defined notions in the field, from now to the end of this chapter, we will be using a non-standard notation. Namely, the symbols $|0\rangle$ and $|1\rangle$ are used here to denote the eigenstates of the symmetry respecting basis rather than the Pauli-Z basis. The author understands that this is potentially confusing but hopes that it will be clear from the context. Furthermore, in the discussion below, each spin is assumed to have d degrees of freedom.

The key technical idea that extends the usefulness of SPT phases from quantum wire to logical gates is the "incoherent addition of computational paths." In this context, computational paths refer to the record of different measurement outcomes obtained in course of a particular run of MBQC. "Addition" of these paths simply means that after applying the by-product operators (which are outcome dependent and always arise in MBQC), the measurement record is discarded and the different computational paths are added.

To apply this idea to our spin chain, consider n consecutive spins, being measured in the wire basis. At the end of the computation, an outcome-dependent byproduct operator is applied to the unmeasured spin and finally, the outcomes are discarded. Such a procedure is known as *oblivious wire* for obvious reasons. The authors in [RWP$^+$17] proved that such an operation effectively acts as a quantum channel that transforms the state of the right boundary (up to normalisation) to,

$$\tau_R = I \otimes \mathcal{L}^n |L\rangle\langle L|, \tag{3.29}$$

wherein $\mathcal{L}^n$ denotes the n-fold iteration of the channel $\mathcal{L}$, $\mathcal{L}^n := \underbrace{\mathcal{L} \circ \mathcal{L} \circ \ldots \circ \mathcal{L}}_{n \text{ times}}$ and

$$\mathcal{L}(\rho) := \sum_{k=0}^{d-1} B[k]\,(\rho)\,B^\dagger[k]. \tag{3.30}$$

Since the ground state is assumed to be unique, the MPS tensors A and thereby the junk tensors B are injective. Thus, the channel $\mathcal{L}$ has a unique fixed point ρ_{fix}, which can be reached

after n-fold application of $\mathcal{L}$ if $n \gg \zeta$,[6]

$$\mathcal{L}^n(\rho) \approx \nu_\rho \, \rho_{\text{fix}}, \tag{3.31}$$

with $\nu_\rho \in \mathbb{R}_+$, for all states ρ of the junk subsystem. Such a contracting channel can be used to prepare our virtual system (where the encoded qubit lives) in a tensor product state $\tau = \sigma \otimes \rho_{\text{fix}}$, where the junk system is always pushed to a defined fixed point and the two subsystems become unentangled.

Now, to perform a rotation about an infinitesimal angle $d\beta$, let us consider a spin chain of length $n+1$, which prepares the junk system in ρ_{fix} using the procedure above. To perform the computation, we measure the first spin in a slightly rotated basis from the wire basis i.e. $\tilde{\mathcal{B}}(d\beta) = \{|0'\rangle, |1'\rangle, \ldots, |d-1\rangle\}$ with

$$|0'\rangle = |0\rangle + d\beta|1\rangle, \tag{3.32}$$

$$|1'\rangle = |1\rangle - d\beta|0\rangle, \tag{3.33}$$

where $d\beta \in \mathbb{R}$. The remaining n spins are measured in the wire basis to perform oblivious wire.

To describe the evolution of the virtual system under these measurements, it is convenient to define the the parameters $\nu_{ij} \in \mathbb{C}$ via,

$$\boxed{\lim_{n\to\infty} \mathcal{L}^n(B[i]\,\rho_{\text{fix}}\,B^\dagger[j]) = \nu_{ij}\,\rho_{\text{fix}} \quad \text{for all } i,j = 0,\ldots,d-1} \tag{3.34}$$

where the matrix ν with elements $[\nu]_{i,j} = \nu_{ij}$ can be given the interpretation of a coupling matrix. Now, the combined first symmetry breaking measurement with outcome $0/1$ (corresponding to post measurement state $|0'\rangle\rangle/|1'\rangle$) and subsequent oblivious channel results in the transformation: $\sigma \otimes \rho_{\text{fix}} \to \mathcal{T}_{0/1}\,(\sigma \otimes \rho_{\text{fix}})$, where

$$\begin{aligned}\mathcal{T}_{0/1}\,(\sigma \otimes \rho_{\text{fix}}) = &\nu_{00/11}\,\sigma \otimes \rho_{\text{fix}} + \frac{d\beta}{2}\left[\nu_{01}^* C - \nu_{01} C^\dagger, \sigma\right] \otimes \rho_{\text{fix}} \\ &\pm \frac{d\beta}{2}\left\{\nu_{01}^* C + \nu_{01} C^\dagger, \sigma\right\} \otimes \rho_{\text{fix}},\end{aligned} \tag{3.35}$$

and $C := C^{-1}[0]C[1]$.

Thereby, upon adding the two channels $\mathcal{T}_0$ and $\mathcal{T}_1$, the evolution of the logical system becomes unitary up to the first order in the rotation angle $d\beta$,

$$\mathcal{T}_0 + \mathcal{T}_1 : \sigma \otimes \rho_{\text{fix}} \longrightarrow (\nu_{00} + \nu_{11})\,\sigma \otimes \rho_{\text{fix}} + d\beta\left[\nu_{10} C - \nu_{10}^* C^\dagger, \sigma\right] \otimes \rho_{\text{fix}}. \tag{3.36}$$

To leading order in the angle $d\beta$ and upto the norm factor $\nu_{00}+\nu_{11}$, we have just implemented

[6] Note that the correlation length ζ was earlier defined (after Theorem 1) in terms of the second largest eigenvalue of the channel as $\zeta := -1/\ln|\lambda_1|$.

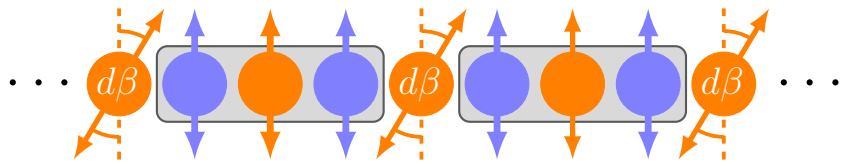

Figure 3.2: SPT-MBQC scheme applied to the cluster phase for an intended z-rotation: the odd (orange) and even (blue) sites are used to perform z and x rotations respectively just like in the cluster state. The desired rotation angle is split into infinitesimal parts (each $d\beta$) so that the resulting operation for each of them only differs slightly from the identity. The sites at which symmetry breaking measurements are performed are separated from each other by a number of sites $\gg \zeta$ (correlation length). These sites (inside the gray boxes) are measured in the wire basis to perform oblivious wire and their precise number depends on our location in the phase diagram.

a unitary gate $U(d\beta)$,

$$U(d\beta) = \exp\left(i\, d\beta\, \frac{\nu_{10} C - \nu_{10}^{*} C^{\dagger}}{(\nu_{00} + \nu_{11})}\right). \tag{3.37}$$

We can redo the above analysis for a continuous set of measurement bases $\tilde{\mathcal{B}}(d\beta, \gamma)$, with

$$|0'(\gamma)\rangle = |0\rangle + d\beta e^{i\gamma}|1\rangle,$$
$$|1'(\gamma)\rangle = |1\rangle - d\beta e^{-i\gamma}|0\rangle,$$

and $d\beta, \gamma \in \mathbb{R}$ to find that the unitary gate being implemented is, (up to leading order in $d\beta$)

$$\boxed{U(d\beta, \gamma) = \exp\left(i\, d\beta\, |\nu_{01}| \frac{\left(e^{-i(\gamma+\delta)} C - e^{i(\gamma+\delta)} C^{\dagger}\right)}{i}\right),} \tag{3.38}$$

where $\nu_{01} = |\nu_{01}| e^{i\delta}$.

Admittedly this is a lot of material to take in, but let us focus on the final result in Eq. 3.38. From here, it is visibly clear why it is important to condition our junk system to a reliable fixed point ρ_{fix} via oblivious wire. The state ρ_{fix} itself, and even the Hilbert space it lives in, are a *priori* unknown but it doesn't matter. The only computationally relevant parameter that needs to known about ρ_{fix} is ν_{01} as defined in Eq. 3.34. This parameter ν_{01} appears as a reduction factor to the intended infinitesimal rotation angle $d\beta$ and can be interpreted as the computation efficiency of the MBQC resource state at hand. Furthermore, if we want to perform finite rotations, we can perform the above transformation repeatedly where each individual rotation angle is infinitesimally small and each overall transformation can be treated independently. Nevertheless, as long as we have infinite resources, this is not a problem and we can implement finite unitary operations this way (See Fig. 3.2 and the discussion below it for a graphical understanding).

Interpretation of the $[\nu]$ *matrix:* The operator $\nu := \sum_{i,j=0}^{d-1} |i\rangle \nu_{ij} \langle j|$ can be given the interpre-

tation of a (mixed) quantum state. However, what part does this fictitious quantum state play in the computational scheme? It turns out that each copy of the state ν implements a single quantum gate on the logical subsystem by interacting with it and subsequently being discarded (traced out). In other words, MBQCs in SPT ordered phases can be shown to simulate quantum circuits in which each gate arises from the interaction between the logical subsystem with a (quasi?) particle prepared in the state ν.

3.5 Higher dimensions and implications

Almost the entirety of this chapter has been devoted to the discussion of SPT phases in 1D spin chains primarily because there are more rigorous results known for such systems and they are of primary interest for this thesis. However, these connections between SPT order and MBQC extend to 2D systems as well. The 2D AKLT states, which possess SPT order, have been shown [WAR11, Miy11, Wei13] to be universal for MBQC in different lattices. Similarly, fixed point states for general 2D phases, which are essentially products of generalized GHZ states, are universal for MBQC [NW15]. In both cases, the trick is to use local measurements to reduce the state at hand to the canonical resource state i.e. the 2D cluster state, as long as some percolation constraints are met. In a different line of work, resource states with *genuine* 2D SPT order were shown to have computational power beyond the 2D cluster state. Namely, the so-called Union Jack State [MM16] can be proven to be universal for MBQC using just Pauli measurements. Such states need to be necessarily outside the stabilizer formalism for compatibility with the Gottesman-Knill theorem [Got98].

Notably, in all of the examples above, the allowed deformations to the path of Hamiltonians are restricted. This is to say, none of them are examples of a 2D SPT phase in which *all* the ground states are universal for MBQC. The first and only known example of such a phase is the 2D cluster phase which can be better understood as inheriting a different type of order known as subsystem symmetry-protected order (SSPT) [SNBV$^+$19]. The relevant symmetries for the 2D cluster phase are *lines* of X operators[7] that only act along the diagonal sites of a 2D lattice and can be well understood by the formalism of PEPS which are straight forward generalizations of the MPS formalism. Overall, this gives rise to the idea of a *universal computational phase of matter* and is an area of active research in its own right.

In general, this deep connection between SPT order and MBQC (arguably) has two main takeaways. From a practical point of view, if we want to prepare our MBQC resource state by cooling a physical system down to sufficiently low temperatures, the idea of a universal phase rather than a universal state gives more room for errors in the preparation procedure. Thus such systems are naturally robust to symmetry preserving errors and we don't need the precise details of our location in the phase diagram to carry out a computation. On the other hand, these results get us a step closer to the answer to our fundamental question about the unifying

[7] to be precise, these line symmetries turn out to be a subgroup of the larger group representing the so-called cone symmetries.

feature that connects MBQC resource states. From our earlier discussion in Chapter 1, we know that while entanglement is necessary for our resource state, as with most things in life, too much of it is a curse [GFE09]. The SPT-ordered states seem to get the entanglement structure just right and sit at the middle of this entanglement measure. In conclusion, it seems like the same structure that allows SPT order to exist is closely related to the structure responsible for computational universality.

Chapter 4

The Curious Case of Finite Systems

4.1 Motivation

In the last two chapters, we have built all the machinery of tensor networks and group cohomology to understand how SPT phases can be classified and used for MBQC. However, these theoretical results hold only in the thermodynamic limit where the spin chain at our hand is arbitrarily large. On the other hand, physical computation is necessarily limited by finite resources and especially in the current era of noisy quantum computers with very few qubits, one would like to have a theory that works for any chain length.

To see that there is a potential discrepancy here, first note that the MPS language introduced earlier is an equally valid construction for finite and infinite systems. Thus, the idea of projective representations on the virtual legs of an MPS is still on firm ground. However, such representations can go through a discontinuous change if and only if the energy gap above the ground state closes [SPGC11].

The typical expectation for finite systems is that the gap never closes exactly and zero gap is approached as some inverse power of the system size. This leaves two possibilities for the analysis in finite chains,

(a) The cocycle of the projective representation never changes as one varies the parameters. This means, to the extent the idea of "phase" is valid in finite systems, all the states are under the same phase.

(b) The gap indeed closes regardless of the finite length of the chain.

In Sec. 4.3, we will explore why (a) is problematic. In [SPGC11], Schuch *et al.* vouch for (b), arguing

> ... The idea of the impossibility proof is to consider a chain of arbitrary length N and show that along any well-behaved path H_γ, P_γ needs to change continuously, which results in a continuous change in the way the symmetry acts on the virtual

system. In turn, such a continuous change cannot change the cohomology class. While this argument is based on the fact that the chain is finite (as the continuity bounds depend on N), it works for arbitrary system size N; also our argument implies that, in order to interpolate between two systems with different cohomology classes, i.e., in different phases, the gap of the Hamiltonian will have to close for a finite chain, and not only in the thermodynamic limit. (This can be understood from the fact that along an MPS path, the virtual representation of the symmetry is well defined even for finite chains. So, it cannot change without closing the gap.. . .)

If true, this would solve our puzzle. However, our physics intuition tells us that the gap indeed doesn't close for finite systems. To resolve the matter, we consider a concrete interpolation Hamiltonian between the fixed points of the trivial and non-trivial "phase".

4.2 Interpolating Hamiltonian and role of the gap

Let us consider the so called transverse field cluster Hamiltonian that is invariant under the same $\mathbb{Z}_2 \otimes \mathbb{Z}_2$ symmetry with periodic boundary conditions

$$H_{\mathsf{P}}(\alpha) = -\cos\alpha \sum_{i=1}^{N} Z_{i-1} X_i Z_{i+1} - \sin\alpha \sum_{i=1}^{N} X_i. \tag{4.1}$$

The two symmetry generators on the physical spins are still given by $X_{\mathsf{odd}} = XIXI \ldots XI$ and $X_{\mathsf{even}} = IXIX \ldots IX$ as they commute trivially with the perturbing Hamiltonian. Let us denote the unique ground state of this Hamiltonian as $|\Psi(\alpha)\rangle$ which inherits the $\mathbb{Z}_2 \otimes \mathbb{Z}_2$ symmetry of the Hamiltonian. It is clear that even in finite systems the ground states $|\Psi(\alpha = 0)\rangle$ and $|\Psi(\alpha = \pi/2)\rangle$ correspond to differing computational power.

According to Schuch's argument, the gap should close at some intermediate value of α between 0 and $\pi/2$ even in finite systems. Please note that it is known that the gap indeed closes at $\alpha = \pi/4$ in the thermodynamic limit and the Hamiltonian can be mapped to non-interacting Majorana fermions via Jordan-Wigner transformation.

At any rate, for finite systems, we can investigate the question of the gap via some numerical method like DMRG. The results (See Fig. 4.1) show no gap closing for any angle $\alpha \in (0, \pi/2)$. Thus, to the extent that the standard notion of phase applies to these finite systems, we conclude that the ground states $|\Psi(\alpha)\rangle$ belong to the same "phase" for all values of α.

4.3 Where does computational power break for finite chains?

As we saw in the last chapter, the standard SPT classification techniques that apply for infinite chain lengths are based on group cohomological arguments. Namely, to go from a computationally useful cluster state to a trivial state, the interpolating cocycle class $[\omega]$ has to go through a

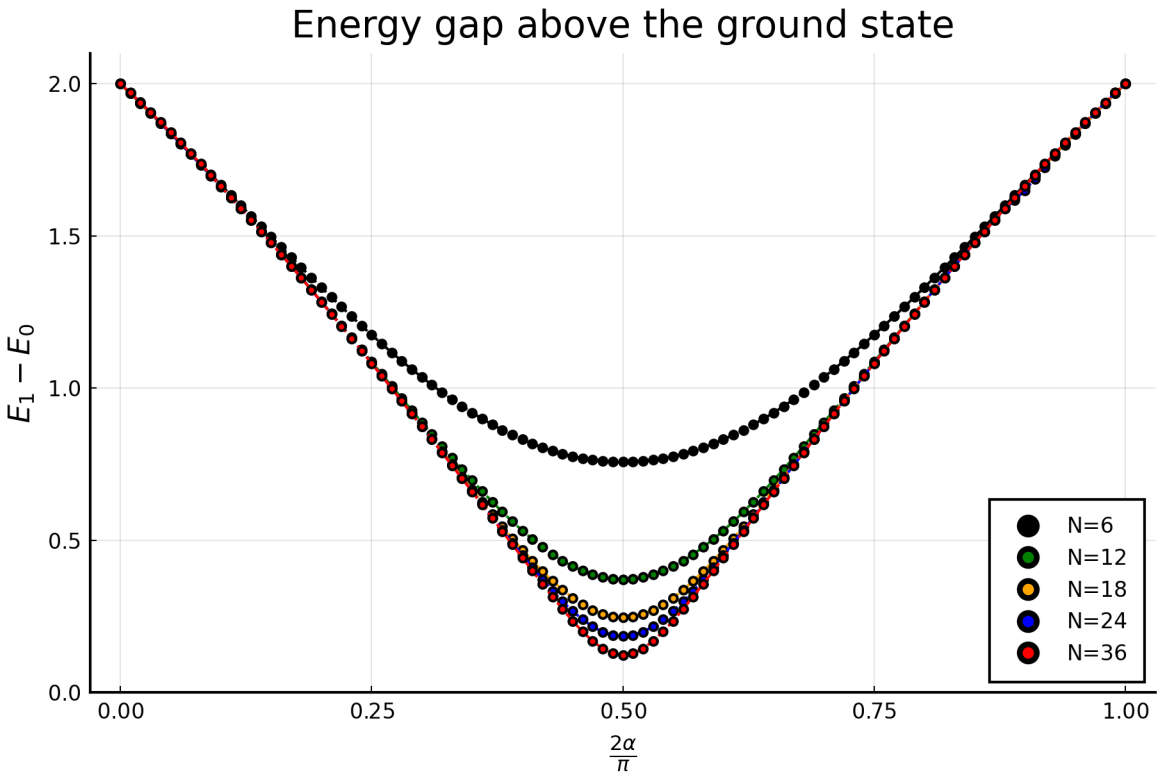

Figure 4.1: Energy gap above the ground state of the Hamiltonian $H_{\mathrm{P}}(\alpha)$ as a function of the sweep parameter α. The different colors are due to varying values of system size N. We see that the gap never closes for finite systems. At the supposed critical point ($\alpha = \pi/4$), the gap scales like $1/N$.

discontinuous change from non-trivial to trivial. In the case of infinite chains, this discontinuous change in $[\omega]$ coincides with phase transition (i.e. closing of the gap above the ground state).

But what does all of this mean for finite systems? We do know for a fact that irrespective of the size of our system, the 1D cluster state ($\alpha = 0$) can be represented by MPS tensors that admit projective representations on the virtual legs, thereby implying $[\omega]_{\alpha=0} \in \mathbb{Z}_2$ for all N.

On the other hand, at $\alpha = \pi/2$, the ground state is $\otimes_{i=1}^{N} |+\rangle_i$. As such a state can always be represented by an MPS with bond dimension 1, we have $[\omega]_{\alpha=\pi/2} = 0$ for all N.

As the Hamiltonian $H(\alpha)$ interpolates between the above two states, the cocycle representation has to change at some intermediate value of $\alpha \in (0, \pi/2)$. As was mentioned earlier, we know that this happens at $\alpha = \pi/4$ for infinite systems as the gap closes. However, for finite systems, the gap never closes and thereby the question becomes

> At which point α_{crit} does the cocycle class $[\omega]_\alpha$ change, in finite systems?

To investigate the matter, we shift our attention to the physical consequences of a non-trivial cocycle class. Note that whenever $[\omega] \in \mathbb{Z}_2$, the MPS tensors representing the ground state can

be decomposed in the wire basis as

$$A[k] = C[k] \otimes B[k],$$

where components $C[k]$ in the wire basis $\{|k\rangle = |+\rangle, |-\rangle\}$ are just the Pauli matrices for our case of interest and the junk matrices are allowed to arbitrarily vary with α. As long as such a decomposition persists for a certain range of α, we can rely on the standard analysis as presented in Sec. 3.4 to conclude that computational power persists even for finite spin chains. This should be easy enough to do using numerical techniques like a DMRG routine with the caveat that there is always a gauge degree of freedom that may obscure this neat tensor decomposition. In other words, if our DMRG routine chooses the "wrong" gauge, it may spit out the tensors,

$$\tilde{A}[k] = E\left(C[k] \otimes B[k]\right) F^{\dagger} \tag{4.2}$$

for arbitrary unitaries[1] E and F, without affecting any physical property of our state. However, this choice of the left and the right unitaries still leaves the singular values of the MPS tensor invariant. As the Pauli matrices come with two singular values of 1, the singular values of the components of A should at least[2] be doubly degenerate. Note that this is a necessary (but not sufficient) condition for Eq. 4.2 to hold. Unfortunately for us, the DMRG results suggest otherwise. The singular values of the MPS tensors jump rapidly throughout the sweep and the cluster point itself $(\alpha = 0)$ seems to be unstable.

Just to be clear, this plot in Fig. 4.2 *doesn't* tell us that a decomposition of the form Eq. 3.17 is *non-existent* but instead that it is very difficult to find such a decomposition away from exactly solvable fixed points (like the cluster state). Note that the decomposition in Eq. 3.17 is not constructive and the sizes of the junk matrices are allowed to be arbitrarily large as we vary α. On the other hand, the DMRG optimization routine aims to approximate the ground state up to some input accuracy and doesn't particularly care about our preferred decomposition. Instead, it will just converge to an alternative approximation[3] of the actual ground state if its bond-dimension is smaller than that prescribed by the nice decomposition.

This immediately means that we cannot directly use the MPS tensors from a standard DMRG routine to analyze the entire range of $\alpha \in (0, \pi/2)$. However, it is crucial for the whole computational scheme (both for quantum wire and unitary operations) that we can extract the junk tensors as the computationally relevant parameters (coupling strength ν_{01} and correlation length ζ) are defined with respect to them.

At this point, we seem to have arrived at an impasse. On one hand, we cannot apply the argument of the energy gap closing affecting a discontinuous change in the cohomology class. On the other hand, the numerical investigations in finite systems also don't seem to get us closer

[1] for a transitionally invariant system, we should have $E = F$ but for finite systems let us allow them to be different just to be general.

[2] it maybe $4, 6, 8, \ldots$ fold degenerate if the components of B have additional structure.

[3] i.e. gets stuck in a local minimum.

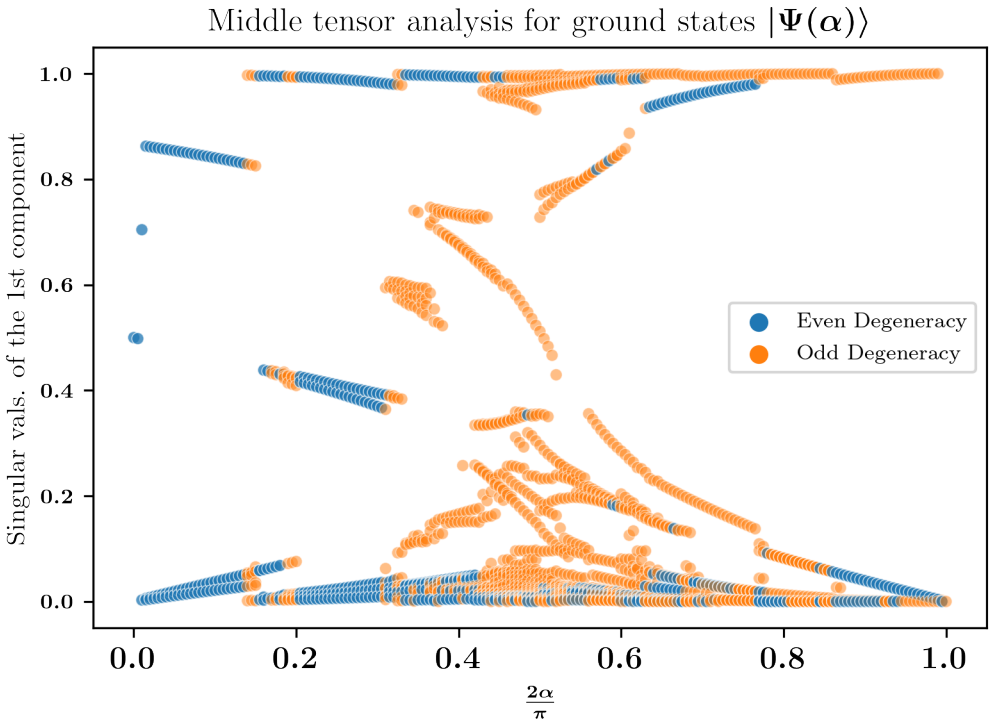

Figure 4.2: Singular values of one of the four (due to two-site blocking) MPS tensors (the first) describing the ground state of the Hamiltonian $H_{\mathrm{P}}(\alpha)$ as a function of the sweep parameter α. The singular values are colored blue if they appear even number of times and orange otherwise. Note that at any particular value of α, for Eq. 4.2 to hold, all the singular values should be colored blue. In this regard, we see that the cluster point ($\alpha = 0$) is very unstable and so is the product point ($\alpha = \pi/2$). The other relevant parameters for plot are system size $N = 24$ and DMRG accuracy$= 10^{-12}$.

as the approximate MPS tensors don't exhibit the structure expected from theoretical arguments (except at exactly solvable points like the cluster state and the product state). Unfortunately, we will not be able to resolve this question in this thesis. We do acknowledge that the puzzle remains unsolved as group cohomology class has to change at some intermediate value of $\alpha \in (0, \pi/2)$, as long as we believe that a different group cohomology class is indicative of different computational power even in finite systems. This fact notwithstanding, in the next chapter, we introduce a rather simplified formalism that doesn't refer to group cohomology classes or MPS tensors at all but is still able to categorize SPT states according to their computational power as resource states for systems of any size.

Chapter 5

Results

This chapter outlines the main results of this thesis which apply to arbitrary chain lengths. The key insight that led to this new formulation is to take a strictly operational point of view. In this formalism, observables (that at least in principle can be measured) rather than MPS tensors (that approximates a quantum state) take center stage. Such a treatment allows us to explicitly calculate a computational "*order parameter*" for any chain length. Using symmetry arguments and the short-range entanglement of our SPT states, we relate this parameter to the conventional string order parameter of topological order in condensed matter physics. Coming back to the question of computational power and efficiency in finite chains, we move on to the discussion of minimizing the inherent decoherence involved in the scheme whenever a non-trivial computation needs to be performed. We show that for *any finite* spin chain the most efficient regime of operation is precisely the opposite extreme of the regime prescribed in the discussion of computation in SPT phases.

5.1 An operational point of view: Simulating MBQC

Having gone through all the trouble that comes with the existing MPS formalism for extracting the computationally relevant parameters, we ask ourselves the obvious question that every physicist would ask themselves when in trouble. If these parameters are indeed physical, how would we *measure* them? In other words, if we are handed a resource state, how do we physically extract the parameters relevant for computation power? Pursuing this line of questioning leads us to a formulation that solely refers to the state at hand itself and doesn't care about the details of its MPS or any other representation.

To this goal, we perform a computer simulation of MBQC in the 1D SPT phase. Therein, by simulating a single site rotation (via a measurement away from the wire basis), we can simulate the "measurement" of the ν-matrix which is of central importance for any 1D MBQC resource state. We can extract the correlation length (ζ), the only other computationally relevant parameter, by simulating two consecutive rotations at spatially separated sites on the 1D chain.

As such MBQC schemes are simplest to analyse both analytically and numerically in odd

chains with open boundary conditions, we consider the ground state $|\Phi(\alpha)\rangle$ of the interpolation Hamiltonian

$$H_{\mathsf{O}}(\alpha) = -\cos\alpha \left(\sum_{i=2}^{N-1} Z_{i-1} X_i Z_{i+1} + X_1 Z_2 + X_N Z_{N-1} \right) - \sin\alpha \sum_{i=2}^{N-1} X_i. \tag{5.1}$$

For the rest of this thesis, all expectation values of observables are taken with respect to these resource states $|\Phi(\alpha)\rangle$ unless specified otherwise. With this choice of boundary conditions, the symmetry generators of the $\mathbb{Z}_2 \otimes \mathbb{Z}_2$ symmetry group are modified to

$$g_{\mathsf{o}} = X_1 X_3 X_5 \dots X_{N-2} X_N \text{ and } g_{\mathsf{e}} = Z_1 X_2 X_4 \dots X_{N-1} Z_N. \tag{5.2}$$

for odd chain lengths N.

Coming back to the computational scheme, let us consider a chain of length N on which our resource state is supported. We measure the first $N-1$ spins in a fixed basis, the outcomes of which are all recorded and the corresponding byproduct operators are applied to the last spin before it is measured also in different bases, for the purpose of state tomography.

The density matrix of our last[1] spin is

$$\rho_N = \sum_{\mathbf{s}} \sigma_N(\mathbf{s}) \langle \mathbf{s}|\Phi(\alpha)\rangle\langle\Phi(\alpha)|\mathbf{s}\rangle \sigma_N^\dagger(\mathbf{s}), \tag{5.3}$$

wherein $|\Phi(\alpha)\rangle$ is our resource state[2], $|\mathbf{s}\rangle$ corresponds to the post-measurement state on sites $1, 2, \dots, N-1$ and $\sigma(\mathbf{s})$ is the outcome-dependent byproduct operator.

The simplest non-trivial simulation "experiment" that comes to mind in this context is that of a single site rotation about the z-axis. To do so all but a special site is measured in the wire i.e. Pauli-X basis. The special site is chosen to be odd[3] and it is measured in the eigenbasis of the observable $O(\beta) = \cos\beta X - \sin\beta Y$. For small angles β, this introduces a unitary evolution $\sim \exp(-2i\nu_{01}\beta(Z/2))$ on our logical qubit up to leading order in β and the our all-important off-diagonal element ν_{01} of ν-matrix can be read off from such numerical simulations. This was done using the ITensor package in Julia [FWS20] and the resulting plot is shown in Fig. 5.1.

Note that these curves are consistent with our expectations since we see them monotonically decreasing as we move away from the cluster point. For small chain lengths, we see that there is some computational power left beyond the supposed transition point at $\alpha = \pi/4$. As we make the distance between the readout qubit and the rotation site smaller, the parameter $2\nu_{01}$ increases. This is understandable as the amount of entanglement required to transmit quantum information decreases as we take the rotation site closer to the read-out qubit.

These results look promising as we can apply such a procedure for any chain length and

[1] note this is the state of the last spin after the proper byproduct operators have been applied.
[2] thus the ground state at sweep parameter α
[3] this is just because we want to perform a z-rotation rather than a x-rotation.

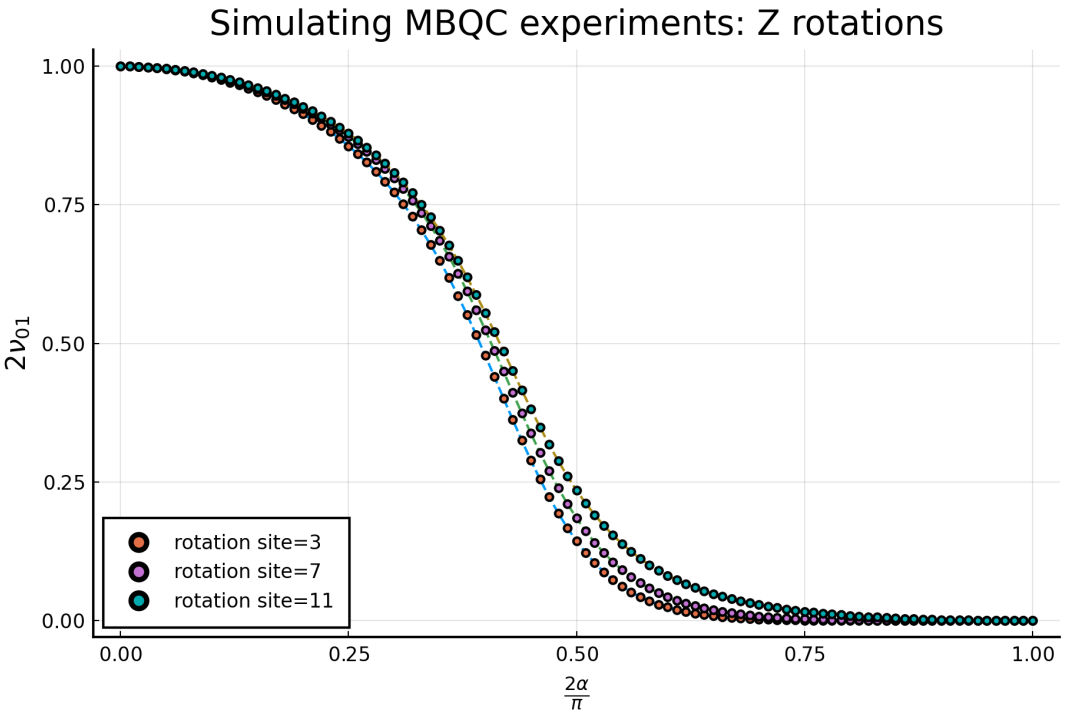

Figure 5.1: Parameter $2\nu_{01}$ as a function of the sweep parameter α for a small chain length of $N = 15$. The reason behind the multiplicity of curves are boundary effects—the curves are labeled by the qubit in the chain by whose non-Pauli measurement the rotation is implemented. The other relevant parameters in the simulation are – intended rotation angle $\beta = 10^{-2}$ radian and DMRG accuracy $= 10^{-12}$.

extract the corresponding ν_{01} parameter. However, it is prohibitively slow for large chain lengths. The reason is as follows. Each term in the expansion of Eq. 5.3 involves a separate MPS contraction which is efficient on its own. However, the number of terms in the sum scales exponentially with the length N, making the computationally accessible range quite limited. In the following section, we show how to overcome this computational barrier using some neat MBQC classical post-processing tricks.

5.2 A computational order parameter

The simulation results in Fig. 5.1 give us hope for classifying the states $|\Phi(\alpha)\rangle$ according to their ability as a resource to perform non-trivial computations. In this section, we improve upon the methods that are used to obtain such a classification. The central result that comes out of this analysis is a computational string-like order parameter. Below we describe how to arrive such a result using only MBQC relations.

If the last qubit in the chain is always measured for tomographic purposes, it suffices to restrict the measured observables A on the last qubit to Pauli operators. Next, we note that

the expectation value of the measurement observable is given by

$$\begin{aligned}
\mathsf{Tr}_N\left(\rho_N A_N\right) &= \mathsf{Tr}_N\left(\sum_{\mathbf{s}} \sigma_n(\mathbf{s})\langle\mathbf{s}|\Phi(\alpha)\rangle\langle\Phi(\alpha)|\mathbf{s}\rangle\sigma_N(\mathbf{s})^\dagger A_N\right) \\
&= \mathsf{Tr}\left(\sum_{\mathbf{s}} |\Phi(\alpha)\rangle\langle\Phi(\alpha)|\,|\mathbf{s}\rangle\langle\mathbf{s}| \otimes \sigma_N(\mathbf{s})^\dagger A_N \sigma_N(\mathbf{s})\right) \\
&= \mathsf{Tr}\left(\sum_{\mathbf{s}} |\Phi(\alpha)\rangle\langle\Phi(\alpha)|\,|\mathbf{s}\rangle\langle\mathbf{s}| \otimes (-1)^{f_A(\mathbf{s})} A_N\right) \\
&= \mathsf{Tr}\left(|\Phi(\alpha)\rangle\langle\Phi(\alpha)| \sum_{\mathbf{s}} (-1)^{f_A(\mathbf{s})}|\mathbf{s}\rangle\langle\mathbf{s}| \otimes A_N\right).
\end{aligned}$$

Therein, for every Pauli observable A, f_A is a linear function on the measurement record $\mathbf{s}$ that depends on which of the three Pauli observables A actually is.
Thus, the goal is to find a compact expression for

$$\tilde{A} := \sum_{\mathbf{s}} (-1)^{f_A(\mathbf{s})}|\mathbf{s}\rangle\langle\mathbf{s}| \otimes A_N. \tag{5.4}$$

We will now work out $\tilde{A}$ in Eq. 5.4 for successively more complicated and interesting cases. In all cases we assume for convenience that N is odd.

1. The Pauli observable for the final measurement is $A = X$, and no rotation is performed on the chain. The latter means that all measurements on the chain are in the X-basis.

   In this case the function f_X is

   $$f_X(\mathbf{s}) = \sum_{i \text{ odd}}^{N-1} s_i.$$

   Thus,

   $$\tilde{A}_X = X_1 X_3 X_5 \ldots X_{N-2} X_N.$$

   Note the subscript X on the l.h.s. denotes that the final qubit is measured in the X-basis. The advantage is that now we only need a single tensor contraction instead of 2^{N-1}.

   However, the case is actually too simple. The above $\tilde{A}$ is a symmetry (g_o), and so the expectation value is 1 for all α.

2. The Pauli observable for the final measurement is $A = Y$, and no rotation is performed on the chain. This means that all measurements on the chain before the last are in the X-basis.

   The function f_Y is

   $$f_Y(\mathbf{s}) = \sum_{i=1}^{N-1} s_i.$$

Thus,

$$\tilde{A}_Y = X_1 X_2 X_3 \ldots X_{N-2} X_{N-1} Y_N.$$

Again, the subscript on the l.h.s. denotes the measurement basis of the final qubit and the advantage is that we only need a single tensor contraction instead of 2^{N-1}.

But, again, this case is too simple. Using symmetry element $g_o = X_1 X_3 X_5 \ldots X_{N-2} X_N$, we have $g_o \tilde{A}_Y = -\tilde{A}_Y g_o$. Then,

$$\begin{aligned} \langle \Phi(\alpha) | \tilde{A}_Y | \Phi(\alpha) \rangle &= -\langle \Phi(\alpha) | g_o^\dagger \tilde{A}_Y g_o | \Phi(\alpha) \rangle \\ &= -\langle \Phi(\alpha) | \tilde{A}_Y | \Phi(\alpha) \rangle \\ &= 0. \end{aligned}$$

We will make use of such symmetry arguments later on.

3. The Pauli observable for the final measurement is $A = X$, and a z-rotation is implemented by measurement of the observable

$$O_k(\beta) = \cos\beta \; X_k - \sin\beta \; (\prod_{j=1}^{\frac{k-1}{2}} X_{2j}) \, Y_k \tag{5.5}$$

on a qubit location k (odd). Note that the product of the X operators on even sites before rotation elucidate the adaptive aspect of MBQC protocols.[4] All measurements on the chain, except for qubit k, are in the X-basis.

(i) The function f_X is $f_X(\mathbf{s}) = s_1 + s_3 + s_5 + \cdots + s_{N-2}$, as before.

(ii) Thus,

$$\tilde{A}_X = X_1 X_3 \ldots X_{k-2} O_k(\beta) X_{k+2} \ldots X_{N-2} X.$$

Inserting Eq. 5.5 and using the two earlier cases (with slight variation), we find

$$\langle \Phi(\alpha) | \tilde{A}_X | \Phi(\alpha) \rangle = \cos\beta, \;\; \forall \alpha. \tag{5.6}$$

4. The Pauli observable for the final measurement is $A = Y$, and a z-rotation is implemented by measurement of the observable $O(\beta)$ of Eq. 5.5.

(i)The function f_Y is

$$f_Y(\mathbf{s}) = \sum_{i=1}^{N-1} s_i.$$

(ii)Thus we find,

$$\tilde{A}_Y = X_1 X_2 \ldots X_{k-1} O_k(\beta) X_{k+1} \ldots X_{N-1} Y_N.$$

[4]Note that only the $\sin\beta$ term gets affected as it is an odd function of the measurement angle β which potentially gets flipped.

Using the same symmetry arguments (involving g_o) as above, we find

$$\begin{aligned}\langle\Phi(\alpha)|\tilde{A}_Y|\Phi(\alpha)\rangle &= -\sin\beta\,\langle\Phi(\alpha)|X_1X_3\ldots X_{k-2}Y_kX_{k+1}\ldots X_{N-1}Y_N|\Phi(\alpha)\rangle \\ &= \sin\beta\,\langle\Phi(\alpha)|Z_kX_{k+1}X_{k+3}\ldots X_{N-3}X_{N-1}Z_N|\Phi(\alpha)\rangle.\end{aligned} \tag{5.7}$$

Note that the operator remaining on the r.h.s. is a (string-like) element from the cluster state stabilizer.

5. The Pauli observable for the final measurement is $A = Z$, and a z-rotation is implemented by measurement of the observable $O(\beta)$ of Eq. 5.5.

   (i)The function f_Z is

   $$f_Y(\mathbf{s}) = \sum_{i\ \text{even}}^{N-1} s_i.$$

   (ii)Thus we find,

   $$\tilde{A}_Z = X_2X_4\ldots X_{k-1}X_{k+1}\ldots X_{N-1}Z_N.$$

   Note that such an operator *anti-commutes* in the symmetry element g_o (specifically at the final site). Thus, using the same arguments as in Eq. 2, we have

$$\begin{aligned}\langle\Phi(\alpha)|\tilde{A}_Z|\Phi(\alpha)\rangle &= \langle\Phi(\alpha)|X_2X_4\ldots X_{k-1}X_{k+1}\ldots X_{N-1}Z_N|\Phi(\alpha)\rangle \\ &= 0 \quad \text{(due to anti-commutation with } g_o\text{)}\ .\end{aligned} \tag{5.8}$$

The expansion Eq. 5.7 has computational advantage over the method of Section 5.1 (1 term vs. 2^{N-1} terms), and it allows to infer a quantity of primary interest, namely ν_{01}. We have

$$\boxed{\nu_{01}(\alpha) = \frac{1}{2}\langle\Phi(\alpha)|Z_kX_{k+1}X_{k+3}\ldots X_{N-3}X_{N-1}Z_N|\Phi(\alpha)\rangle.} \tag{5.9}$$

Such an expression[5] looks very close to the standard string order parameter that the topological condensed matter physicist is so familiar with. We will explore this connection next in Sec. 5.4. At any rate, keeping Eq. 5.6 and Eq. 5.7 in mind, we see that the entire computational scheme is defined merely by classical MBQC processing relations and we can explicitly write down the quantum channel that is applied on our logical qubit as

$$\boxed{\mathcal{T}(\rho_{\text{in}}) = \left(\frac{1}{2}+\nu_{01}\right)e^{-i\frac{\beta}{2}Z}(\rho_{\text{in}})\,e^{i\frac{\beta}{2}Z} + \left(\frac{1}{2}-\nu_{01}\right)e^{i\frac{\beta}{2}Z}(\rho_{\text{in}})\,e^{-i\frac{\beta}{2}Z}.} \tag{5.10}$$

As the Pauli measurements are tomographically complete, Eq. 5.10 represents the unique channel

[5]It is might be interesting to note that if we have done the above analysis for rotation at an even site (for a $x-$rotation), we arrive at a similar result, $2\nu_{01} = \langle Z_kX_{k+1}X_{k+3}\ldots X_N\rangle$, which again belongs to the stabilizer group of the cluster state.

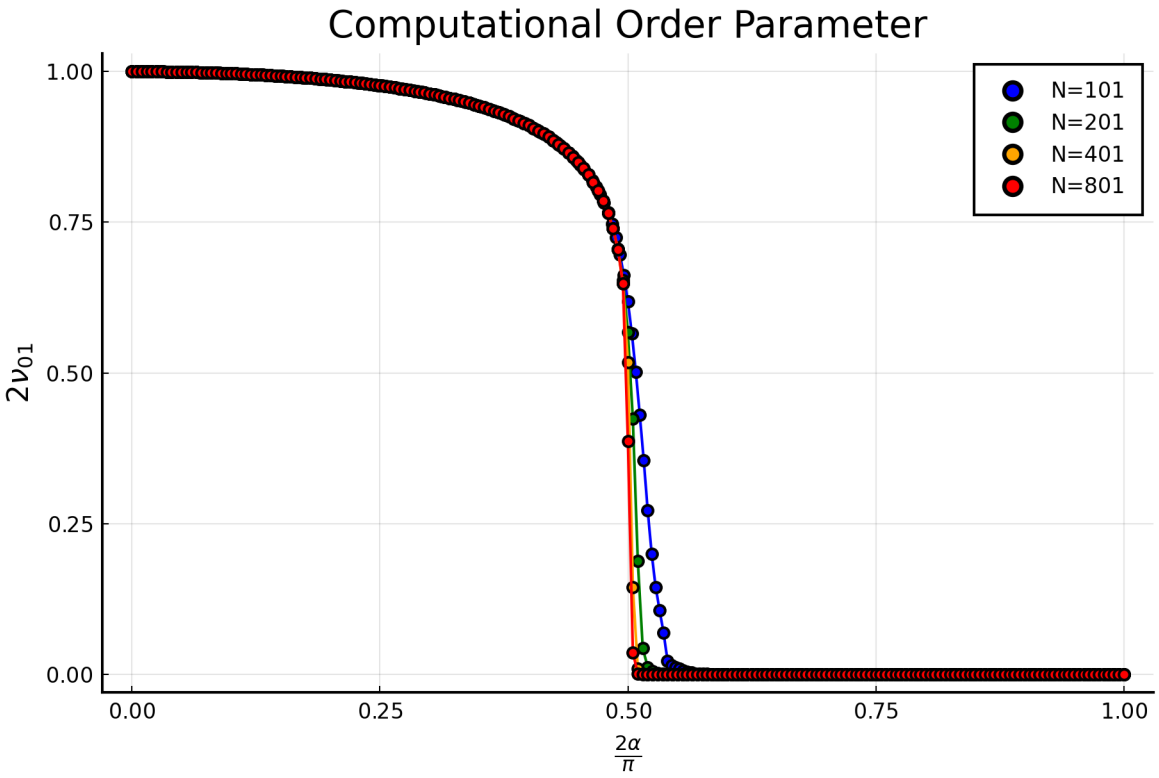

Figure 5.2: Plot of the computational order parameter $2\nu_{01}$ as a function of the sweep parameter α for different chain lengths N. Close to the supposed phase transition at $\alpha = \pi/4$, the curves get sharper with increasing system size. It is in this sense that ν_{01} is an order parameter as, in the thermodynamic limit, it exhibits a kink at the critical point $\alpha = \pi/4$.

action. To get an intuitive understanding of this mapping, see Fig. 5.3 and the discussion below. Notably, this expression is exact for arbitrary values of the rotation angle β, thereby improving on the expression in Eq. 3.38 which is reproduced in the small-angle limit (as expected).

5.3 Detour: Standard string order parameters

Standard string-like order parameters are expectation values of non-local operators which are used to distinguish between different SPT phases.

A translationally invariant state Ψ supported on a spin chain is said [PGWS$^+$08] to possess string order if there exist a local unitary (on-site symmetry) $u \neq \mathbb{I}$ and local operators A, B (which can be taken to be hermitian) such that

$$\lim_{L\to\infty} |\mathrm{SOP}_L(A, B, u, \Psi)| > 0, \tag{5.11}$$

$$\mathrm{SOP}_L(A, B, u, \Psi) := \left\langle \Psi \middle| A \otimes u^{\otimes L} \otimes B \middle| \Psi \right\rangle . \tag{5.12}$$

If we assume that we are dealing with SRE states with correlation length ζ, the value of SOP_L becomes independent of L for $L \gg \zeta$. It is instructive to note that these parameters are defined

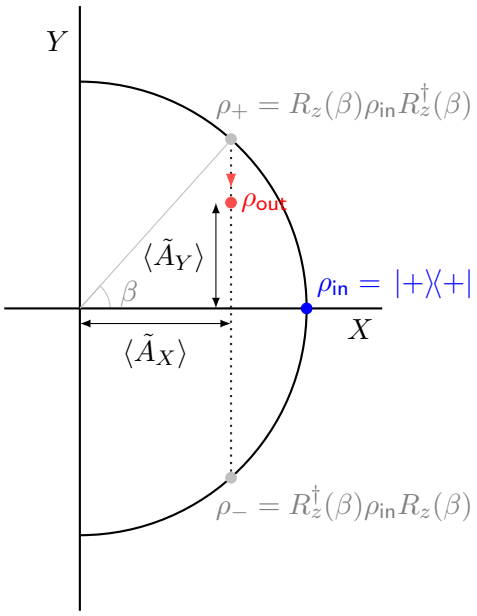

Figure 5.3: Bloch sphere graphical representation of the channel $\mathcal{T} : \rho_{\text{in}} \mapsto \rho_{\text{out}}$: for simplicity, we consider simulating a circuit with $\rho_{\text{in}} = |+\rangle\langle+|$. The downward pointing (red) arrow represents the deviation of the actual output state ρ_{out} from the desired final state ρ_+. As α is ramped up, the red dot representing ρ_{out} approaches the x-axis along the dotted vertical line. We note that for $\nu_{01}(\alpha) = 0$, the red dot is situated on the x-axis and no logical rotation is performed, as expected.

at the bulk and have two endpoints (wherever A and B's non-trivial action ends). This fact will become important when we try to relate them to the computational order parameter that we just defined in the last section. More on that later.

Coming back to the cluster case at hand, we have the bulk on-site symmetry generators, $u_{\text{o}} = XI$ and $u_{\text{e}} = IX$. Following the recipe above, we can define, for example,

$$\text{SOP}_L(Z, Z, u_{\text{e}}) := \langle Z_k X_{k+1} X_{k+3} \cdots X_{k+2L-1} Z_{k+2L} \rangle \text{ for odd values of } k. \tag{5.13}$$

For the cluster state ($\alpha = 0$) itself, the value of SOP is just unity as the string operator can be constructed by merely stringing together the cluster stabilizers

$$\begin{aligned} \text{SOP}_L(Z, Z, u_{\text{e}}, C) &= \langle K_{k+1} \cdot K_{K+3} \cdots K_{k+2L-1} \rangle_C \\ &= 1 \text{ regardless of the length } 2L. \end{aligned}$$

wherein the stabilizers $K_k := Z_{k-1} X_k Z_{k+1}$ and we have used Eq. 3.5 to arrive at the second line.

However, for other points under consideration, we do need to put in some honest work. Well, not quite. In practice, we make our laptop do the work for us by finding an efficient DMRG approximation to these ground states and then calculating the expectation value of

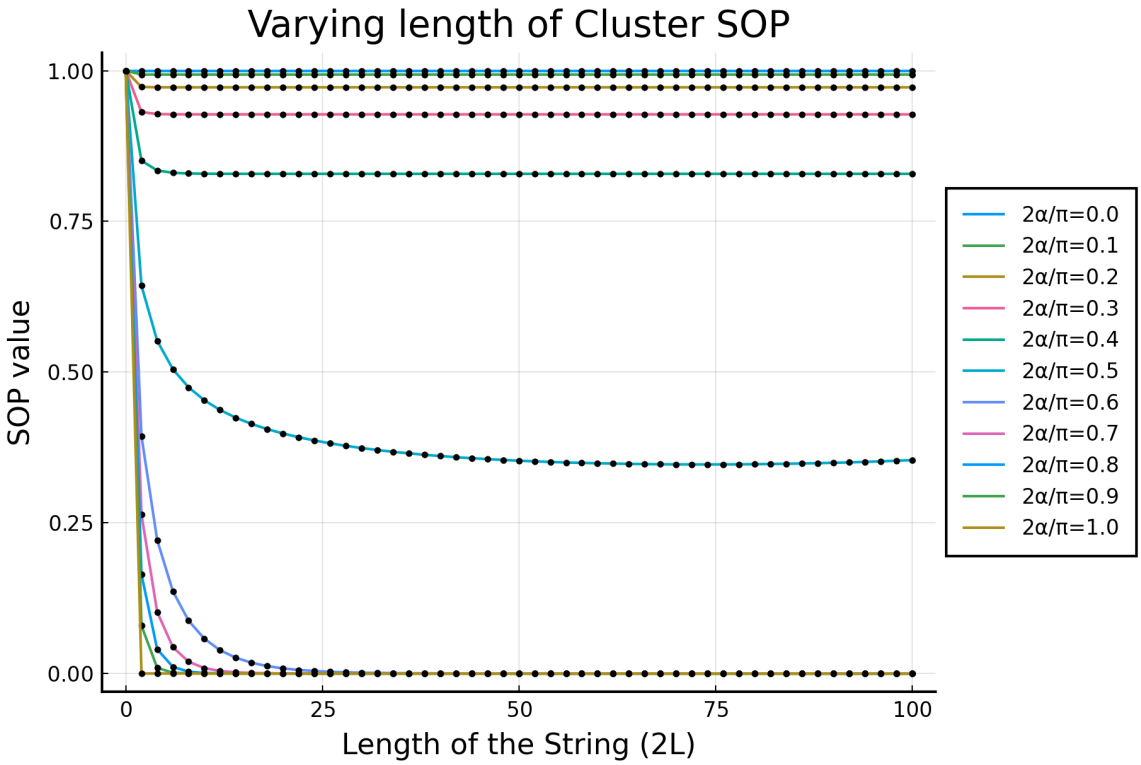

Figure 5.4: Numerical confirmation of convergence of SOP_L as a function of L for chain length $N = 201$ and DMRG accuracy 10^{-15}. The multiplicity of plots are due to different value of the sweep parameter α. See text for relevant discussion.

these non-local operators. This is bread and butter for DMRG/ITensor and in Fig. 5.4, we do see a non-vanishing SOP for $\alpha \in (0, \pi/4)$.

Finite size effects: As far as the SOP_L is concerned, we expect it to have some weak dependence on L. Namely, (a) $\text{SOP}_0 = 1$ as it is just the expectation value of the identity operator. (b) For "large" values of L, it approaches a constant. (c) In-between, we expect a length dependence with a characteristic length scale (ζ) that increases as the sweep parameter α is ramped up. All of these predictions are numerically confirmed by the numerics in Fig. 5.4.

5.4 Properties of order parameters

Having defined the computational order parameter and reviewed the concept of standard order parameters in the cluster phase, we are now fully equipped to explore the relationship between them. Furthermore, properties of these order parameters also allow us to extract ζ, the only other relevant parameter for computation, as a function of the sweep parameter α. In this regard, it is useful to (re)define the following operators for a chain of length N (odd),

$$
\begin{aligned}
K_k^+ &:= Z_k X_{k+1} X_{k+3} \dots X_N, && \text{for } k \text{ even},\\
K_k^+ &:= Z_k X_{k+1} X_{k+3} \dots X_{N-1} Z_N, && \text{for } k \text{ odd},\\
K_l^- &:= X_1 X_3 \dots X_{l-1} Z_l, && \text{for } l \text{ even},\\
K_l^- &:= Z_1 X_2 X_4 \dots X_{l-1} Z_l, && \text{for } k \text{ odd},\\
\overline{K}_{l,k} &:= Z_l X_{l+1} X_{l+3} \dots X_{k-3} X_{k-1} Z_k, && \text{for } k,l \text{ both odd or even}.
\end{aligned}
\tag{5.14}
$$

For future reference, note that $\mathrm{SOP}_{L=(|k-l|/2)} \equiv \langle \overline{K}_{l,k} \rangle$ and $2\nu_{01} \equiv \langle K^+ \rangle$.

Square relation between order parameters: We observe that, as a consequence of the definitions of Eq. 5.14, the product $K_l^- \overline{K}_{l,k} K_k^+$, for all choices of k, l both odd or both even, is a symmetry (g_o or g_e) of the considered spin chain. Therefore, for all sweep parameters α it holds for the expectation values of any symmetric state, in particular the ground state, that

$$
\langle K_l^- K_k^+ \rangle_{\Phi(\alpha)} = \langle \overline{K}_{l,k} \rangle_{\Phi(\alpha)}. \tag{5.15}
$$

Furthermore, if k and l are sufficiently far apart and the ground state $|\Phi(\alpha)\rangle$ is short range entangled, then $\langle K_l^- K_k^+ \rangle_{\Phi(\alpha)} = \langle K_l^- \rangle_{\Phi(\alpha)} \langle K_k^+ \rangle_{\Phi(\alpha)}$. This arises as follows. If $|\Phi(\alpha)\rangle$ is short-range entangled, then we can create it from a product state $|+(N)\rangle := |+\rangle_1 \otimes |+\rangle_2 \otimes .. \otimes |+\rangle_N$ by a short-range entangling unitary $U(\alpha)$. Then, defining further $\tilde{K}^-_{l+\delta(\alpha)} := U^\dagger(\alpha) K_l^- U(\alpha)$, $\tilde{K}^+_{k-\delta(\alpha)} := U^\dagger(\alpha) K_k^+ U(\alpha)$,

$$
\begin{aligned}
\langle K_l^- K_k^+ \rangle_{\Phi(\alpha)} &= \mathrm{Tr}\left(U(\alpha) |+(N)\rangle\langle +(N)| U^\dagger(\alpha) K_l^- K_k^+ \right)\\
&= \mathrm{Tr}\left(|+(N)\rangle\langle +(N)| \left[U^\dagger(\alpha) K_l^- U(\alpha)\right] \left[U^\dagger(\alpha) K_k^+ U(\alpha)\right] \right)\\
&= \langle \tilde{K}^-_{l+\delta(\alpha)} \rangle_+ \langle \tilde{K}^+_{k-\delta(\alpha)} \rangle_+ .
\end{aligned}
$$

The last line follows by observing that the operator $\tilde{K}^-_{l+\delta(\alpha)}$ has support only the left $l+\delta(\alpha)$ qubits, and $\tilde{K}^+_{k-\delta(\alpha)}$ has support only qubits $k-\delta(\alpha)$ onwards. Therefore, if $l+\delta(\alpha) < k-\delta(\alpha)$, and since the expectation value is taken w.r.t. a product state, the expectation value factorizes.

An analogous argument to the above yields

$$
\langle K_l^- \rangle_{\Phi(\alpha)} = \langle \tilde{K}^-_{l+\delta(\alpha)} \rangle_+, \ \langle K_k^+ \rangle_{\Phi(\alpha)} = \langle \tilde{K}^+_{k-\delta(\alpha)} \rangle_+ .
$$

Putting the last three relations together yields $\langle K_l^- K_k^+ \rangle_{\Phi(\alpha)} = \langle K_l^- \rangle_{\Phi(\alpha)} \langle K_k^+ \rangle_{\Phi(\alpha)}$. Furthermore, for $l \gg 0$ and $k \ll N$ the expectation values become constant in k and l respectively, and we may drop those indices. Also, by reflection symmetry, $\langle K^+ \rangle_{\Phi(\alpha)} = \langle K^- \rangle_{\Phi(\alpha)}$. Therefore, finally,

$$
\boxed{\langle \overline{K} \rangle_{\Phi(\alpha)} = \langle K^+ \rangle^2_{\Phi(\alpha)} = \langle K^- \rangle^2_{\Phi(\alpha)}.} \tag{5.16}
$$

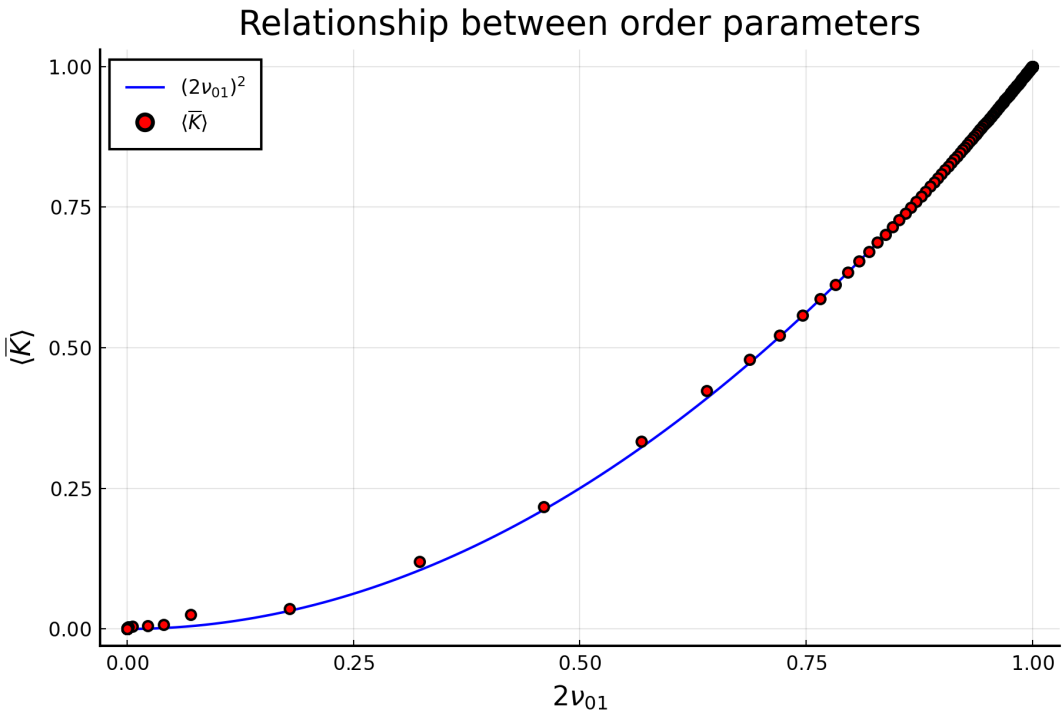

Figure 5.5: Numerical confirmation of Eq. 5.16 for chain length $N = 201$, DMRG accuracy$=10^{-15}$. Note that $2\nu_{01} = \langle K^+\rangle = \langle K^-\rangle$. The small deviations are presumably because of the questionable reliability of DMRG close to criticality where the gap becomes vanishingly small for large systems and the bond dimension of the MPS representation blows up.

Even-odd decoupling: From Fig. 5.4, we can infer that if we wanted to perform two z-rotations on a chain, the wise thing to do will be separating them out (which is expected from the picture that emerges from the standard treatment of SPT-MBQC, e.g. Fig. 3.2). To be more specific, when the rotations are separated by large distance, we can treat them independently and just add up the decoherence introduced by each of the operations (See Fig. 5.8 and Eq. 5.23 for more lucid explanations). If the rotation sites are close together, the total decoherence on our logically qubit is *greater* than the sum of the decoherence incurred by individual operations. A pair of rotations implemented on an even and an odd site, respectively – that is a x and a z-rotation – do not interact in this fashion. Rather, the total amount of decoherence introduced appears to be independent of the separation. This goes back to the now numerically established fact that

$$\langle K_l^+\rangle_{\Phi(\alpha)}\langle K_{l+1}^+\rangle_{\Phi(\alpha)} = \langle K_l^+ K_{l+1}^+\rangle_{\Phi(\alpha)}. \tag{5.17}$$

This relation holds, to eyesight accuracy, almost in the entire cluster phase (See Fig. 5.6 for graphical display). Deviations appear near the phase transition, but these may well be numerical inaccuracies.

The even-odd decoupling seems weird. Qualitatively and quantitatively, Fig. 5.6 displays a similar decoupling as Fig. 5.5. However, the physical mechanism is different. For the expectation

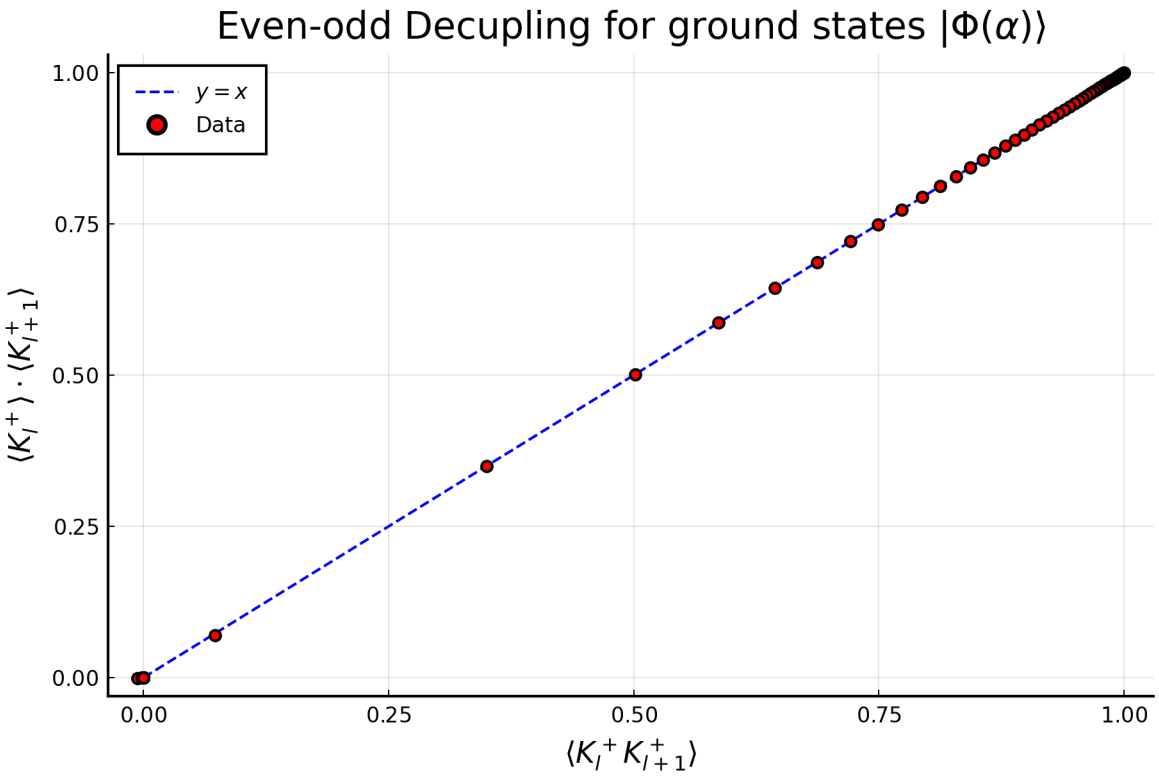

Figure 5.6: Even-odd decoupling (for a chain length of $N = 201$ and DMRG accuracy $= 10^{-12}$). On the vertical axis, the product of expectation values $\langle K_l^+\rangle_{\Phi(\alpha)}\langle K_{l+1}^+\rangle_{\Phi(\alpha)}$ is plotted, and on the horizontal axis the expectation value of the product observable, $\langle K_l^+ K_{l+1}^+\rangle_{\Phi(\alpha)}$, with the sweep angle α as an implicit parameter. Within eyesight accuracy, the order parameters $\langle K_l^+\rangle_{\Phi(\alpha)}$ and $\langle K_{l+1}^+\rangle_{\Phi(\alpha)}$ are uncorrelated. The value of l chosen here is 51 but the particular value is irrelevant as long as it is in the bulk.

values plotted in Fig. 5.5, the parabolic relation $\langle K_l^- K_k^+\rangle_{\Phi(\alpha)} = \langle K_l^-\rangle_{\Phi(\alpha)}\langle K_k^+\rangle_{\Phi(\alpha)}$ holds only when $|k-l|$ is much larger than the correlation length. This relation is based on the short-rangeness of entanglement. However, the uncorrelatedness displayed in Fig. 5.6 must have a different origin. The starting points of the operators K_l^+ and K_{l+1}^+ are only a single site apart, which is short deep into the phase.

Correlation length scaling: The correlation length ζ can be extracted from the pattern of SOP decay as shown in Fig. 5.4. Such a correlation length is expected to follow a scaling relation like $\zeta(\alpha) \propto |1 - 4\alpha/\pi|^{-\gamma}$ near the phase transition at $\alpha = \pi/4$ due to scale invariant physics of quantum phase transitions. The scaling exponent γ has been extracted from a logarithmic plot shown in Fig. 5.7. From the plot, it looks like $\gamma \approx 0.66$ which is somewhat weird.[6] We expect the scaling exponent to be 1 as the model under consideration can be mapped (modulo

[6]Without meaning to cause more confusion, for the sake of full disclosure, to extract the correlation length from Fig. 5.7, we have ignored the first point ($\text{SOP}_{L=0} = 1$) in the SOP decay plot and used an exponential fit. If one doesn't do so and fits a double-exponent curve to the plot, one arrives at an messier plot that for some reason provides the proper scaling exponent (See here).

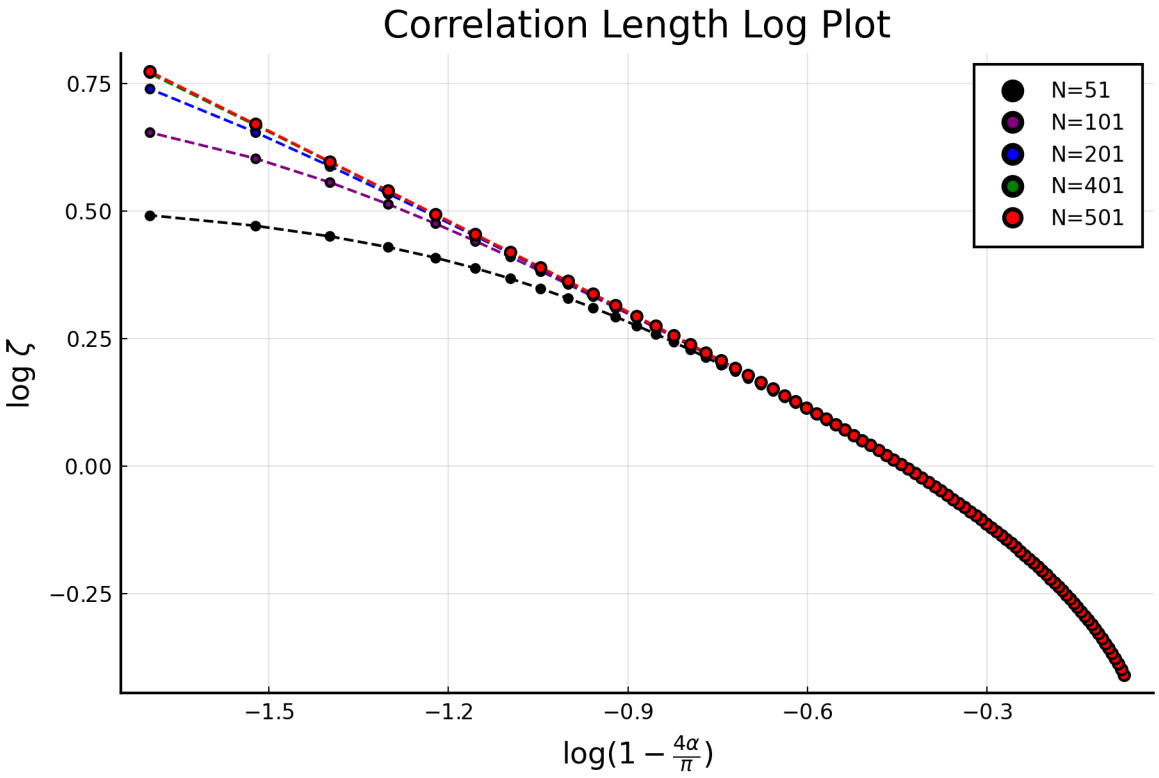

Figure 5.7: Correlation length scaling as a function of distance from the critical point (DMRG accuracy 10^{-12}). The multiplicity of plots are due to different lengths of the chain. We see finite-size effects on the left-hand side of the plot where the correlation length diverges.

boundary conditions) to a 2D Ising model. The only resolution that comes to mind is as follows: the mapping used between the two models (via a Jordan-Wigner transformation) is likely *non-local* and it might be possible that such a non-local mapping does not preserve even the most fundamental properties like the scaling behaviour of quantum phase transitions.

5.5 Decoherence management for finite chains

At this point of the thesis, we have shown how simple MBQC side processing is enough to analyse computational power of SPT ordered states. The obvious advantage of this formalism is its applicability to finite systems and arbitrarily rotation angles. Such a prescription stands on its own legs but in this section, we show that it in fact allows us to investigate regimes of computation that were inaccessible to previous methods. To this end, we discuss the management of the inherent logical decoherence (involved with performing non-trivial logical operations) in finite spin chains. The culmination of this analysis reveals dependent but efficient regimes of operation.

Imagine we are given a quantum state that has n (assumed to be even) qubits at the bulk (thereby protected from boundary effects) and lies somewhere in the cluster "phase".[7] With

[7] the term "phase" is being used loosely here keeping in mind that we are dealing with finite systems; equiva-

the aim of performing a (small) single-qubit logical rotation on our encoded qubit, we would like to make the best use of our resources. In this section, we lay out the optimal measurement scheme on these n qubits to minimize the loss in purity of our logical qubit.

5.5.1 Testing the waters: Splitting rotation angle in two

To set up our notation, let us label the n sites of interest from left to right and consider the simple situation where the actual logical rotation to be performed is split up into two (by performing measurements away from the symmetry respecting basis) on the two sites labeled as k and l. The distance between these two special sites ($\Delta = |k - l|$) is allowed to vary. It was already known from previous work that as long as the separation Δ is considerably larger than the relevant (correlation) length scale in the problem, the two rotations are independent of each other and this amounts to a reduction in the logical error by a factor of 2. In the following paragraphs, we extend this notion by quantifying the logical error for arbitrary values of Δ.

To get to such an expression, it is imperative to apply the techniques developed in the previous section to our two-site rotation scenario. Due to arguments presented there, it is sufficient to consider only Pauli measurements on the readout qubit and all that remains to figure out is the expectation value of the operator $\tilde{A}$ defined in Eq. 5.4.

1. To start, we consider the case when the Pauli observable for the readout qubit is X and two z-rotations (each by an angle $\gamma = \beta/2\,\langle K^+ \rangle$) are performed on sites k and l (both odd) via the measurement of the observables

$$O_i\,(\gamma) \,= \cos\gamma\; X_i - \sin\gamma\; (\prod_{j=1}^{\frac{i-1}{2}} X_{2j})\, Y_i, \tag{5.18}$$

for two special sites $i = k, l$. All other sites in the chain are measured in the X-basis.

(i) The function f_X is $f_X(\mathbf{s}) = s_1 + s_3 + s_5 + .. + s_{N-2}$, as is always the case for X measurements on the final qubit.

(ii) Thus, by definition

$$\widetilde{A}_X = X_1 X_3 ... X_{k-2} O_k\,(\gamma)\, X_{k+2} ... X_{l-2} O_l\,(\gamma)\, X_{l+2} ... X_N.$$

(iii) Now inserting Eq. 5.18 we see that there are four terms that can potentially contribute to the expectation value of $\langle \Phi(\alpha)|\widetilde{A}_X|\Phi(\alpha)\rangle$ where $|\Phi(\alpha)\rangle$ denotes the ground state of our interpolation Hamiltonian. However, the terms consisting of a single Y at either one of the odd sites anti-commute with the symmetry element $g_o = X_1 X_3 X_5 ... X_{N-2} X_N$ and thereby don't contribute to the expectation value. Taking the other two terms into

lently one can just think of the interpolation parameter α lying in the interval $(0, \frac{\pi}{4})$.

account and using the same symmetry element g_{o}, we find

$$\begin{aligned}\langle\Phi(\alpha)|\widetilde{A}_X|\Phi(\alpha)\rangle &= \cos^2\gamma - \sin^2\gamma\,\langle Z_k X_{k+1} X_{k+3} ... X_{l-1} Z_l\rangle \\ &=: \cos^2\gamma - \sin^2\gamma\,\langle\overline{K}_{k,l}\rangle,\end{aligned}$$

where the second (new) term arises when we consider the contribution from the measurement pattern corresponding to Y in both the sites k and l.

2. When the final measurement is performed in the Pauli-Y basis, with all other parameters left unchanged from the above discussion:

   (i) The function f_Y is $f_Y(\mathbf{s}) = s_1 + s_2 + s_3 + s_4 + \ldots + s_{N-2} + s_{N-1}$.

   (ii) Therefore, we can readily write down

$$\widetilde{A}_Y = X_1 X_2 ... X_{k-1} O_k(\gamma)\, X_{k+1} X_{k+2} ... X_{l-1} O_l(\gamma)\, X_{l+1} X_{l+2} ... Y_N.$$

   (iii) Using the same symmetry arguments involving g_{o}, we arrive at the expression

$$\begin{aligned}\langle\widetilde{A}_Y\rangle_{\Phi(\alpha)} &= \sin\gamma\,\cos\gamma\,\langle Z_k X_{k+1} X_{k+3} ... X_{N-1} Z_N + Z_l X_{l+1} X_{k+3} ... X_{N-1} Z_N\rangle \\ &= \sin\gamma\,\cos\gamma\,\langle K_k^+ + K_l^+\rangle.\end{aligned}$$

Before moving on, let us note that the expectation values of all the string order parameters involved in the expression above are exactly 1 for $\alpha = 0$ as they belong to the stabilizer group of the cluster state. This reduces the relevant expressions to

$$\langle\widetilde{A}_X\rangle_C = \cos 2\gamma = \cos\beta \qquad \text{and} \qquad \langle\widetilde{A}_Y\rangle_C = \sin 2\gamma = \sin\beta\,,$$

which is consistent with what we know about the cluster state. In particular, this tells us that for the cluster state itself, spacing rotations out is unnecessary as the expectation values are independent of the site labels k and l.

To quantify the logical error introduced into the computational scheme for resource states away from the cluster point, we introduce the following decoherence metric[8]

$$\text{Loss of Purity (LP)} := \left[1 - \langle\widetilde{A}_X\rangle^2 - \langle\widetilde{A}_Y\rangle^2\right]. \tag{5.19}$$

We also restrict ourselves to small rotation angles and thus be satisfied by results to leading order in perturbation theory. Under these considerations, we can approximate the 2-site rotation expectation values to

$$\langle\widetilde{A}_X\rangle = 1 - \gamma^2 - \gamma^2\,\langle\overline{K}_{k,l}\rangle + O(\gamma^4), \qquad \langle\widetilde{A}_Y\rangle = \gamma\,\langle K_k^+ + K_l^+\rangle + O(\gamma^3).$$

[8] In the standard definition of decoherence metric, there would be contributions from $\langle\tilde{A}_Z\rangle$ as well. However, for the situation at hand, this is always zero due to anti-commutation arguments presented in Eq. 5.8.

Thereby, using the decoherence metric (defined in Eq. 5.19), we arrive at the expression

$$\mathsf{LP}_2 = \gamma^2 \left(2 + 2\,\langle \overline{K}_{k,l} \rangle - \langle K_k^+ + K_l^+ \rangle^2\right) + O(\gamma^4), \tag{5.20}$$

where the subscript on the l.h.s. just denotes the number of sites at which a measurement away from the X basis has been performed. The expression looks simple enough but it turns out it can be further simplified making use of two central properties of the order parameters.

(i) As long as we are working with sites at the bulk, $\langle K_k^+ \rangle = \langle K_l^+ \rangle =: \langle K^+ \rangle = 2\nu_{01}$, regardless of the site labels.

(ii) $\langle \overline{K}_{k,l} \rangle$ depends on $\Delta =\mid k - l \mid$ only.[9] Moreover, $\langle \overline{K}_{\Delta} \rangle$ is a strictly decreasing function of Δ with $\langle \overline{K}_{\Delta=0} \rangle = 1,\ \langle \overline{K}_{\Delta \gg 0} \rangle \to \langle K^+ \rangle^2$.

All this can be conveniently summed up in the expression

$$\boxed{\langle \overline{K}_{\Delta} \rangle = \langle K^+ \rangle^2 + \left(1 - \langle K^+ \rangle^2\right)\ f(\Delta),} \tag{5.21}$$

where $f(x)$ is a strictly (and rapidly) decreasing function of its argument with $f(x=0) = 1,\ f(x \gg 0) \to 0$ and thus easier to deal with.

This expression will be central to proving our final result about the optimal measurement pattern as we will see later. For now, we can just substitute Eq. 5.21 to Eq. 5.20 and simplify to

$$\begin{aligned} \mathsf{LP}_2 &\approx \gamma^2 \left[2 + 2\,\langle K^+ \rangle^2 + 2\left(1 - \langle K^+ \rangle^2\right) f(\Delta) - 4\,\langle K^+ \rangle^2\right] \\ &= \gamma^2 \left(1 - \langle K^+ \rangle^2\right)\,(2 + 2f(\Delta))\,, \end{aligned} \tag{5.22}$$

which can be used to calculate the decoherence metric (to leading order) for arbitrarily spaced out rotations as long as we know the functional form of $\langle \overline{K}_{\Delta} \rangle$ from some numerical simulation method like DMRG (See Fig. 5.8).

This is a marked difference between this new formalism compared to that discussed in [RWP$^+$17] where only the scaling laws were known for large values of Δ. For the sake of consistency, we see that the decoherence metric is indeed reduced in half if the two rotations are "separated far enough and don't talk to each other"

$$\frac{\mathsf{LP}_2(\Delta \gg 0)}{\mathsf{LP}_2(\Delta = 0)} = \frac{2 + 2 \cdot f(\Delta \gg 0)}{2 + 2 \cdot f(\Delta = 0)} \to \frac{2}{2+2} = \frac{1}{2}\,. \tag{5.23}$$

Having gone through this toy example, we might start to wonder if this is a general feature. That is to say, given access to a constant number of qubits in a chain, can the rotation angle be

[9] When we say "only", we are considering its' value at a particular value of α which is always an implicit parameter.

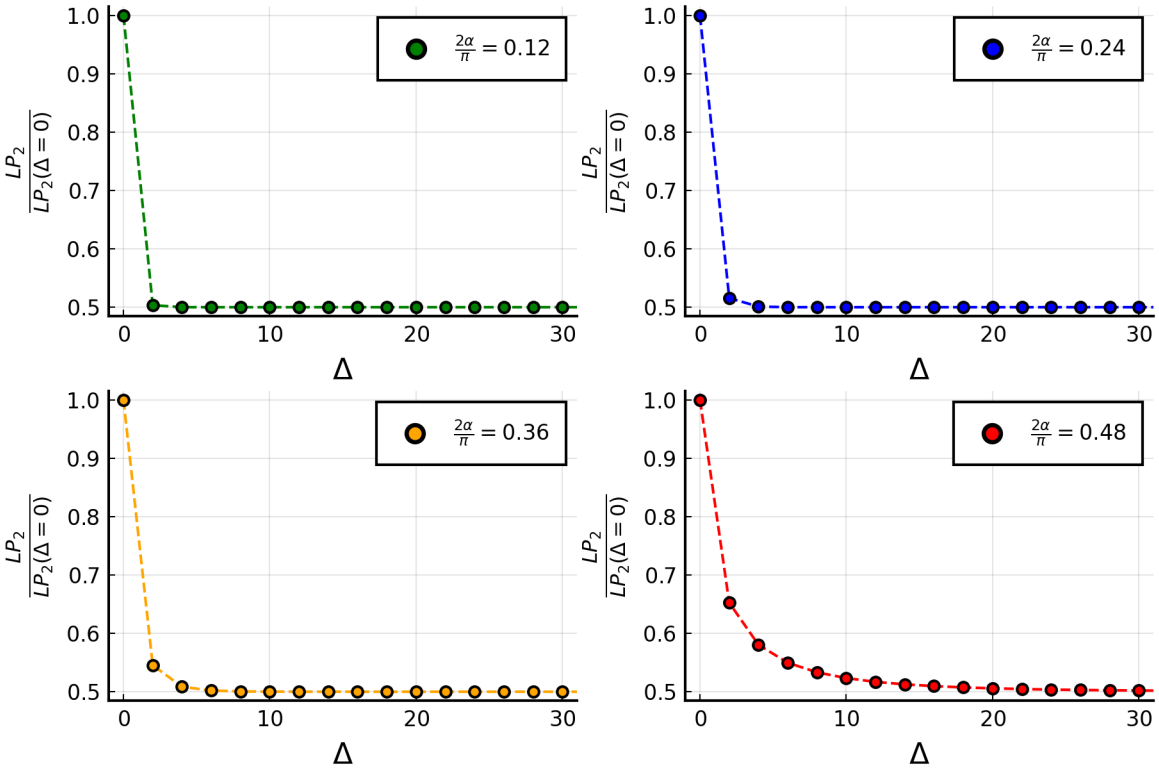

Figure 5.8: Divide and conquer at play: Reduction in the (normalised) decoherence metric as a function of the distance Δ between two rotation sites for a chain length of $N = 201$. The different plots are for varied values of our sweep parameter α and for each of them, after some characteristic length scale ($\sim \zeta(\alpha)$), the metric approaches the value of 0.5. We further see signs of the correlation length $\zeta(\alpha)$ diverging as we approach criticality at $\frac{2\alpha}{\pi} = 0.50$.

split up as much as possible to reduce the decoherence metric as defined in Eq. 5.19 ? Notice that as long as n is finite, the more the rotation angle is split up, two consecutive rotations become closely spaced and arguments of the type in Eq. 5.23 don't go through. Hence, it is not a priori clear what the optimal splitting strategy should be and if it is dependent on the value of our interpolation parameter α.

5.5.2 Error for arbitrary splitting of the rotation angle

Now, we consider the task of performing a logical rotation by β about the z-axis with the goal of minimising decoherence. Following the divide and conquer strategy, we split the rotation angle up into m parts. Consequently, the measurement observables in the chain are given by

$$O_i = \begin{cases} \cos(\gamma)X_i - \sin(\gamma)Y_i\ , & \text{for } i \in \mathcal{R} \qquad \text{where } \ \gamma = \frac{\beta}{m\langle K^+ \rangle} \\ X_i\ , & \text{otherwise} \end{cases} \tag{5.24}$$

wherein $\mathcal{R} := \{r_1, r_2, ..., r_m\}$ just contains the site labels where a measurement is performed away from the X basis. Furthermore, as the rotations are equally spaced if we denote the spacing

between two consecutive rotations by Δ, for n sites at our disposal, we have the constraint, $m \cdot \Delta = n$. Following the exact recipe laid out in the last section, we arrive at the following expressions for our all important expectation values

$$\langle \widetilde{A}_X \rangle = (\cos\,\gamma)^m - (\cos\,\gamma)^{m-2}\,(\sin\,\gamma)^2 \sum_{a,b\in\mathcal{R}} \langle \overline{K}_{a,b} \rangle + \text{ terms including } (\sin\,\gamma)^4,$$
$$\langle \widetilde{A}_Y \rangle = (\sin\,\gamma)(\cos\,\gamma)^{m-1} \sum_{a\in\mathcal{R}} \langle K^+_a \rangle + \text{ terms including } (\sin\,\gamma)^3.$$

For small angles γ, we can ignore the higher-order terms and this is what are going to do in the calculations that follow. However, as a side comment, we do note that if we were diligent enough we can perform exact calculations for arbitrary values of m, although the expressions that come out wouldn't be pretty and would have little explanatory power.
Thus, to leading order approximations we have

$$\begin{aligned}
\langle \widetilde{A}_X \rangle &\approx 1 - \frac{m\gamma^2}{2} - \gamma^2 \sum_{a,b\in\mathcal{R}} \langle \overline{K}_{a,b} \rangle\,, \\
\langle \widetilde{A}_Y \rangle &\approx \gamma \sum_{a\in\mathcal{R}} \langle K^+_a \rangle\,, \\
\mathsf{LP}_m &\approx \gamma^2 \left[m + 2 \sum_{a,b\in\mathcal{R}} \langle \overline{K}_{a,b} \rangle - (\sum_{a\in\mathcal{R}} \langle K^+_a \rangle)^2 \right].
\end{aligned} \tag{5.25}$$

The final expression can be further simplified using familiar properties of the string order parameters as noted in Eq. 5.21. Putting everything together and rearranging, we arrive at the rather compact expression

$$\mathsf{LP}_m = \gamma^2 \,\left(1 - \,\langle K^+ \rangle^2\right)\,\left[m + 2 \sum_{j=1}^{m-1} (m-j)\, f(j\Delta) \right] \,+\, O\left(\gamma^4\right).$$

Plugging in the value of γ needed to perform a logical z-rotation by β, we have

$$\mathsf{LP}_m = \left(\frac{\beta}{m}\right)^2 \,\left(\frac{1}{\langle K^+ \rangle^2} - 1\right)\,\left[m + 2 \sum_{j=1}^{m-1} (m-j)\, f(j\Delta) \right] \,+\, O\left(\gamma^4\right). \tag{5.26}$$

To see the explicit dependence on m, it is instructive to write the above as

$$\boxed{\mathsf{LP}_m \approx \beta^2 \,\left(\frac{1}{\langle K^+ \rangle^2} - 1\right)\, F(m),} \tag{5.27}$$

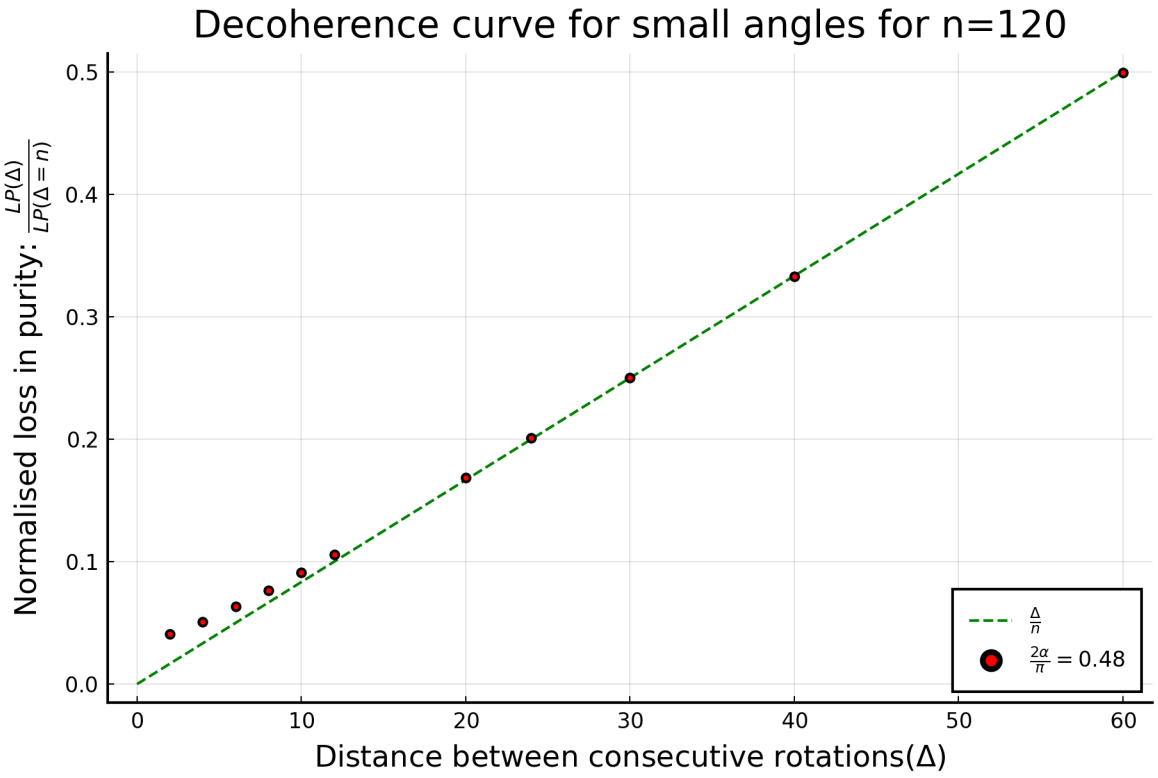

Figure 5.9: Numerical simulation of the normalised decoherence metric as a function of the distance between two consecutive rotation sites Δ, close to the phase transition. Deviations from the green straight line indicate the regime $\Delta \gtrsim \zeta$ where the individual rotations cannot just be considered separately. Remarkably, we see that it is in this regime that the decoherence is minimised.

wherein

$$F(m) = \frac{m + 2\sum_{j=1}^{m-1}(m-j)\cdot f(j\Delta)}{m^2}.$$

As m and Δ are dependent parameters we can always equivalently write

$$F(\Delta) = \frac{\Delta}{n}\left(1 + 2\sum_{j\Delta=\Delta}^{n-\Delta} f(j\Delta)\right) - \frac{2\Delta}{n^2}\sum_{j\Delta=\Delta}^{n-\Delta} \cdot(j\Delta)f(j\Delta)\ . \tag{5.28}$$

Although $f(\Delta)$ is a rapidly decreasing function, $F(\Delta)$ turns out to be a *strictly increasing function of* Δ.[10] Thus, to minimise the loss in purity, *consecutive rotations should be spaced as close as possible corresponding to* $\Delta = 2$ (See Fig. 5.9). In this regime, the rotations are dependent on each other as they are within the relevant (correlation) length scale. However, the penalty paid for this dependence is more than compensated by the gain from the increased

[10] Thereby a strictly decreasing function of the number of splittings m.

splitting of the logical rotation angle. Combining this information with Eq. 5.27 we have

$$\mathsf{LP}^{\mathsf{min}} \approx \beta^2 \left(\frac{1}{\langle K^+ \rangle^2} - 1 \right) F(\Delta = 2). \tag{5.29}$$

For large values of n, $F(\Delta = 2)$ can be approximated as

$$F(\Delta = 2) = \frac{2}{n} \left(1 + \sum_{j=1}^{\frac{n}{2}-1} f(2j) \right) + O\left(\frac{1}{n^2} \right).$$

In this entire discussion, we have suppressed the implicit dependence of our expressions on the interpolation parameter just to avoid cluttering the notation. Plugging them back, we arrive at the final result of this section

$$\mathsf{LP}^{\mathsf{min}}(\alpha) = \eta(\alpha). \frac{\beta^2}{n} + O\left(\frac{1}{n^2} \right) + O\left(\beta^4 \right), \tag{5.30}$$

therein the parameter

$$\eta(\alpha) = 2 \left(\frac{1}{\langle K^+ \rangle^2} - 1 \right) \left(1 + \sum_{j=1}^{\frac{n}{2}-1} f(2j) \right), \tag{5.31}$$

can be thought of as quantifying the overhead of the computation procedure in the phase.

5.5.3 Conclusion: Counter-intuitive regimes are efficient.

It is easy to get lost in all the notation and numerical data in this section. Here is the take-home message:

> Given access to a chain of fixed length, to perform a (small z) rotation, the optimal strategy for minimising decoherence is to split up the rotation angle as much as possible with the smallest possible spacing ($= 2$) between consecutive rotation sites.

The result is counter-intuitive as it goes directly against the conventional wisdom of separating out the rotation sites more than the relevant length scale in the problem (so that the individual rotations can be treated independently). We have shown both analytically and numerically that we actually gain in efficiency by spacing the rotation sites as close as possible because it allows us to split up the rotation angle maximally (See Fig. 5.11). In this counter-intuitive regime, we cannot treat the logical operations implemented by the individual measurements on their own. Rather, they "interact" with each other and care needs to be taken to deal with memory effects.

Anyone familiar with the earlier work by Raussendorf *et al.* [RWP+17] might start to wonder how our result fits with the previously established notion that decoherence effects can be reduced

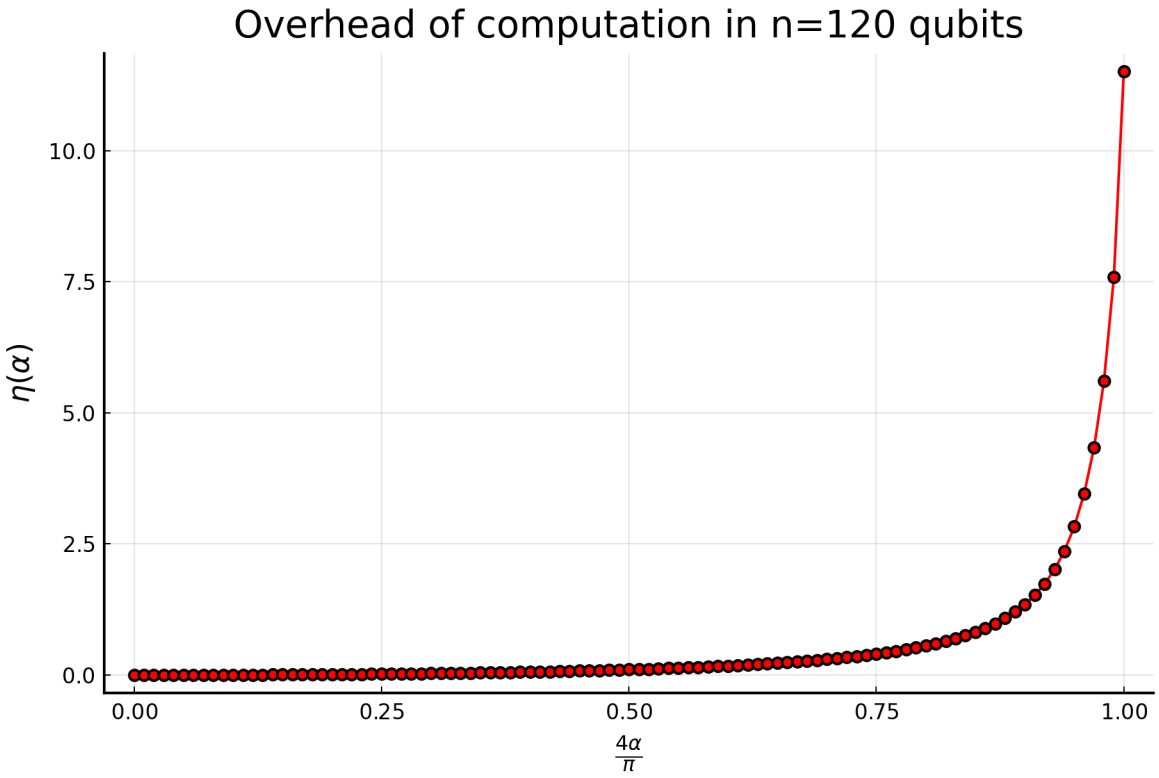

Figure 5.10: Computational overhead in the cluster "phase": as we approach criticality, we see a blowup. This is caused by an ever-increasing correlation length and ever decreasing order parameter as the distance to the phase transition approaches zero. The finite value of the overhead at the critical point is merely a signature of finite size effects.

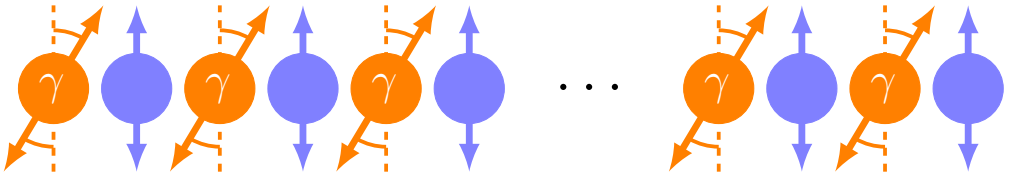

Figure 5.11: Optimal measurement pattern for performing a z-rotation in the cluster phase regardless of the specific location in the phase diagram. We see that the symmetry breaking measurements are as closely packed as possible corresponding to $\Delta = 2$ even if they become dependent on each other when the correlation length is comparable to or less than Δ. Contrast this new result with the earlier prescription in Fig. 3.2 where the rotation sites were "far" apart.

to zero in infinite chains (i.e. SPT phases) when the rotation sites are separated by $\Delta \gg \zeta$ (correlation length). Our analysis shows that the zero decoherence limit is actually approached from the opposite regime ($\Delta = 2$). The only reason that one doesn't pay an extra price for separating the rotation sites by a large distance in thermodynamic limit is the fact that the individual rotation angles can be made arbitrarily small. This fact is immediately evident from Eq. 5.28 where the function $F(\Delta) \to 0$ as $n \to \infty$ regardless of the value of Δ. However, when we do not have that luxury of infinite resources, our aim should be to pack the rotation sites

as closely as possible corresponding to $\Delta = 2$ for *any* finite chain length regardless of where we are located in the cluster phase.

If we wanted to generalise this notion by considering z-rotations followed by rotations about the x-axis, in the optimal measurement pattern, a (small) symmetry breaking measurement is performed at every single site (See Fig. 5.12). An important caveat to stress here is that while the measurement pattern in Fig. 5.11 has firm analytical and numerical backing for any resource state connected to the cluster state (via symmetry respecting local quantum circuits), the pattern in Fig. 5.12 only holds for the ground states $|\Phi(\alpha)\rangle$. This is because Eq. 5.17 is only numerically confirmed and we know that such relations don't hold in more general resource states in the cluster "phase".

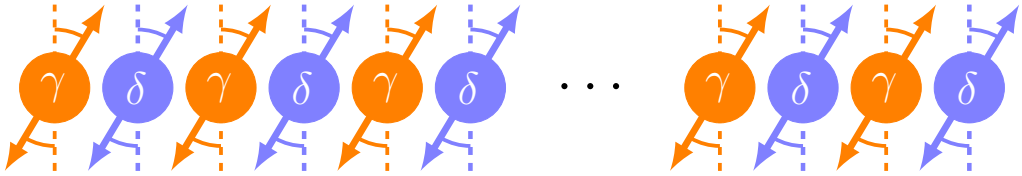

Figure 5.12: Optimal measurement pattern for performing a z-rotation followed by a x-rotation using ground states $|\Phi(\alpha)\rangle$. This is due to the numerically confirmed even-odd decoupling relations, as displayed in Fig. 5.6. However, do note that such decoupling holds only for the transverse field cluster Hamiltonian and *not* for arbitrary symmetry respecting perturbations to the cluster Hamiltonian.

To conclude the chapter, we observe that although the analysis above was primarily suited to odd chains, the same physical principles apply in even rings (i.e. periodic boundary conditions). One just needs to be a little more careful about classical post-processing relations and how to interpret MBQC observables like $\tilde{A}_X$. This will be relevant if we wanted to experimentally verify the efficiency of the dependent regime outlined above as small rings (which we can afford in the era of quantum computers of low depth) can protect against boundary effects.

Chapter 6

Conclusions and Outlook

In this thesis, we investigated the relationship between measurement-based quantum computation (MBQC) and symmetry-protected topological (SPT) order in finite spin chains. In general, this work contributes to the broader line of work done with the aim of bringing the fields of quantum computation and condensed matter physics together. More specifically, we started our exploration by asking the following question: can the traditional methods of group cohomology and matrix product state (MPS) tensors, used to classify abelian SPT phases according to their computational power, be applied to finite (i.e. more realistic) spin chains? In our own excursions, we did not find such a straightforward adaptation. Be that as it may, we came up with our own (rather simplified) formalism that is comfortable in dealing with spin chains of arbitrary length. This operational formalism shifts the attention from the analysis of MPS tensors (representing the resource state at hand) to observables (that can be measured on the resource state). Along the way, we showed that the non-trivial computational power of SPT ordered states can be directly related to some non-vanishing string-like order parameter – thereby establishing the most obvious connection between the standard analysis of SPT ordered states and their use as resources in MBQC. Furthermore, using the techniques developed, we were able to investigate regimes of computation that were inaccessible to the work done in the last decade. Remarkably, such counter-intuitive regimes turned out to be *more efficient* than the safer regimes prescribed earlier.

The immediate questions that follow from our analysis are in two directions. Firstly, all the results in this thesis pertain to spin chains i.e. 1D systems. Can they be extended to higher dimensions? As was noted in Sec. 3.5, two-dimensional extensions of computational phases of matter already exist and recently the cluster phase has been discovered as the first example of universal quantum computational phase of matter. These analyses were based on the traditional techniques of PEPS (2D generalizations of MPS) symmetry and group cohomology. Now that we have (seemingly) better techniques in our armor, can they be used to simplify these analyses or better, be used to find other unorthodox universal phases of matter? If such extensions are indeed possible, we will go a long way towards the ultimate goal of classifying schemes of MBQC merely by symmetry.

The other potential line of investigation is rather modest in comparison but still intriguing. In this thesis, we have mainly dealt with the 1D cluster phase and associated the computational power with a non-vanishing string order parameter. Nevertheless, these results generalises rather trivially to other 1D abelian SPT phases that contain short range entangled states (meaning small correlation lengths). For example, consider the twin of the cluster state defined as the unique ground state of the Hamiltonian $H_{\text{twin-clus}} = -\sum_i Z_{i-1}Y_iZ_{i+1} =: -\sum_i K_i^{\text{twin}}$. If we wanted to investigate the twin cluster phase by interpolating between the twin-cluster Hamiltonian and the product Hamiltonian $H_{\text{trivial}} = -\sum_i X_i$, a relevant computational order parameter can be constructed out of the stabilisers K_i^{twin} as follows

$$\begin{aligned} O_k^+ &:= (K_{k+1}^{\text{twin}}).(K_{k+1}^{\text{twin}}).(K_{k+3}^{\text{twin}}).(K_{k+4}^{\text{twin}}) \dots (K_{N-1}^{\text{twin}}), \\ &= Z_k X_{k+1} X_{k+2} X_{k+4} X_{k+5} \dots X_{N-1} Z_N. \end{aligned}$$

A non-zero expectation value of this string-like observable can be taken as the smoking gun for non-trivial computational power for ground states of the interpolation Hamiltonian which are short-range entangled.

The situation becomes much more interesting when we are dealing with long-range entangled states corresponding to a vanishingly small energy gap above the ground state in the thermodynamic limit. A particularly fascinating example is the so-called one parameter Kitaev-Gamma chain spin-$1/2$ Hamiltonian

$$H_{K-\Gamma}(\Phi) = \sum_{\langle i,j\rangle \in \gamma \text{ bond}} -\cos\Phi\ S_i^\gamma S_j^\gamma - \sin\Phi\ (S_i^\alpha S_j^\alpha + S_i^\beta S_j^\beta), \text{ where } \alpha, \beta \neq \gamma,$$

with an enormous symmetry group [YNT$^+$20]. Without going into the precise details about Hamiltonian, let us just note that a large section[1] of the phase diagram is gapless with the gap above the unique ground state scaling like $1/N$ where N is the system size. This would be the end of the story if our whole analysis was based on previous techniques that relied on a non-vanishing thermodynamic gap as the central notion for computationally useful resource state. However, for us, we simply don't care about this behavior at the thermodynamic limit as the new techniques are perfectly at home with finite systems. To get us started, we just need a non-vanishing order parameter in finite systems and it turns out that they can be merely built out of truncated symmetries as

$$\text{SOP}_L(X) := \langle X^{\otimes L}\rangle, \quad \text{SOP}_L(Z) := \langle Z^{\otimes L}\rangle.$$

Such operators commute with all the Hamiltonian terms except at the two boundaries where they are truncated and thereby have some probability of being non-zero in finite systems. This

[1] the other sections in the phase diagram contain numerous ground state degeneracies, making reliable computation impossible.

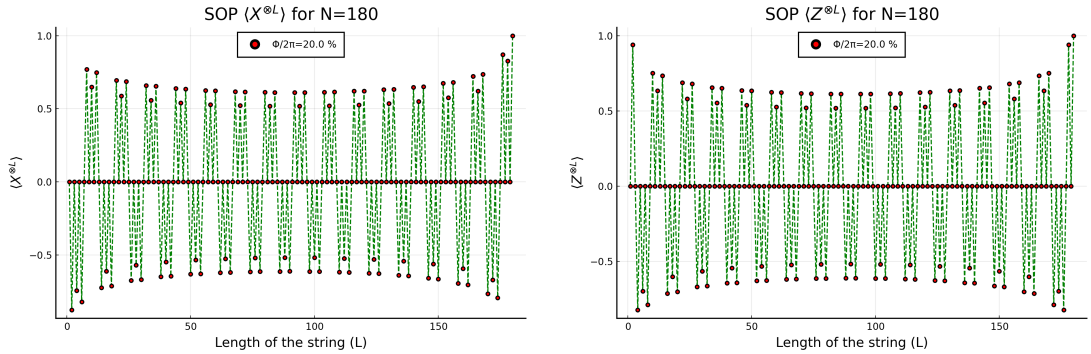

(a) Expectation values of a strings Pauli-X operators in the ground state of $K-\Gamma$ chain.

(b) Expectation values of strings of Pauli-Z operators in the ground state of $K-\Gamma$ chain. This looks exactly like Fig. 6.1a just two sites shifted.

Figure 6.1: String-like order parameters in the Kitaev-Gamma chain as a function of their length. In particular, the starting point of the string is fixed at the first site and it is the end point that is varied. The two plots are taken at the point $\Phi = 2\pi/5$ in the phase diagram for a chain length of $N = 180$. The primary take-away from these plots is that for all even values of string length, there exist the much coveted non-zero string order parameters. A secondary feature is that the correlation length is very large – maybe even comparable to the system size. This is the footprint of the long range entanglement present in the ground state.

is numerically confirmed for all even[2] values of L in Fig. 6.1.

However, from the same figure, it is also clear that the Kitaev-Gamma chain has a very large correlation length whose value cannot quite be resolved from the figures themselves as the SOPs seem to decay polynomially. At any rate, such a large correlation length complicates potential MBQC schemes that can be realized on these chains. Specifically, this would mean that no matter how separated we make our symmetry-breaking measurements, these will always be dependent on each other and one cannot reach a fixed point state via some procedure like oblivious wire. However, in Sec.5.5 we discussed how dependent operations can still be handled although they introduce additional logical error in the computational scheme. An intriguing question that arises is the following: *can the same techniques used in analyzing the unconventional regime in the cluster phase be adapted to make the Kitaev-Gamma chain (and other spin-chains with long-range entanglement) useful for MBQC?*

As a final comment, it would be really nice if we can use our newly gained knowledge from this formalism to somehow devise a simple experiment that can potentially be implemented in real-life devices like the IBM quantum processors. This is a point of ongoing investigation in our group currently and we hope these noisy devices are coherent enough to capture the theoretical predictions that come from exploring non-traditional regimes of computation.

[2]This is not entirely relevant for the discussion at hand but if you are curious, for odd lengths, the vanishingly small value of SOPs is due to their anti-commutation among themselves.

Bibliography

[AAB+19] Frank Arute, Kunal Arya, Ryan Babbush, Dave Bacon, Joseph C. Bardin, Rami Barends, Rupak Biswas, Sergio Boixo, Fernando G.S.L. Brandao, David A. Buell, Brian Burkett, Yu Chen, Zijun Chen, Ben Chiaro, Roberto Collins, William Courtney, Andrew Dunsworth, Edward Farhi, Brooks Foxen, Austin Fowler, Craig Gidney, Marissa Giustina, Rob Graff, Keith Guerin, Steve Habegger, Matthew P. Harrigan, Michael J. Hartmann, Alan Ho, Markus Hoffmann, Trent Huang, Travis S. Humble, Sergei V. Isakov, Evan Jeffrey, Zhang Jiang, Dvir Kafri, Kostyantyn Kechedzhi, Julian Kelly, Paul V. Klimov, Sergey Knysh, Alexander Korotkov, Fedor Kostritsa, David Landhuis, Mike Lindmark, Erik Lucero, Dmitry Lyakh, Salvatore Mandrà, Jarrod R. McClean, Matthew McEwen, Anthony Megrant, Xiao Mi, Kristel Michielsen, Masoud Mohseni, Josh Mutus, Ofer Naaman, Matthew Neeley, Charles Neill, Murphy Yuezhen Niu, Eric Ostby, Andre Petukhov, John C. Platt, Chris Quintana, Eleanor G. Rieffel, Pedram Roushan, Nicholas C. Rubin, Daniel Sank, Kevin J. Satzinger, Vadim Smelyanskiy, Kevin J. Sung, Matthew D. Trevithick, Amit Vainsencher, Benjamin Villalonga, Theodore White, Z. Jamie Yao, Ping Yeh, Adam Zalcman, Hartmut Neven, and John M. Martinis. Quantum supremacy using a programmable superconducting processor. *Nature*, 574(7779), 2019. → page 1

[AAG20] Anurag Anshu, Itai Arad, and David Gosset. Entanglement subvolume law for 2D frustration-free spin systems. In *Proceedings of the Annual ACM Symposium on Theory of Computing*, 2020. → page 80

[AKLT87] Ian Affleck, Tom Kennedy, Elliott H. Lieb, and Hal Tasaki. Rigorous results on valence-bond ground states in antiferromagnets. *Physical Review Letters*, 59(7):799–802, 1987. → page 15

[BBC+93] Charles H. Bennett, Gilles Brassard, Claude Crépeau, Richard Jozsa, Asher Peres, and William K. Wootters. Teleporting an unknown quantum state via dual classical and Einstein-Podolsky-Rosen channels. *Physical Review Letters*, 70(13), 1993. → page 9

[BBMR10] Stephen D. Bartlett, Gavin K. Brennen, Akimasa Miyake, and Joseph M. Renes. Quantum computational renormalization in the haldane phase. *Physical Review Letters*, 105(11), 2010. → page 35

[BCO17] Johannes Bausch, Toby Cubitt, and Maris Ozols. The Complexity of Translationally Invariant Spin Chains with Low Local Dimension. *Annales Henri Poincare*, 18(11), 2017. → page 78

[BK05] Sergey Bravyi and Alexei Kitaev. Universal quantum computation with ideal Clifford gates and noisy ancillas. *Physical Review A - Atomic, Molecular, and Optical Physics*, 71(2), 2005. → page 5

[BL08] Jacob D. Biamonte and Peter J. Love. Realizable Hamiltonians for universal adiabatic quantum computers. *Physical Review A - Atomic, Molecular, and Optical Physics*, 78(1), 2008. → page 78

[BM08] Gavin K. Brennen and Akimasa Miyake. Measurement-based quantum computer in the gapped ground state of a two-body hamiltonian. *Physical Review Letters*, 101(1), 2008. → page 32

[CGLW13] Xie Chen, Zheng Cheng Gu, Zheng Xin Liu, and Xiao Gang Wen. Symmetry protected topological orders and the group cohomology of their symmetry group. *Physical Review B - Condensed Matter and Materials Physics*, 87(15), 2013. → pages 2, 24

[Cho14] Jaeyoon Cho. Sufficient condition for entanglement area laws in thermodynamically gapped spin systems. *Physical Review Letters*, 113(19), 2014. → page 80

[CLN05] Andrew M. Childs, Debbie W. Leung, and Michael A. Nielsen. Unified derivations of measurement-based schemes for quantum computation. *Physical Review A - Atomic, Molecular, and Optical Physics*, 71(3), 2005. → page 9

[Deu85] D. Deutsch. QUANTUM THEORY, THE CHURCH-TURING PRINCIPLE AND THE UNIVERSAL QUANTUM COMPUTER. *Proceedings of The Royal Society of London, Series A: Mathematical and Physical Sciences*, 400(1818), 1985. → page 1

[DOE10] Niel De Beaudrap, Tobias J. Osborne, and Jens Eisert. Ground states of unfrustrated spin Hamiltonians satisfy an area law. *New Journal of Physics*, 12, 2010. → page 80

[EN14] Dominic V. Else and Chetan Nayak. Classifying symmetry-protected topological phases through the anomalous action of the symmetry on the edge. *Physical Review B - Condensed Matter and Materials Physics*, 90(23), 2014. → page 25

[ESBD12] Dominic V. Else, Ilai Schwarz, Stephen D. Bartlett, and Andrew C. Doherty. Symmetry-protected phases for measurement-based quantum computation. *Physical Review Letters*, 108(24), 2012. → pages 29, 30

[Fey82] Richard P. Feynman. Simulating physics with computers. *International Journal of Theoretical Physics*, 21(6-7), 1982. → page 1

[FWS20] Matthew Fishman, Steven R. White, and E. Miles Stoudenmire. The ITensor software library for tensor network calculations, 2020. → page 47

[GFE09] D. Gross, S. T. Flammia, and J. Eisert. Most quantum states are too entangled to be useful as computational resources. *Physical Review Letters*, 102(19), 2009. → pages 2, 5, 40

[GI09] Daniel Gottesman and Sandy Irani. The quantum and classical complexity of translationally invariant tiling and hamiltonian problems. In *Proceedings - Annual IEEE Symposium on Foundations of Computer Science, FOCS*, 2009. → page 78

[Got98] D Gottesman. The heisenberg representation of quantum computers. 6 1998. → pages 13, 39

[Gro96] Lov K. Grover. A fast quantum mechanical algorithm for database search. In *Proceedings of the Annual ACM Symposium on Theory of Computing*, volume Part F129452, 1996. → page 1

[Hal83] F. D.M. Haldane. Continuum dynamics of the 1-D Heisenberg antiferromagnet: Identification with the O(3) nonlinear sigma model. *Physics Letters A*, 93(9), 1983. → page 15

[Has07] M B Hastings. An area law for one-dimensional quantum systems. *Journal of Statistical Mechanics: Theory and Experiment*, 2007(08), 2007. → pages 79, 80

[hgw] Xiao-Gang Wen (https://physics.stackexchange.com/users/9444/xiao-gang wen). Definition of short range entanglement. Physics Stack Exchange. URL:https://physics.stackexchange.com/q/136096 (version: 2014-10-16). → page 16

[HPGCS12] Jutho Haegeman, David Pérez-García, Ignacio Cirac, and Norbert Schuch. Order parameter for symmetry-protected phases in one dimension. *Physical Review Letters*, 109(5), 2012. → page 3

[Hua21] Yichen Huang. Two-dimensional local Hamiltonian problem with area laws is QMA-complete. *Journal of Computational Physics*, 2021. → page 80

[HWVE14] Mark Howard, Joel Wallman, Victor Veitch, and Joseph Emerson. Contextuality supplies the 'magic' for quantum computation. *Nature*, 510(7505), 2014. → page 1

[JL03] Richard Jozsa and Noah Linden. On the role of entanglement in quantum-computational speed-up. *Proceedings of the Royal Society A: Mathematical, Physical and Engineering Sciences*, 459(2036), 2003. → page 1

[KKR04] Julia Kempe, Alexei Kitaev, and Oded Regev. The complexity of the local Hamiltonian problem. *Lecture Notes in Computer Science (including subseries Lecture Notes in Artificial Intelligence and Lecture Notes in Bioinformatics)*, 3328, 2004. → page 78

[KLZ98] Emanuel Knill, Raymond Laflamme, and Wojciech H. Zurek. Resilient quantum computation. *Science*, 279(5349), 1998. → page 5

[KSV02] A. Yu. Kitaev, A. H. Shen, and M. N. Vyalyi. *Classical and Quantum Computation*. American Mathematical Society, USA, 2002. → page 77

[KTTW15] Anton Kapustin, Ryan Thorngren, Alex Turzillo, and Zitao Wang. Fermionic symmetry protected topological phases and cobordisms. *Journal of High Energy Physics*, 2015(12), 2015. → page 25

[Lan36] L. Landau. The theory of phase transitions [3], 1936. → page 14

[LG12] Michael Levin and Zheng Cheng Gu. Braiding statistics approach to symmetry-protected topological phases. *Physical Review B - Condensed Matter and Materials Physics*, 86(11), 2012. → page 27

[LVV15] Zeph Landau, Umesh Vazirani, and Thomas Vidick. A polynomial time algorithm for the ground state of one-dimensional gapped local Hamiltonians. *Nature Physics*, 11(7), 2015. → page 79

[Mas09] Lluís Masanes. Area law for the entropy of low-energy states. *Physical Review A - Atomic, Molecular, and Optical Physics*, 80(5), 2009. → page 80

[Mic12] Spyridon Michalakis. Stability of the area law for the entropy of entanglement. *arXiv preprint arXiv:undefined*, 2012. → page 80

[Miy11] Akimasa Miyake. Quantum computational capability of a 2D valence bond solid phase. *Annals of Physics*, 326(7), 2011. → page 39

[MM15] Jacob Miller and Akimasa Miyake. Resource quality of a symmetry-protected topologically ordered phase for quantum computation. *Physical Review Letters*, 114(12), 2015. → page 35

[MM16] Jacob Miller and Akimas A. Miyake. Hierarchy of universal entanglement in 2D measurement-based quantum computation. *npj Quantum Information*, 2(1), 2016. → page 39

[NW15] Hendrik Poulsen Nautrup and Tzu Chieh Wei. Symmetry-protected topologically ordered states for universal quantum computation. *Physical Review A - Atomic, Molecular, and Optical Physics*, 92(5), 2015. → page 39

[PGVWC07] D. Perez-Garcia, F. Verstraete, M. M. Wolf, and J. I. Cirac. Matrix product state representations. *Quantum Information and Computation*, 7(5-6), 2007. → page 20

[PGWS+08] D. Pérez-García, M. M. Wolf, M. Sanz, F. Verstraete, and J. I. Cirac. String order and symmetries in quantum spin lattices. *Physical Review Letters*, 100(16), 2008. → page 52

[PR21] A. S. Popova and A. N. Rubtsov. Cracking the quantum advantage threshold for gaussian boson sampling. *arXiv preprint arXiv:2106.01445*, 2021. → page 1

[PW15] Abhishodh Prakash and Tzu Chieh Wei. Ground states of one-dimensional symmetry-protected topological phases and their utility as resource states for quantum computation. *Physical Review A - Atomic, Molecular, and Optical Physics*, 92(2), 2015. → page 31

[RB01] R. Raussendorf and H. J. Briegel. A one-way quantum computer. *Physical Review Letters*, 86(22), 2001. → pages 1, 5

[RWP+17] Robert Raussendorf, Dong Sheng Wang, Abhishodh Prakash, Tzu Chieh Wei, and David T. Stephen. Symmetry-protected topological phases with uniform computational power in one dimension. *Physical Review A*, 96(1), 2017. → pages 2, 16, 35, 36, 61, 65

[Sch11] Ulrich Schollwöck. The density-matrix renormalization group: A short introduction, 2011. → page 22

[Sho97] Peter W. Shor. Polynomial-time algorithms for prime factorization and discrete logarithms on a quantum computer. *SIAM Journal on Computing*, 26(5), 1997. → page 1

[SNBV+19] David T. Stephen, Hendrik Poulsen Nautrup, Juani Bermejo-Vega, Jens Eisert, and Robert Raussendorf. Subsystem symmetries, quantum cellular automata, and computational phases of quantum matter. *Quantum*, 3, 2019. → page 39

[SPGC11] Norbert Schuch, David Pérez-García, and Ignacio Cirac. Classifying quantum phases using matrix product states and projected entangled pair states. *Physical Review B - Condensed Matter and Materials Physics*, 84(16), 2011. → pages 29, 41

[SPGWC10] Mikel Sanz, David Pérez-García, Michael M. Wolf, and Juan I. Cirac. A quantum version of Wielandt's inequality. *IEEE Transactions on Information Theory*, 56(9), 2010. → page 20

[Ste17] David Thomas Stephen. Computational power of one-dimensional symmetry-protected topological phases. Master's thesis, University of British Columbia, 2017. → pages 21, 31, 36

[SWP+17] David T. Stephen, Dong Sheng Wang, Abhishodh Prakash, Tzu Chieh Wei, and Robert Raussendorf. Computational Power of Symmetry-Protected Topological Phases. *Physical Review Letters*, 119(1), 2017. → pages 2, 16, 34, 35

[TSG82] D. C. Tsui, H. L. Stormer, and A. C. Gossard. Two-dimensional magnetotransport in the extreme quantum limit. *Physical Review Letters*, 48(22), 1982. → page 15

[WAR11] Tzu Chieh Wei, Ian Affleck, and Robert Raussendorf. Affleck-Kennedy-Lieb-Tasaki State on a honeycomb lattice is a universal quantum computational resource. *Physical Review Letters*, 106(7), 2011. → page 39

[Wei13] Tzu Chieh Wei. Quantum computational universality of Affleck-Kennedy-Lieb-Tasaki states beyond the honeycomb lattice. *Physical Review A - Atomic, Molecular, and Optical Physics*, 88(6), 2013. → page 39

[Wen95] Xiao Gang Wen. Topological orders and edge excitations in fractional quantum Hall states. *Advances in Physics*, 44(5), 1995. → pages 2, 15

[Whi92] Steven R. White. Density matrix formulation for quantum renormalization groups. *Physical Review Letters*, 69(19), 1992. → page 22

[YNT+20] Wang Yang, Alberto Nocera, Tarun Tummuru, Hae-Young Kee, and Ian Affleck. Phase diagram of the spin-$1/2$ kitaev-gamma chain and emergent su(2) symmetry. *Phys. Rev. Lett.*, 124:147205, Apr 2020. → page 69

[Yos16] Beni Yoshida. Topological phases with generalized global symmetries. *Physical Review B*, 93(15), 2016. → page 27

[ZCZW15] Bei Zeng, Xie Chen, Duan-lu Zhou, and Xiao-gang Wen. Quantum Information Meets Quantum Matter, 2015. → page 21

[ZSW20] Yiqing Zhou, E. Miles Stoudenmire, and Xavier Waintal. What Limits the Simulation of Quantum Computers? *Physical Review X*, 10(4), 2020. → page 1

[ZWD+21] Han Sen Zhong, Hui Wang, Yu Hao Deng, Ming Cheng Chen, Li Chao Peng, Yi Han Luo, Jian Qin, Dian Wu, Xing Ding, Yi Hu, Peng Hu, Xiao Yan Yang, Wei Jun Zhang, Hao Li, Yuxuan Li, Xiao Jiang, Lin Gan, Guangwen Yang, Lixing You, Zhen Wang, Li Li, Nai Le Liu, Chao Yang Lu, and Jian Wei Pan. Quantum computational advantage using photons. *Science*, 370(6523), 2021. → page 1

Appendix A

Gapped Local Hamiltonians and Area Laws

In the general setting of a many-body quantum system, the condensed matter physicist is interested in N (usually large) qubits (spin-$1/2$ systems) sitting on a $\mathcal{D}$-dimensional lattice. Thus, the Hilbert space of the entire system is just $\mathcal{H} = (\mathbb{C}^2)^{\otimes N}$ with dimension 2^N. Typically, we consider physically motivated *local* Hamiltonians acting on these lattices, which are of the form $H = \sum_i h_i$ where each h_i term acts non-trivially only on a small k number of terms around spin site i. Such Hamiltonians are called "k-local" and encode nearest neighbour interactions in most physical systems. To describe an arbitrary state of the system, we need to specify exponentially many coefficients which is the basic reason for the complexity in describing them. In particular, for large values of N, it becomes intractable to even store all these coefficients in some memory – let alone tracking how they evolve during any dynamical process.

However, we as physicists are interested in the low-lying energy manifold (i.e. ground state(s) and few excitations above it) that decide many of the defining features of the material we are interested in[1]. We might suspect that such states are particularly simple admitting efficient polynomial-size descriptions. This wishful thinking was proven to be fallacious by Kitaev [KSV02]. Formally, he defined the *local Hamiltonian problem* as,

The local Hamiltonian problem

Given a k-local Hamiltonian supported on N qubits, approximate the ground state energy E_0 within an error $\propto 1/\text{poly}(N)$.

A subtle but important point to note here is that for this problem we don't consider a single Hamiltonian but actually a family of Hamiltonians $\{H_N\}_{N=1}^{\infty}$ wherein each H_N denotes the Hamiltonian supported on a system with N degrees of freedom. Surprisingly, using the formalism of quantum computational complexity theory, one can prove that this seemingly innocuous

[1]This is particularly true for systems cooled down to low enough temperatures but it turns out that even at room temperatures, the low energy sector has great implications.

problem is hopelessly hard. It is in fact, so hard that even if we have a universal fault-tolerant quantum computer, it is very unlikely that a (general) solution to this problem can be found. Without getting deep into the technical discussion, below we try to explain some practical consequences that follow from this result.

First of all, we need to clarify what we exactly mean by "very unlikely". In the language of quantum computation, an algorithm is said to be efficient if it solves a problem by using a polynomial sized quantum circuit. Thus, we believe that there exists *no* such quantum circuit of size poly(N) that can approximate the (a) ground state of H_N. The underlying reason behind this belief is the fact that if such a circuit exists it would collapse the sacred complexity hierarchy of (quantum) computer science. Technically, solving this problem would immediately mean solving the hardest complexity problems (QMA-complete) that can be merely be verified by quantum computers thereby implying QMA=BQP where BQP denotes the set of problems efficiently solvable by quantum computers. Among computer scientists, this is a no-go as it is the quantum analogue of the **P vs NP** conjecture.

Understandably, such results raise difficult questions about the overall viability of many-body physics itself. If even the "simplest" (i.e. ground states of local Hamiltonians) quantum states are exponentially complex, what hope do we have in investing large degrees of freedom except for some mean-field theory crude approximation? Some suggested symmetry principles like translational invariance, only 2-body nearest neighbour interaction and Hamiltonians constructed out of simple Pauli operators may come to the rescue but detailed analysis that even with these restrictions, the hardness of the problem remains exactly the same [KKR04, GI09, BCO17, BL08].

To see how we can possibly get around such a bleak picture, let us first note that the fundamental reason behind the exponential complexity of quantum systems is quantum entanglement. If we can somehow bound the entanglement present in a quantum state, we can hope to find an efficient description of it. Specifically, if we have an completely unentangled product state, we would need only $O(N)$ parameters to completely specify it. To quantify the entanglement present across any bi-partition of a quantum state, it helps to recall the Schmidt decomposition,

$$|\Psi\rangle = \sum_{\alpha} \lambda_\alpha |O_\alpha\rangle |I_\alpha\rangle$$

where the set of numbers $\{\lambda_\alpha^2\}$ satisfying $\sum_\alpha \lambda_\alpha^2 = 1$ can be given the interpretation of a probability distribution. Using a such distribution, we can look at its Shannon entropy which is defined as the entanglement entropy between the two subsystems under consideration,

$$\text{Entanglement Entropy}: \; S_L := -\sum_{\alpha} \lambda_\alpha^2 \log \lambda_\alpha.$$

Using this measure of entanglement present between the a subsystem L and its environment, we can think of an area law pointing to the situation when $S_L \propto \delta L$. States abiding an area law are very special and incredibly rare in the Hilbert space as, for random states, we have the scaling

$S_L \propto |L|$ (volume law). Existence of an area law roughly says that the relevant correlations between the two subsystems under consideration are essentially only at the boundary. Thus, such area laws are taken a defining signature for locality of quantum states.

Now, coming back to the question of the ground states of local Hamiltonians, under which conditions can we expect them to abide by some area law? Here is where the area law conjecture comes in. Before stating it, it is useful to define the gap above the ground state $|E_0\rangle$ as

$$\delta\epsilon := E_1 - E_0 \text{ where } H|E_i\rangle = E_i|E_i\rangle.$$

Note that for gapped systems $\delta\epsilon > 0$ even in the thermodynamic limit. Formally, the area conjecture is stated as follows,

The area-law conjecture

Ground states of local Hamiltonians on a $\mathcal{D}$-dimensional lattice with spectral gap $\delta\epsilon = O(1)$ satisfy an area law.

Intuitively speaking, we believe this conjecture to be true because a large gap implies fast convergence to the the lowest energy state and thereby reveals weak correlations. One can make this a little rigorous via a back of the envelope calculation where one applies an ground state projector to a product state. If the gap is large, we will rapidly approach the ground state,

$$\left(\mathbb{I} - \frac{H}{\|H\|}\right)^l |0\rangle^{\otimes N} \xrightarrow[\text{"large" } l]{} |E_0\rangle.$$

However, it has turned out to be very difficult to use this intuition in proving rigorous claims. To date, the area law conjecture has been fully proven [Has07] only in 1D systems.

Hastings's 1D Area law

The ground state of chain of d-dimensional spins with gap $\delta\epsilon$ satisfies:

$$S_{1D}(L) = e^{O(log(d)/\delta\epsilon)} = \text{constant}.$$

As a corollary, it was shown that there existent an efficient MPS representation for the ground state. Thus, the 1D gapped local Hamiltonian (GLH) problem is at least inside the complexity class NP. If we can indeed find an classical algorithm to find this efficient description is a independent question. Note that although we know that DMRG works well under these settings, such an heuristic algorithm cannot be analysed analytically. In fact, we know that DMRG can get struck in local minimums and has substantial trouble with periodic boundary conditions for large systems. At any rate, this problem was solved in [LVV15] where the authors constructed a rigorous classical algorithm using the so-called approximate ground state projectors (AGSP) with provable guarantees of obtaining efficient description for ground states of 1D GLHs. This result, which bounds the 1D GLH problem to the complexity class P, was a seminal achievement in

theoretical quantum computer science. However, it would be fair to say that these new methods are not widely used in practice in computing ground states due to poor (still polynomial) scaling and from a numerical point of view, it is heuristic algorithms like DMRG that have stood the test of time.

Extending these ideas to 2D systems is far from trivial and till now there exists no formal general proof of area laws in 2D [2] systems. However, in the last decade, 2D area laws have been proven to hold in systems with,

(a) sub exponential number of low energy states [Has07, Mas09],

(b) frustration free spin-1/2 degrees of freedom [DOE10],

(c) adiabatic assumptions [Mic12],

(d) local consistency and overlap condition [Cho14],

(e) frustration free local gap [AAG20].

As a final comment, we note that the extensions to 2D and 3D systems maybe the hardest problems in this domain as for very high dimensions the area law holds trivially due to applicability of mean field theory arguments.

[2] We hate to be the harbinger of bad news again but it seems like in 2D, even states admitting an area law *don't*, in general, have efficient classical descriptions [Hua21].

Appendix B

Computational Methods: The ITensor Package

Below attached is a sample Julia ITensor code used to obtain the order parameter $2\nu_{01}(\alpha)$.

```
using ITensors

    N=41 # Odd chain
    starting_loc=Int64(round((N-1)/2)) # Specify the rotation site
    if (starting_loc %2)==0
        starting_loc+=1
    end
    # Create N spin-half degrees of freedom
    sites = siteinds("S=1/2",N)
    # Create an initial guess for the ground state
    bond_dim=50
    psi_i = randomMPS(sites,bond_dim)
    # Create arrays to store values as alpha varies
    Ndel=100 # Number of points we want in the interpolation
    swe = Array{Float64,1}(undef, Ndel+1)
    swe_para= Array{Float64,1}(undef, Ndel+1)
    nu_01=Array{Float64,1}(undef,Ndel+1)

    for nloop=1:(Ndel+1) # Sweep parameter

      alpha= pi*(nloop-1)/(2*Ndel)
      s_p=((nloop-1)*100/Ndel);
      cs=cos(alpha)
      ss=sin(alpha)
```

```
 # operator terms that define the Interpolation Hamiltonian
 ampo = AutoMPO()
 for j=2:N-1
    ampo += -8*cs,"Sz",j-1,"Sx",j,"Sz",j+1;
 end
 ampo+= -4*cs,"Sz",N-1,"Sx",N;
 ampo+= -4*cs,"Sx",1,"Sz",2;
 for j=2:N-1
    ampo+= -2*ss,"Sx",j
 end
 # Convert these terms to an MPO tensor network
 H = MPO(ampo,sites)

 println("$s_p % into the sweep")

 sweeps = Sweeps(10) # Decide on the number of sweeps for the DMRG algorithm
 # Increased bond dimension for the later sweeps
 maxdim!(sweeps,10,20,40,50,100,150,200,250,400,500)
 # Set a cutoff below which the singular values can be ignored
 cutoff!(sweeps,1E-15)
 # Run the DMRG algorithm, returning energy and optimized MPS
 e0,psi0 = dmrg(H,psi_i,sweeps,outputlevel=1)
  @show nu_01[nloop]=SOP(psi0,starting_loc,N)
 # Store some parameters in the arrays
 swe[nloop]=alpha*2/pi;
 swe_para[nloop]=nloop-1;
end

#Calculate expectation value of the operator ZXIXIX...Z
function SOP(T::MPS,start,finish)
 if start==finish
     return 1
     else
     mps=copy(T)

     s = siteind(mps,start)
     newpsi= 2*op(s,"Sz")*mps[start]
     noprime!(newpsi)
     mps[start]= newpsi
```

```
    for o = (start+1):2:(finish-1)
         s = siteind(mps,o)
         newpsi= 2*op(s,"Sx")*mps[o]
         noprime!(newpsi)
         mps[o]= newpsi
    end

     s = siteind(mps,finish)
     newpsi= 2*op(s,"Sz")*mps[finish]
     noprime!(newpsi)
     mps[finish]= newpsi

     expectation=inner(mps,T)
     return expectation
 end
end
```